2007

# Development of a portable laboratory facility to demonstrate alternative energy technologies

Peter Thomas Swanson
*Iowa State University*

# Development of a portable laboratory facility to demonstrate alternative energy technologies

by

Peter Thomas Swanson

A thesis submitted to the graduate faculty

in partial fulfillment of the requirements for the degree of

MASTER OF SCIENCE

Major: Mechanical Engineering

Program of Study Committee:
Michael B. Pate, Major Professor
Ron M. Nelson
Adin J. Mann

Iowa State University

Ames, Iowa

2007

# Table of Contents

# LIST OF FIGURES

# Chapter 1 INTRODUCTION

## *Project Background*

Issues related to energy are becoming increasingly pressing. Petroleum, natural gas, and coal are currently the major resources by which the power-consuming technologies of society operate, but these are finite in supply and have negative side effects. Alternative sources and ways of converting energy from one form to another are thus becoming of more and more interest to engineers and others in order to meet society's energy needs in the future. Energy is the source of all kinds of activity in the world, from transportation to industrial processing to residential appliances and other conveniences. Many factors contribute to an increasing demand for energy including growing industry, a climbing world population, and escalating standards of living. Figure 1-1 below shows the historical use of different sources of energy, reflecting both the past trends and the relative amounts of current energy source usage.

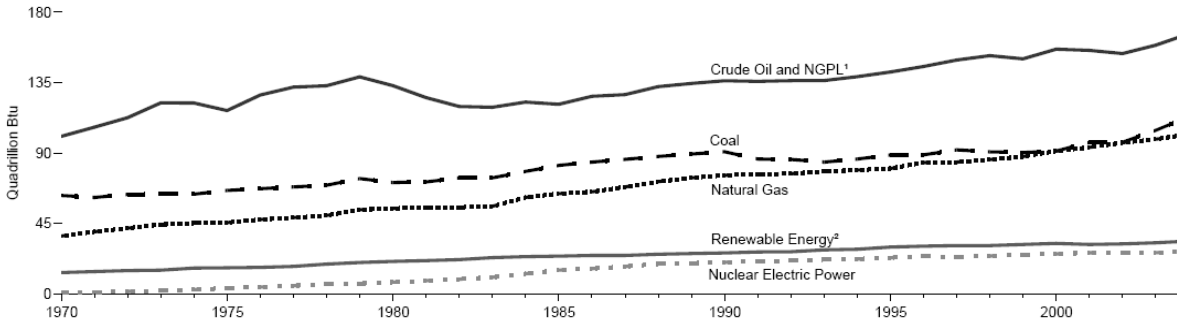


**Figure 1-1 World primary energy production by source.[1]**

Global warming, pollution issues, the limited supply of conventional energy sources, political concerns about the location of these energy resources are the topics of worldwide discussion. While the particular issue of global warming is still debated, there is no debate that petroleum-based fuels have adverse health effects, especially in urban areas. Some big cities with heavy traffic even include an "air quality forecast" to warn against being outdoors on days of intense air pollution. Large-scale harm of the environment in areas such as water quality, ozone, acid rain, and various other specific air pollutants all are either primarily or partially caused by the existing power industry. In third-world countries, lack of cheap

[1] World Primary Energy Production by Source, 1970-2004. Energy Information Administration, Department of Energy. 2006. <http://www.eia.doe.gov/emeu/aer/pdf/pages/sec11_2.pdf> Last accessed August 7, 2007

power forces people to use wood for cooking and heating, resulting in deforestation and erosion[2]. Fossil fuel supply predictions are controversial, but current estimates reported by the DOE are between about 1080 and 1300 billion barrels in world reserves[3]. With the estimated world consumption in 2005 being 84,035,000 barrels/day[4] these reserves would last between about 35 and 42 years at this same consumption rate. This prediction is somewhat misleading, though, since new oil is being discovered all the time, and advances in recovery technology and changes in the economy can make new reserves both available and economically feasible to tap, thus increasing the reserve.[5] Despite presently increasing reserves, however, there is a finite energy supply and the harmful side effects could be avoided with different technology. Both of these reasons strongly encourage the pursuit of alternative energy technologies.

In addition to these concerns about conventional energy, there is also much discussed about the hopeful prospects of new energy technologies. These prospects range from simply increasing the efficiency of current technologies to radically new visions of how the world will be powered, where the world's energy will come from, and how this energy will be allocated. Up to this point, these new technological proposals have had relatively little, though not altogether insignificant, impact in comparison with conventional technologies as Figure 1-1 also shows. According to that figure, alternative energy accounts for only about 7% of total energy production, though the inclusion of nuclear power brings the total to around 14%.

---

[2] Sub-Saharan Africa: Environmental Issues. Energy Information Administration, Department of Energy. <http://www.eia.doe.gov/emeu/cabs/subafricaenv.html> Last accessed May 10, 2007.

[3] International Energy Annual 2004. Energy Information Administration, Department of Energy. <http://www.eia.doe.gov/pub/international/iea2004/table81.xls> Last accessed August 7, 2007.

[4] International Petroleum Monthly, July 2007. Energy Information Administration, Department of Energy. <http://www.eia.doe.gov/emeu/ipsr/t46.xls> Last accessed August 7, 2007.

[5] How much Oil and Natural Gas is Left? Society of Petroleum Engineers. <http://www.spe.org/spe/jsp/basic/0,,1104_1008218_1109511,00.html> Last accessed May 10, 2007.

There is potential for much more energy to come through alternative means rather than from fossil fuel and education about these other means is an important technical and social need for reaching this potential. Some particular areas of possible energy resources and energy technologies that are under investigation worldwide and options for student education are the following:

- Pumped Storage
- Ocean Tidal
- Ocean Thermal
- Hydro Power
- Photovoltaic
- Solar Thermal
- Fuel Cell
- Geothermal
- Ocean Wave
- Wind Power
- Biomass
- Passive Solar
- Fusion

Engineers will be needed to conceive, design, build, and maintain these energy technologies, and therefore must become familiar with and understand the various technologies available. The education of engineering students that takes place in such courses as Iowa State University's (ISU) alternative energy course would be greatly improved by the addition of alternative energy technology demonstrations to experiment with, investigate, and analyze. Therefore the research reported in this thesis focuses on filling this need for portable and convenient laboratory demonstrations of various alternative energy technologies for classroom educational use.

## *Research Objectives*

The objective of this research is to design, build, and test a portable laboratory facility that demonstrates important contemporary alternative energy technologies for use in a classroom setting. In addition, the objective includes formulating laboratory exercises that can be performed in the future by students seeking to achieve both an operational and performance understanding of the chosen alternative energy technologies.

## *Research Project Overview*

A survey of alternative energy technologies was conducted to determine six alternative energy technologies for inclusion in the laboratory demonstrations. Considerations such as laboratory demonstration feasibility, accuracy in representing real-world use of the

technology, world-wide importance and potential, and variety guided the choice of the six technologies. A chapter devoted to each chosen technology reports four aspects of the research for each technology: background, theory, demonstration, and experimentation. Background information about the technology gives a general understanding of the role, scope, and importance of the technology in the energy industry presenting reasons why the technology was chosen for inclusion in the laboratory. From this background a relevant laboratory demonstration of the technology appropriate and feasible for student education was chosen. Theories and models for the performance of the demonstration were developed and demonstration devices, parts, and sensors were sized, designed, purchased, and built according to the constraints and guidelines given in the Demonstration Design section below. Discussion of the demonstration's reasonableness and limitations in illustrating design and operational performance of corresponding real-world systems is presented justifying the demonstration's design. Experimental investigations with the demonstration were executed and the data from the experimental investigations along with analysis is presented. Analysis of the experimental results will include comparison with theory and models which will indicate the demonstration's suitability to aid in student understanding of the benefits and limitations of theory. Analysis will also include comparison with real-world alternative energy systems in commercial use throughout the world. This comparison will show how accurately the small-scale demonstrations simulate real-world technologies giving students some familiarity with real-world technologies as they exist in use. The deviances from real-world performance will be discussed and causes identified recognizing the limitations of size and portability for realistic simulations. Each chapter will also supply a framework for student use of the technology and will educate them on the components and significance of the technology. The experimental results and analysis will provide a benchmark for the experiments and exercises carried out by students when doing their own experimentation.

### *Research Project Scope*

The scope of this research project includes the following tasks:

- Determine six important alternative energy technologies for student education.
- Identify appropriate and feasible demonstrations exemplifying each of the six technologies for inclusion in a mobile laboratory facility for classroom use.
- Design and build demonstrations of these six technologies to accurately simulate real-life alternative energy technologies and systems.
- Develop theory and models of the performance of the demonstrations.
- Perform experimentation with the demonstrations to collect data.
- Evaluate demonstration performance by comparison of experimental data with theory and with real-world performance of the technology being considered.
- Provide a framework for student use of demonstrations.

# Chapter 2 DEMONSTRATION DESIGN

Many large-scale renewable and alternative energy laboratories exist. The National Renewable Energy Laboratory, the Florida Solar Energy Center, Sandia National Laboratories are all governmental laboratories heavily focused on developing, improving, and discovering alternative energy sources. While they do have very helpful educational resources available including web sites, publications, and books, they do not provide concrete demonstrations for normal education use. Institutes of higher learning with research and courses in alternative energy include University of California in Berkeley, Lawrence Technological University, University of Colorado at Boulder, University of Montana in Missoula, and Iowa State University. Some of these schools also have demonstrations of alternative technologies but from internet investigation it seems that none integrate these demonstrations with theoretical instruction and lecture but have separate laboratory courses. Many private companies selling alternative technologies demonstrations exist selling such technologies as fuel cells, hydrogen production, PV cells, etc., but the demonstrations are separate and not included as part of a comprehensive package aimed at classroom use with the practicality of integrated storage and mobility. Nothing was found for educational institutions desiring a convenient portable laboratory facility for education about a wide variety of alternative energy technologies.

Since the laboratory facility to be developed is intended for classroom use, it must fit through standard doorways. For the sake of convenience and cost, it should also be integrated into a single, self-contained unit. All the demonstrations of the various technologies need to be stored onboard the mobile base and should require minimal preparation time for a particular demonstration to be ready to use. Each demonstration must be able to operate on the electric power available in classrooms. Various sensors will also be required to measure necessary parameters during experiments for further engineering analysis to be performed by the students.

A steel cart with wheels was chosen to provide the mobility and the base necessary to house and hold the demonstrations both during use and during storage and is shown in Figure 2-1 below.

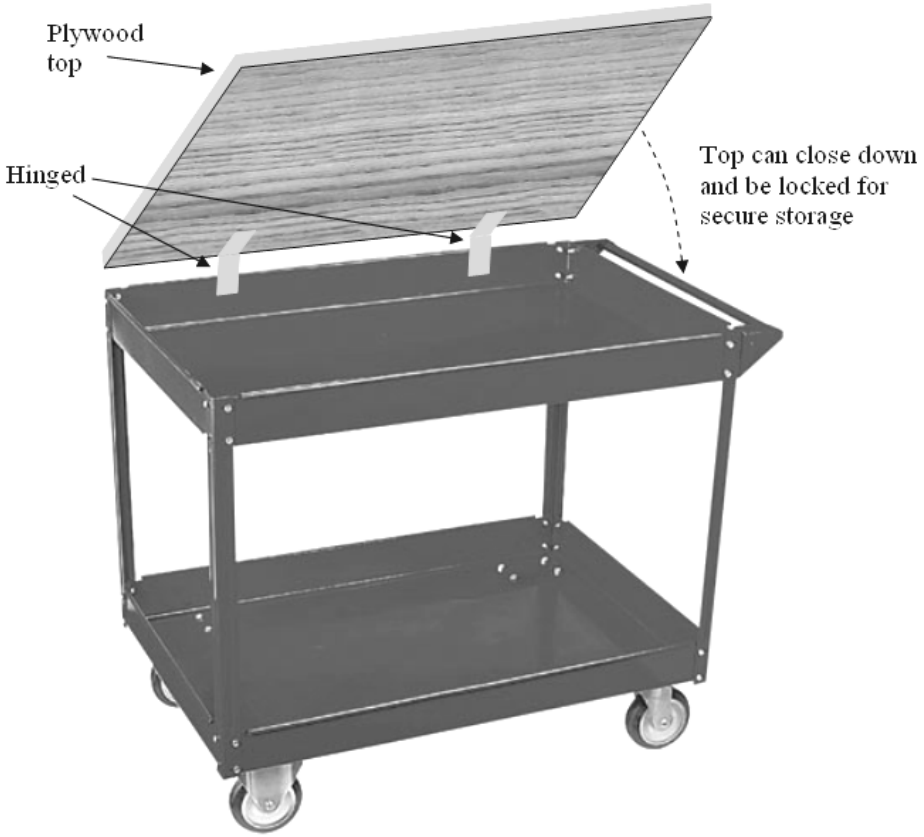


**Figure 2-1 36''L x 24''W x 32''H steel cart with hinged plywood top.**

This cart will constrain the size of the demonstrations. In order to provide a more versatile working surface for in-class use, as well as to enable secure storage of expensive small parts like the fuel cell and sensors, a plywood top was attached via hinges to the side, enclosing the upper tray (also shown in Figure 2-1). Fixtures for a padlock were added for securing the upper tray (not shown).

An extension cord will be stored on the cart to provide access to electricity for the demonstrations that require it, and no device will require more than the standard maximum current of 15 amps and 120 volts.

The six technologies chosen for inclusion in the design and to be detailed further in this survey are:

- Hydrogen Economy (Electrolyzer and Fuel Cell)
- Wind Turbine
- Photovoltaic Panel
- Concentrating Solar Power
- Active Solar Water Heating
- Passive Solar Building Heating

There are several reasons these particular technologies were included that are discussed in much more detail in the chapter on the particular technology, but an overview is given here. First, they were all seen to be important alternative energy technologies for student education. Second, they all are able to be scaled down and simplified to a demonstration suitable for educational use. The exact device chosen for the demonstration of each technology will be discussed in its chapter and justification for its effective illustration of that technology for classroom use will be discussed. Thirdly, each technology chosen is one of widespread research and development in both industry and educational institutions, and many of them are currently in use in various parts of the world. Finally, they represent a wide range of technologies to give students familiarity with as many areas of alternative energy technology as possible. The cart fully loaded with the demonstrations developed is shown in Figure 2-2 below.

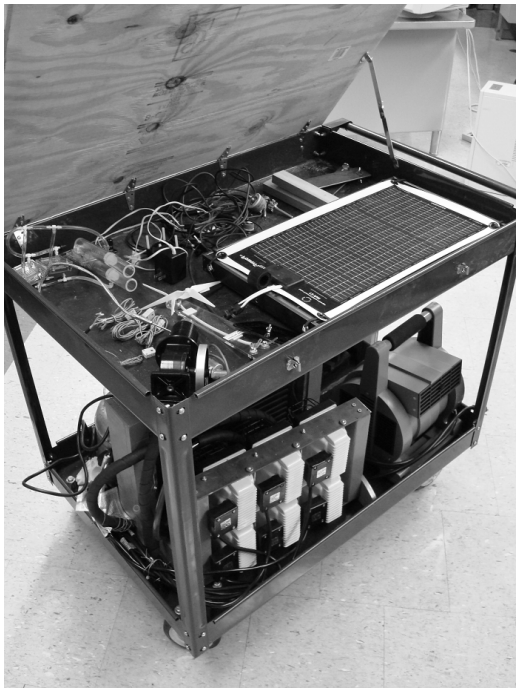

**Figure 2-2 Cart fully loaded with the six alternative energy demonstrations.**

# Chapter 3 HYDROGEN ECONOMY

## *Background*

Various parties involved in the energy industry have proposed differing degrees of the use of hydrogen as an energy "currency", hence the term 'hydrogen economy.' On one end of the spectrum is a very small degree of use as is the case currently with hydrogen being produced on a small scale primarily for use with fossil fuels in a process called "cracking." On the other end of the spectrum is an extremely large-scale and widespread all-hydrogen energy economy wherein most energy, including all energy for mobile applications, is stored and possibly delivered in the form of hydrogen. Hydrogen, in this vision, will be the medium to store energy harnessed from renewable sources like wind or solar power for use in such things devices as laptops and cars. Hydrogen could also aid in supplying energy to stationary applications in residences and industry, by providing enormous storage of energy to even out energy supply from various non-stable energy sources. For example, it could even out supply from solar sources during night time and wind turbines in times of low wind when those primary sources are incapacitated. Between both of these ends of the spectrum there are many other possibilities of a hydrogen economy that makes more or less use of hydrogen as an energy storage and transfer medium.

Though currently the integrated system of renewable energy sources producing hydrogen cannot compete with fossil fuels, hydrogen will be one of the main competitors for the storage and transfer of energy once adequate and cheap sources of renewable energy are available. Other competitors for energy storage and transfer, though not quite as versatile as hydrogen, include ethanol, biodiesel, and various other fuels derived from biomass. Electrochemical batteries are a different kind of competitor for energy storage, and a more obscure competitor is storing energy in kinetic form in high-speed, high-density flywheels.

Some of the other issues that will play a part in the question of the development of a hydrogen economy are infrastructure and storage. How hydrogen will get to its final destination from the source of production is a significant question with various answers that all have many implications for a hydrogen infrastructure. Hydrogen could be piped in various forms. It could be compressed or liquefied and the transported by road or rail. It could also be produced on site using electric energy transferred through a grid. The devices utilized to make valuable use of hydrogen, such as fuel cells, also need to be developed and are an essential part of the hydrogen economy. Fuel cells will be discussed further below.

The storage of hydrogen is possibly the largest technical hurdle yet to be overcome in a transition to a full hydrogen economy. While hydrogen's specific energy is almost three times that of gasoline, its energy density is extremely low at atmospheric pressure and temperature, as will be investigated in more detail below. This low density results in a considerable storage volume required in order to contain as much energy as typical volumes of other transportable forms of energy such as gasoline and batteries. This problem can be alleviated by changing the hydrogen in some way, including compressing hydrogen, liquefying hydrogen, and storing it as a component of a solid compound. These options will be discussed in more detail below.

## *Theory*

The model for the hydrogen economy includes primary power sources, hydrogen production, hydrogen transfer, hydrogen storage, and hydrogen use. Figure 3-1 below illustrates some of the alternatives available within a hydrogen economy.

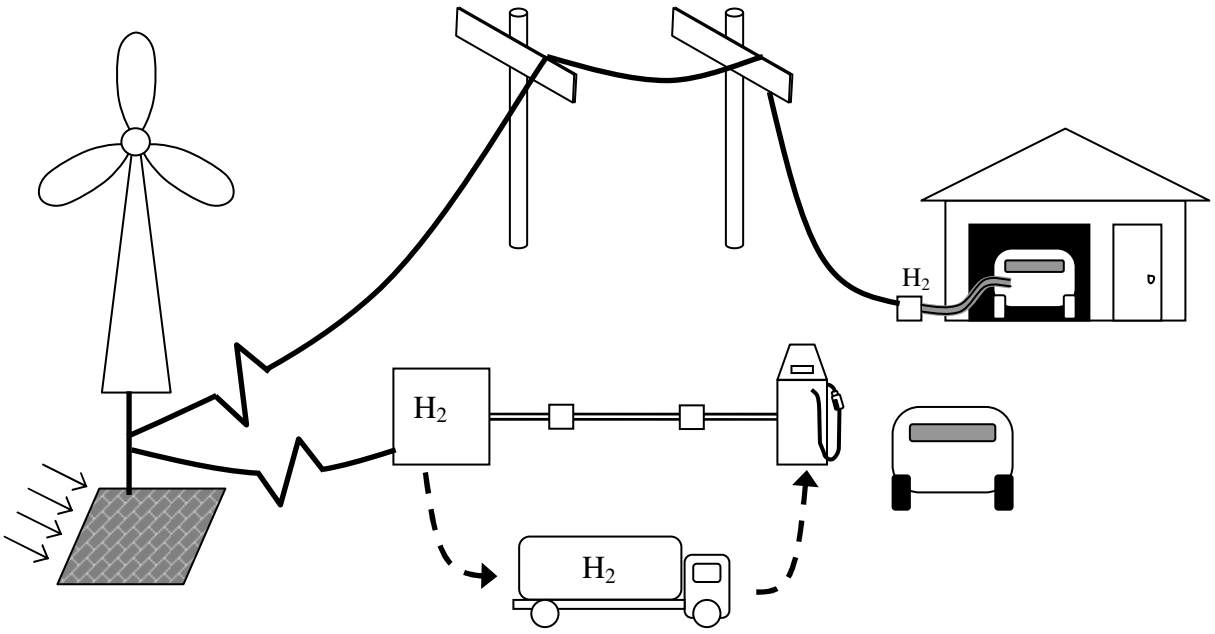


**Figure 3-1 Hydrogen economy alternatives in production, storage, and use**

The key elements of the hydrogen economy to be investigated in the demonstration being developed are the production of hydrogen and its use for power in fuel cells. Because storage is also such an important element of the hydrogen economy and has a large influence

on the answer to the transfer of hydrogen question, its will be discussed as well, though no investigation will be included in the laboratory demonstration.

## Hydrogen Production

Hydrogen can be produced in various ways. A brief overview of some of these ways follows. One method of hydrogen production is via biological processes. Various anaerobic microbes produce hydrogen as a byproduct of photosynthesis. Oxygen is also produced, though, which causes problems in a sustained and high rate production of hydrogen because of the sensitivity of these microbes to oxygen. Work is being done to discover or modify microbes to be more tolerant of oxygen while increasing hydrogen production.[6] This technology may be useful in land fills and wastewater treatment plants because of their waste product's potential for anaerobic digestion by these microbes. Other kinds of microbes produce methane as a byproduct, which can in turn be transformed into hydrogen providing another pathway of renewable hydrogen production.

Another way to produce hydrogen is photoelectrochemical water splitting, which generates hydrogen directly from sunlight. A conversion efficiency of 12.4% has been demonstrated for this technology, though the lifetime of the demonstration was only 20 hours at the most recent state of development.[7] The advantage of this technology is not only the increased simplicity and efficiency because of the integrated electrolysis, but also the economic benefit in that the need for a separate electrolyzer is eliminated.[8]

The thermochemical reforming of biomass is another pathway of hydrogen production. Hydrogen is one of the gasification byproducts, and non-hydrogen compounds can be further converted into hydrogen via the control of temperature and pressure to promote reactions with hydrogen as a product such as the water-gas shift reaction.[9] An advantage of this method is that materials that would otherwise be wasted are made into valuable products, with even the non-hydrogen byproducts representing a valuable product stream for other non-energy related uses.

---

[6] Hydrogen Production and Delivery. National Renewable Energy Laboratory. <http://www.nrel.gov/hydrogen/proj_production_delivery.html> Last accessed August 7, 2007.

[7] John A. Turner. Photoelectrochemical Water Splitting. National Renewable Energy Laboratory. 2003. <http://www1.eere.energy.gov/hydrogenandfuelcells/pdfs/merit03/15_nrel_john_turner.pdf> Last accessed August 7, 2007

[8] Photoelectrochemical Systems for Hydrogen Production. Proceedings of the 2002 U.S. DOE Hydrogen Program Review. National Renewable Energy Laboratory. <http://www1.eere.energy.gov/hydrogenandfuelcells/pdfs/32405a22.pdf> Last accessed August 7, 2007

[9] Robert Brown, *Biorenewable Resources: Engineering New Products from Agriculture*. Iowa State University Press, 2003. p. 188.

A method that can be used to promote hydrogen production is the use of extremely high temperatures from concentrated sunlight. These high temperatures make certain chemical reactions feasible for hydrogen production that at lower temperatures are impractical. In these reactions methane is converted into hydrogen and carbon. Though methane typically does not come from renewable sources, it can be a product of various biomass conversion processes as mentioned above. This high temperature methane reforming method can compliment the gasification method discussed above.

Electrolysis is a method of producing hydrogen that is conducive to use with renewable electricity sources and is the hydrogen production technology chosen to be included in the laboratory demonstration. This method uses electricity to split water molecules into hydrogen and oxygen. One advantage of electrolysis is the freedom to use any source of electricity including wind, solar power, tidal power, nuclear power, etc. Another advantage is that hydrogen may be produced wherever electricity is available, not only where there is an energy source. This flexibility in location can decouple the power source from the hydrogen production through an existing electricity grid. Through this possibility many of the difficulties associated with mass transportation of hydrogen are avoided because it can be produced when and where the hydrogen is going to be used. A PEM electrolyzer is included in the laboratory demonstration and more details about its design and operation will be included in sections to follow.

All the methods of hydrogen production are still being investigated and improved. Hydrogen production is only the first step of the hydrogen economy. Once the hydrogen is produced, it needs to be conveniently stored; the next section will discuss the different challenges and benefits of various storage options.

## Hydrogen Storage

Hydrogen storage presents a significant challenge to the dream of a hydrogen economy. The most challenging application for convenient hydrogen storage is on mobile devices, so this section will discuss hydrogen's use in the auto industry. At standard conditions[10], the density of hydrogen is 0.0824 kg/m$^3$. Taking the LHV of hydrogen as 120.1 MJ/kg, this results in an energy density of about 10 MJ/m^3, whereas gasoline energy density is about 31,700 MJ/m^3[11]. For an easier comparison, the energy contained in a typical 15 gallon tank filled with hydrogen in this form would total about 0.560 MJ. The amount of energy in the

[10] I.e., 298K and 1atm.
[11] This assumes a gasoline LHV of 43 MJ/kg.

same tank filled with gasoline is about 1,800 MJ, a huge difference with about 3000 times more energy per volume in gasoline than in hydrogen. The energy density of stored hydrogen must be made more comparable to that of gasoline for practical reasons—a multiple-thousand gallon tank will not work for mobile transportation. The fuel-to-wheel efficiency of hydrogen is about twice that of gasoline because of both the higher efficiency of fuel cells themselves and the smaller mechanical drive train in fuel cell vehicles.[12] Even with this higher efficiency, however, there is still need for hydrogen to be stored in a form with many hundred times the energy density as that at standard conditions for practical storage.

Compression

One method to help solve this problem of low energy density is to compress the hydrogen. As hydrogen is compressed, its energy density will increase. Figure 3-2 below shows the total energy contained in a 15 gallon tank of hydrogen as a function of pressure with the temperature at standard 25°C. The hydrogen tank energy content is to be compared with the 1,800 MJ benchmark for a gasoline tank.

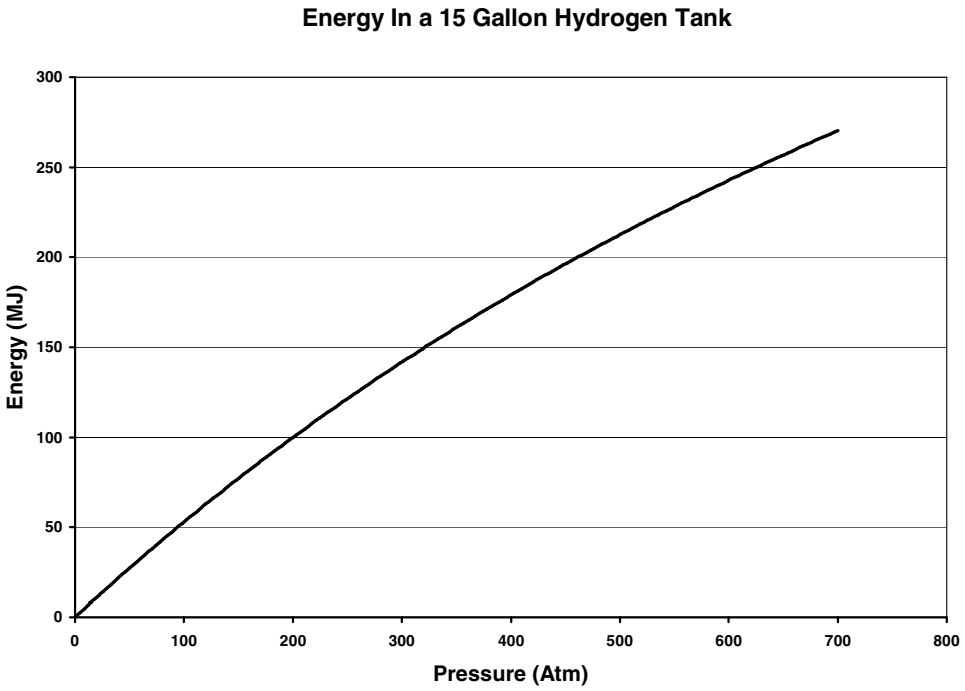


**Figure 3-2 Energy contained in a 15 gallon tank filled with hydrogen as a function of tank pressure.[13]**

[12] Frank Kreith and R.E. West. *Gauging Efficiency, Well to Wheel*. Mechanical Engineering Power 2003. The American Society of Mechanical Engineers. <http://www.memagazine.org/mepower03/gauging/gauging.html> Last accessed August 7, 2007.

[13] Thermophysical Properties of Fluid Systems. National Institute of Standards and Technology. <http://webbook.nist.gov/chemistry/fluid/> Last accessed January, 1 2007.

Note that even at 700 atm of pressure, there is still less than a sixth of the energy of a tank filled with gasoline. Besides low energy content, two additional problems with compression are the weight of the storage vessel needed and the energy necessary for compression. 700 atm of pressure is very high and requires a heavy storage vessel. A steel vessel storing 4.6 kg of hydrogen, which gives a reasonable driving range, would have a mass of around 600 kg, while a carbon fiber vessel would be about 150 kg.[14] The more sophisticated and lighter materials, however, are more expensive.

The second problem is that the energy required for compression is lost without doing useful work. To compress a certain amount of hydrogen to 700 atm requires a significant portion of that hydrogen's energy content—around 10%.[15] This energy would either go to waste or be recaptured (though with some loss) through another mechanism, hence continuing the increase in weight, complication, and cost.

Liquefaction

Another way of increasing the density of hydrogen is by cooling it until it changes to a liquid phase. Hydrogen changes to a liquid phase below about 20K at atmospheric pressure and obtains an energy density of about 8,500 MJ/m^3. A 15 gallon tank full of liquid hydrogen would contain about 480MJ of energy compared with the 1800MJ for gasoline, which is higher than the energy density obtainable by compression at 700 atm. Therefore, in conjunction with the higher energy efficiency possible with hydrogen-powered fuel cells, liquid hydrogen can make for a reasonable driving range. While liquefying hydrogen reduces the need for a high pressure vessel, it requires an extremely well insulated container and a refrigeration mechanism to keep the hydrogen cold. Because of this, the mass of liquid hydrogen vessels is not much less than those for compressed hydrogen.[16]

Solid State Storage

A third way of storing hydrogen is in a solid state as part of a compound called a hydride. With this method, a metal alloy acts as a kind of sponge that absorbs gaseous hydrogen into itself, resulting in a metal hydride with much higher density hydrogen storage than any

[14] Dr. Ulrich Eberle. *Hydrogen Storage: Technology Status and Research Needs*. GM Fuel Cell Activities. Adam Opel AG. 361. WE-Heraeus-Seminar—October 2005, Bad Honnef, Germany.
[15] Douglas J. Nelson. *Hydrogen as a Transportation Fuel*. Virginia Polytechnic Institute and State University. <http://www.hrccc.org/presentations/4StorageH2_Trans.pdf> Last accessed August 8, 2007.
[16] Dr. Ulrich Eberle. *Hydrogen Storage: Technology Status and Research Needs*. GM Fuel Cell Activities. Adam Opel AG. 361. WE-Heraeus-Seminar—October 2005, Bad Honnef, Germany.

method discussed so far. The hydrogen energy density obtainable is about 21,500MJ/m^3[17], or about 1220MJ stored in a 15 gallon tank. Some complications accompanying this storage method surround controlling the release of hydrogen in gaseous form from the metal hydride. Release temperature, release rate, energy consumption, and re-fueling time are all important parameters that need to be considered in the design of solid state storage. Much work is being done related to these parameters to improve this storage method's feasibility.[18] Like compression, this method of storage has drawbacks regarding weight. One manufacturer, for example, has a storage vessel for 4.1 kg of hydrogen, giving a fairly reasonable driving range that weighs about 300 kg[19], compared with roughly 15 kg for a gasoline tank. This is a considerable weight difference for a mobile application. In summary, Figure 3-3 below shows the results of how much energy can be stored in a 15 gallon tank given the different storage methods discussed for comparison.

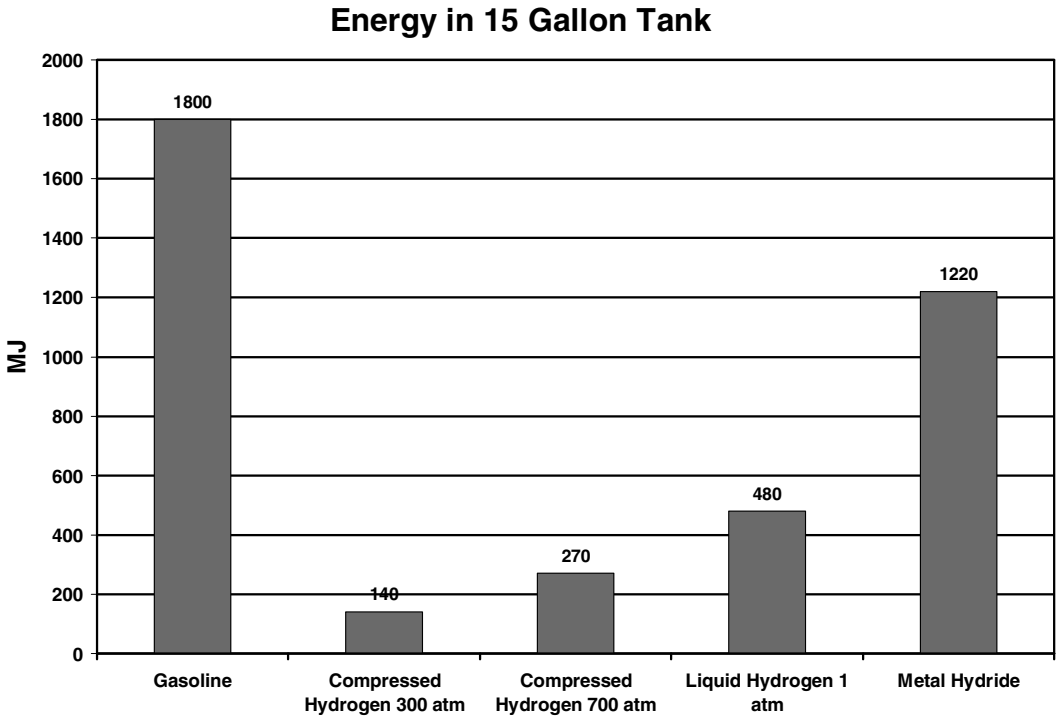


**Figure 3-3 Energy content in a 15 gallon tank for gasoline and hydrogen in various storage forms**

[17] This is based on an atomic number density of $10.7*10^{22}$ atoms/cm$^3$ according to Dr. Ulrich Eberle. *Hydrogen Storage: Technology Status and Research Needs*. GM Fuel Cell Activities. Adam Opel AG. 361. WE-Heraeus-Seminar—October 2005, Bad Honnef, Germany.

[18] Dr. Ulrich Eberle. *Hydrogen Storage: Technology Status and Research Needs*. GM Fuel Cell Activities. Adam Opel AG. 361. WE-Heraeus-Seminar—October 2005, Bad Honnef, Germany.

[19] Stationary and Bulk Storage Products. Ovonic Hydrogen Solutions. <http://www.ovonic-hydrogen.com/products/stationary.htm> Last accessed August 8, 2007.

## Hydrogen Fuel Cell

A fuel cell is an electrochemical energy conversion device. In contrast to heat engine devices that convert chemical energy into electricity through means of a cyclic thermal process, a fuel cell takes fuel and directly produces both electricity and heat directly. The benefits of fuel cell use include a higher possible efficiency and the emission of less pollution depending on the source of the fuel. There are many kinds of fuel cells, each with characteristics that make them best suited for particular applications. One kind of fuel cell, a PEM fuel cell, will be the focus of the next section.

### PEM Fuel Cell

Many efforts to develop fuel cells for mobile applications are focused on what is called a polymer electrolyte membrane or proton exchange membrane (PEM) fuel cell.[20] Because the PEM fuel cell is one of the more promising technologies for many applications, it will be the kind included in the laboratory demonstration so the theory behind its operation will be the focus of this section. The distinctive component of a PEM fuel cell is a membrane that allows the passage of protons (hydrogen ions) while preventing the passage of electrons. The electrons can then be run through an external circuit to provide electric power. The two half-reactions describing this are as follows:

$$H_2 \leftrightarrow 2H^+ + 2e^-$$

**Eq. 3-1**

$$4H^+ + 4e^- + O_2 \leftrightarrow 2H_2O$$

**Eq. 3-2**

The reaction shown by Eq. 3-1 occurs at the anode where hydrogen fuel in the form of gas ($H_2$) is supplied as fuel. By means of a catalyst that increases reaction rates, the hydrogen is split into protons (hydrogen ions) and electrons. The hydrogen ions pass through the electrolyte membrane, while the electrons flow through some external circuit. Both hydrogen ions and electrons arrive at the cathode where the second half of the reaction, shown in Eq. 3-2, occurs with the addition of oxygen. The oxygen, hydrogen ions, and

[20] Types of Fuel Cells. Hydrogen, Fuel Cells & Infrastructure Technologies Program. Department of Energy. <http://www1.eere.energy.gov/hydrogenandfuelcells/fuelcells/fc_types.html#pem> Last accessed August 8, 2007.

electrons react to form water and also output heat. The overall reaction then for one mole of water is shown in Eq. 3-3.

$$H_2 + \frac{1}{2}O_2 \leftrightarrow H_2O$$

**Eq. 3-3**

The forward reaction happens in the fuel cell. This same reaction backwards is the one that occurs in an electrolyzer. A schematic of a PEM fuel cell is shown in schematic form in Figure 3-4 below.

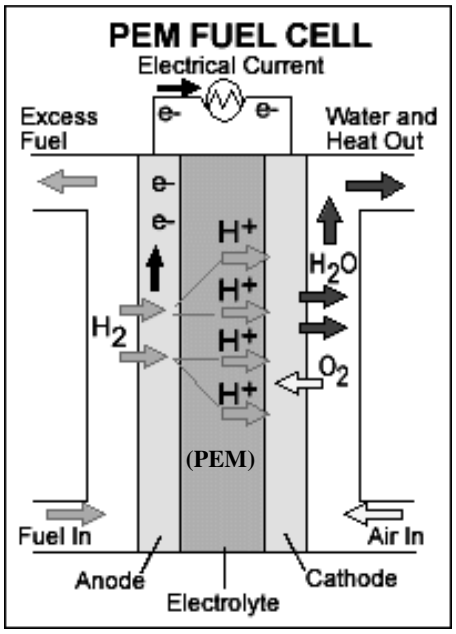


**Figure 3-4 Schematic of a PEM fuel cell showing the electric circuit**[21]

Figure 3-5 gives additional detail on the mechanical design of a fuel cell, especially the method of supplying the fuel. Metallic plates with channels etched out of one side allow for the supply and uniform distribution of gas over the surface of the cell. Only a single cell is shown in Figure 3-5, but practically the design of a fuel cell requires combining many of these cells in series to form a fuel cell stack to output higher voltage.

[21] Types of Fuel Cells. Hydrogen, Fuel Cells & Infrastructure Technologies Program. Department of Energy. <http://www1.eere.energy.gov/hydrogenandfuelcells/fuelcells/fc_types.html#pem> Last accessed August 8, 2007.

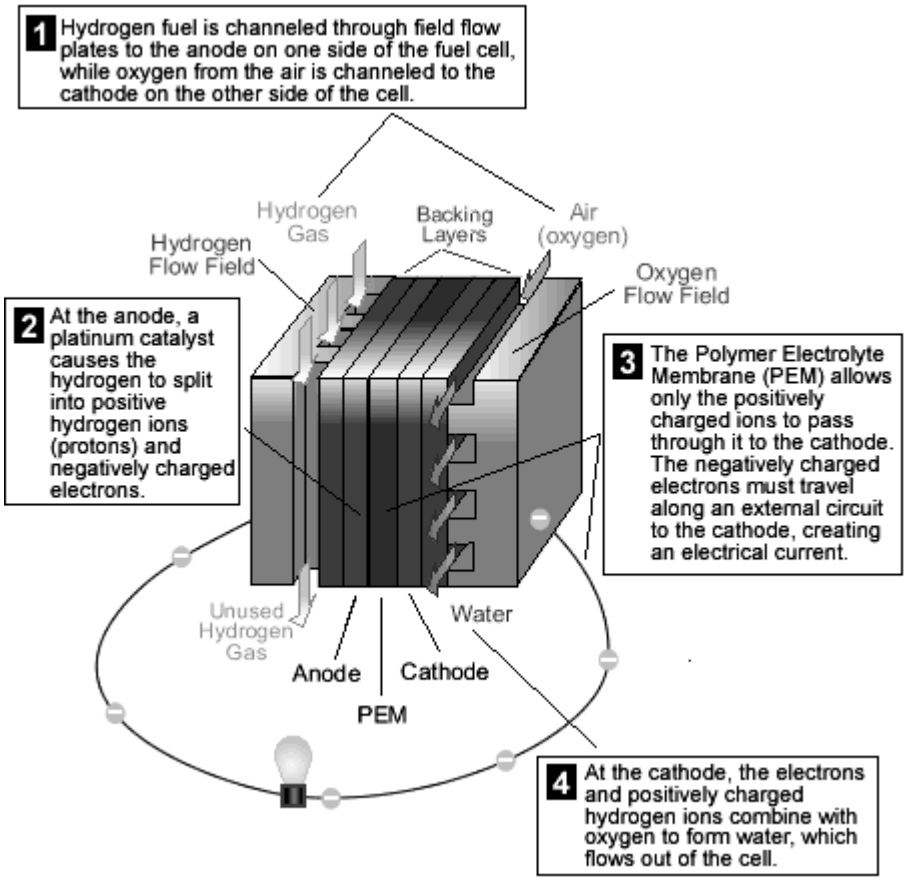


**Figure 3-5 PEM fuel cell schematic showing mechanical features**[22]

PEM fuel cells have an advantage over other kinds of fuel cells because of their faster start up time, higher specific power, and low sensitivity to orientation.[23] These fuel cells can run off compressed or liquefied hydrogen tanks and use oxygen from the atmosphere. Hydrogen can also be supplied by onboard reforming of other hydrogen-containing compounds such as methane. This kind of fuel cell operates at only about 80°C, which is very low relative to other kinds of fuel cells and is responsible for the shorter cold start-up time. This short start-up time and the PEM fuel cell's low sensitivity to orientation are particularly important for mobile applications like automobiles.

PEM fuels do have some drawbacks, however. Because of the low operating temperature, the use of platinum as a catalyst is necessary to improve reaction rates, but

[22] *How They Work: PEM Fuel Cells*. Energy Efficiency and Renewable Energy. Department of Energy. <http://www.fueleconomy.gov/feg/fcv_PEM.shtml> Last accessed August 8, 2007.
[23] Types of Fuel Cells. Hydrogen, Fuel Cells & Infrastructure Technologies Program. Department of Energy. <http://www1.eere.energy.gov/hydrogenandfuelcells/fuelcells/fc_types.html#pem> Last accessed August 8, 2007.

platinum is very expensive. The platinum catalyst also has durability problems by being very susceptible to damage from impurities in the fuel, therefore requiring the use of an extra reactor when using certain kinds of fuel to ensure the removal of impurities. The catalyst is a current area of investigation, with alternative materials and designs being explored.

Thermodynamics

The thermodynamics of electrolyzers and fuel cells is helpful for understanding the experimental results to follow. The two main thermodynamic properties relevant to both electrolyzers and fuel cells are enthalpy and Gibbs free energy. The relevant enthalpy terms are those of the enthalpy of formation, $\Delta\bar{h}_f$ , and the enthalpies of the products and reactants as a function of temperature. Assuming a reaction temperature the same as the reference temperature for the enthalpy of formation, the enthalpy of formation quantifies the energy needed to be supplied to break apart the gaseous or liquid water as in the case of an electrolyzer, and the energy available in the $H_2$ to be transformed into electricity by a fuel cell. However, not all of this energy is needed by the electrolyzer or available in the $H_2$ in electrical form in these reactions, and the Gibbs free energy, $\Delta\bar{g}_f$ , quantifies this effect. Entropy, $\bar{s}$ , also aids in understanding the reactions under consideration. Table 1 below contains values for gaseous and liquid $H_2O$, $H_2$, and $O_2$.

**Table 1 Thermodynamics data for electrolyzers and fuel cells.**[24]

| | $\Delta\bar{h}_f^{0\,25}$ (MJ/kmol) | $\Delta\bar{g}_f^0$ (MJ/kmol) | $\bar{s}^0$ (kJ/kmol·K) |
|---|---|---|---|
| $H_2O$ (g) | -241.8 | -228.6 | 188.7 |
| $H_2O$ (l) | -285.9 | -237.2 | 70.0 |
| $H_2$ (g) | 0 | 0 | 130.6 |
| $O_2$ (g) | 0 | 0 | 205.0 |

[24] Aldo V. Da Rosa, *Fundamentals of Renewable Energy Processes*. Academic Press, 2005. p. 306.

[25] $\bar{x}^0$ means on a per kilomole basis at standard temperature and pressure for property x. The subscript signifies the property is that of formation.

For a reversible electrolyzer, the entropy change will be zero. Assuming liquid water is the reactant at the reaction occurs at standard conditions, the entropy will start at 70.0 kJ/kmol·K and will end up as

$$\frac{1}{2}\bar{s}^0_{O_2} + \bar{s}^0_{H_2} = 205.0/2 + 130.6 = 233.1\,\text{kJ/kmol·K}$$

**Eq. 3-4**

where kmols are those of $H_2$. But since the assumption is that the electrolyzer is reversible, this means that heat must be absorbed equal to

$$Q = \Delta\bar{s}\text{T} = (233.1 - 70.0)\,\text{kJ/kmol·K} \times 298K = 48.6\,\text{MJ/kmol}$$

**Eq. 3-5**

where again kmols are those of $H_2$. Therefore, 48.6 MJ/kmol$_{H_2}$ of heat enters into the enthalpy of the products, contributing with the electrical input to the final enthalpy. Therefore, the necessary amount of electrical work to be supplied to reach the enthalpy of the products according the conservation of energy is decreased by this same amount to 285.9-48.6=237.3MJ/ kmol$_{H_2}$, which is the Gibbs free energy change. This is expected since Gibbs free energy is g=h-tΔs assuming an isothermal reaction. The efficiency, then, is the enthalpy of the products divided by the electrical work input necessary and is shown in Eq. 3-6 below.

$$\eta = \frac{\Delta\bar{h}}{\Delta\bar{g}} = \frac{285.9}{237.3} = 120.5\%$$

**Eq. 3-6**

This is the reversible, HHV efficiency of an electrolyzer. The reversible efficiency of a fuel cell, then, will be the inverse of the reversible electrolyzer efficiency. In a fuel cell, the change in Gibbs free energy will be delivered as electricity while the change in enthalpy (the enthalpy of formation) being supplied as the energy input. The difference will appear as waste heat to the environment. This efficiency is

$$\eta = \frac{\Delta\bar{g}}{\Delta\bar{h}} = \frac{237.3}{285.9} = 83.0\%$$

**Eq. 3-7**

### *Demonstration*

A small size electrolyzer and fuel cell was purchased for the demonstration of the production and final use aspects of the hydrogen economy. The electrolyzer is a 0.7W PEM electrolyzer and is coupled to a twin-column storage mechanism with one column each for hydrogen and oxygen. None of the sophisticated storage mechanisms discussed above is feasible for the laboratory demonstration both because of cost and because of the small amount of $H_2$ to be produced. The gaseous products will be stored at nearly atmospheric pressure though the design of the storage mechanism allows for a slight pressure to be applied, forcing the gases into the fuel cell.

The fuel cells included in the laboratory demonstration are two PEM fuel cells that can be connected either in parallel or in series. Together they are capable of a roughly 250 mW power output. A picture of the electrolyzer and fuel cell is shown in Figure 3-6 below.

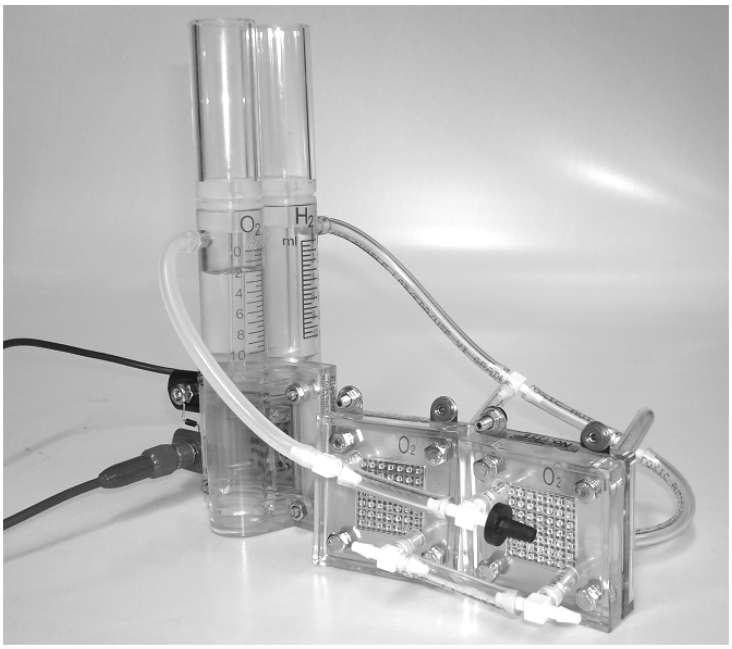


**Figure 3-6 Electrolyzer and fuel cell to be used for the laboratory demonstration.**

Figure 3-7 below shows a diagram of the demonstration with the relevant components and substances labeled.

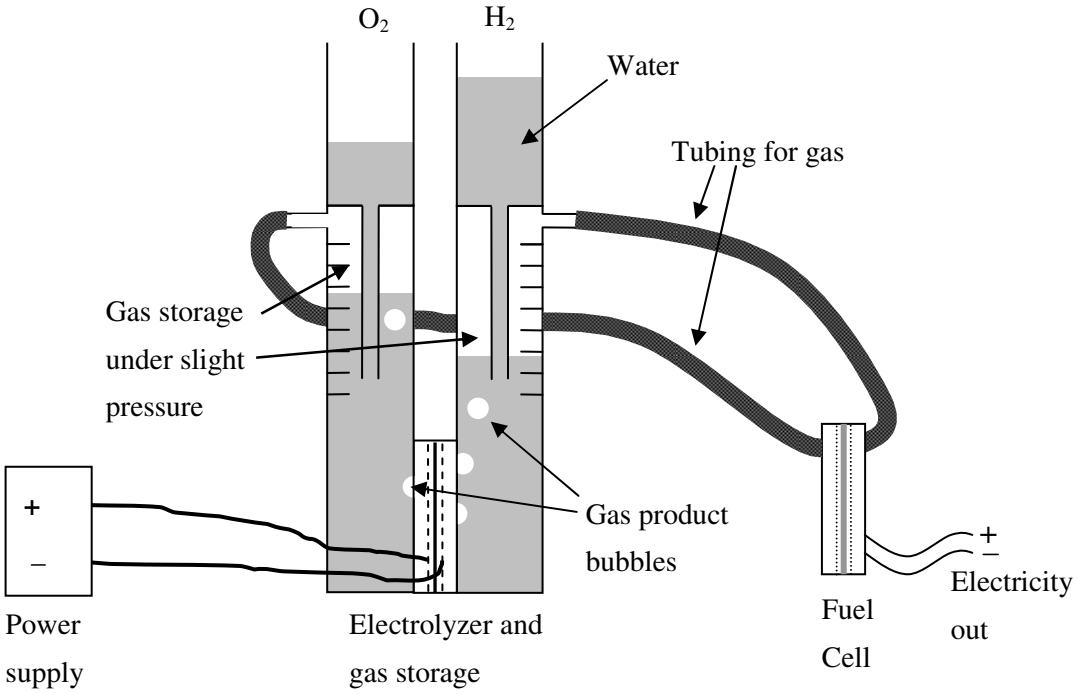


**Figure 3-7 Diagram of the hydrogen production and fuel cell demonstration included in the laboratory demonstration.**

The main features of the electrolyzer and fuel cell to be investigated are their power consumption and output and their efficiencies. Electric power into the electrolyzer, the amount of gas produced, and the power out of the fuel cell must be measured to determine these two efficiencies. Measurement of temperatures in the electrolyzer, the products of reactions, and the fuel cell would give additional data for comparison with theoretical predictions, but with power levels all less than 1W and such small components, accurate temperature measurement is not feasible. How the power amounts and efficiencies can be determined is developed for the electrolyzer and fuel cell in the next two subsections.

## Electrolysis

To calculate the electrical power input, a digital multimeter showing both voltage and current will be used. These measurements can then be used in the following equation to determine electric power into the electrolyzer, $P_{in,elec}$.

$$P_{in,elec} = V_{in} I_{in}$$

**Eq. 3-8**

From the amount of gas produced by a certain amount of electric energy input, the electrolyzer efficiency can be determined. Considering a control volume around the electrolyzer as shown in Figure 3-8, an energy balance can be developed to determine the efficiency. All the non-negligible parameters are included in the diagram and kinetic and potential energy effects are neglected.

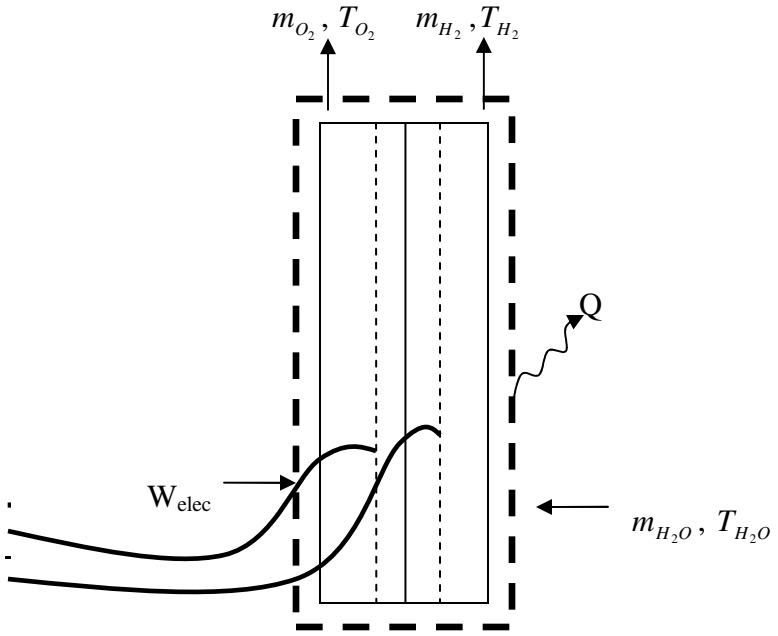


**Figure 3-8 Electrolyzer diagram with control volume and relevant parameters.**

The overall energy balance for the control volume is

$$W_{elec} - Q + \sum m_r h_r - \sum m_p h_p = 0$$

**Eq. 3-9**

with $H_2O$ as the reactants and $H_2$ and $O_2$ as the products, according to Eq. 3-3 above. The work term is the work entering the control volume in the form of electricity. Eq. 3-9 can be made more explicit as follows:

$$W_{elec} - Q + m_{H_2O} h_{H_2O} - m_{H_2} h_{H_2} - m_{O_2} h_{O_2} = 0$$

**Eq. 3-10**

The gases are assumed to be ideal gases, at atmospheric pressure, and at the experiment room temperature of 23°C. If the enthalpy reference temperature is 25°C, then the equation must take this temperature change into account as follows:

$$W_{elec} - Q + m_{H_2O}\left(h_{H_2O}(T) - h_{H_2O}(T_{ref})\right) + m_{H_2O}\Delta h_f^0 - m_{H_2}\left(h_{H_2}(T) - h_{H_2}(T_{ref})\right) - m_{O_2}\left(h_{O_2}(T) - h_{O_2}(T_{ref})\right) = 0$$

**Eq. 3-11**

$\Delta h_f^0$ is the heat of formation of 1 kilogram of liquid water at 1 atm and 25°C. Adding in specific heat information simplifies this equation:

$$W_{elec} - Q + m_{H_2O}\left(c_{p,H_2O}(T - T_{ref}) + \Delta H_f^0\right) - m_{H_2}c_{p,H_2O}(T - T_{ref}) - m_{O_2}c_{p,O_2}(T - T_{ref}) = 0$$

**Eq. 3-12**

For $H_2O_{(l)}$ $\Delta h_f^0$ is -15,864 MJ/kg. The masses of $H_2$ and $O_2$ can be determined easily from the ideal gas equation but, because of the nature of the electrolyzer, the mass of $H_2O$ reacted cannot be directly measured. The difficulty can be overcome by measuring the amount of $H_2$ produced. From this measurement and stoichiometry, the $H_2O$ mass can be calculated.

According to the ideal gas law for a gas at pressure, P, 1 atm and temperature, T, 23°C, its mass can be found according to Eq. 3-13 below with the volume, $V_{H_2}$, as the input from experimental results.

$$n_{H_2} = \frac{PV_{H_2}}{RT}$$

**Eq. 3-13**

The following equation can be used assuming the conditions stated above:

$$n_{H_2}(kmol) = V_{H_2}(ml)\frac{101.3(kPa)}{8.314\left(\frac{kJ}{kmol \times K}\right)298.15(K)}10^{-6}\left(\frac{m^3}{ml}\right)$$

$$n_{H_2}(kmol) = V_{H_2}(ml) \times 4.114 \times 10^{-8}\left(\frac{kmol}{ml}\right)$$

**Eq. 3-14**

Multiplying the number of moles of $H_2$ and $O_2$ by their molar weights gives the mass required in the energy balance. To get the mass of $H_2O$, a simple stoichiometric analysis shows that for every kmol of $H_2$ product, there was one kmol of $H_2O$ reactant. The molar mass of $H_2O$ is 18.015 kg/kmol so

$$m_{H_2O} = 18.015 \frac{kg_{H_2O}}{kmol_{H_2O}} \times 1 \left( \frac{kmol_{H_2O}}{kmol_{H_2}} \right) \times V_{H_2}(ml) \times 4.114 \times 10^{-8} \left( \frac{kmol_{H_2}}{ml} \right)$$

**Eq. 3-15**

Finally, this can be simplified to determine the mass of $H_2O$ and can be expressed as

$$m_{H_2O}(kg) = V_{H_2}(ml) \times 7.412 \times 10^{-7} \frac{kg_{H_2O}}{ml}$$

**Eq. 3-16**

Substituting Eq. 3-16 and the analogous equation for $H_2$ and $O_2$ back into the energy balance gives

$$W_{elec} - Q + V_{H_2} \times 7.412 \times 10^{-7} \left( c_{p,H_2O}(T - T_{ref}) + \Delta H_f^0 \right) - V_{H_2} \times 8.294 \times 10^{-8} c_{p,H_2O}(T - T_{ref}) - V_{O_2} \times 1.317 \times 10^{-6} c_{p,O_2}(T - T_{ref}) = 0$$

**Eq. 3-17**

where volume is in milliliters and mass is in kilograms.

Once a certain amount of electrical work with its corresponding gaseous products is measured, efficiency can be easily calculated. Since the energy from the electric input will either go to turning the reactants into the products or into heat, the efficiency can be expressed as follows:

$$\eta = \frac{W_{elec} - Q}{W_{elec}}$$

**Eq. 3-18**

## Fuel Cell

The efficiency of the fuel cell can be calculated in a similar way based on results from experimentation. The demonstration includes two fuel cells connected in series. A diagram for a single cell with a control volume and relevant parameters is shown below in Figure 3-9.

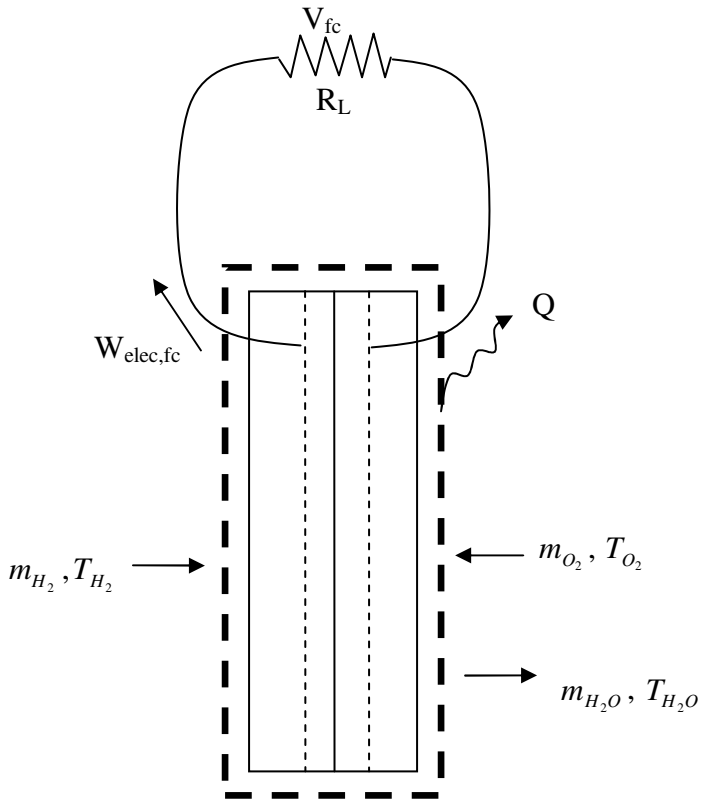


**Figure 3-9 Fuel cell diagram with control volume and relevant parameters.**

According to the diagram in Figure 3-9, the energy balance can be written on a rate basis as follows:

$$\sum \dot{m}_p h_p - \sum \dot{m}_r h_r - P_{elec,fc} - \dot{Q} = 0$$

**Eq. 3-19**

This equation is written on a rate basis because total quantities are not accurately measurable, but input and output rates are. Power and heat transfer terms are positive, and the reactants are $H_2$ and $O_2$ with $H_2O$ as the product. Some of the equations developed above for the electrolyzer apply to the fuel cell as well and will be used as needed. One difference in the fuel cell experiment is that only the output voltage across a load can be measured. The demonstration does not allow for accurate metering of the reactant input rates. If the load resistance is known, the $P_{elec,fc}$ term of the energy balance can be calculated, but the other terms remain unknown. However, the electrical power input to the electrolyzer integrated with the fuel cell, $P_{elec}$, is known, and from the previous analysis of the electrolyzer efficiency, the reactant input rates can be found indirectly. The reaction rates can in turn be

used to calculate out the efficiency of the fuel cell by itself. In practice however, a combined efficiency of the electrolyzer and the fuel cell, along with storage efficiency, would also be very important, since it would quantify the total efficiency to be compared with possible alternative energy systems and would be necessary for answering many economic questions.

### Reasonableness of Demonstration Developed

The main features of the hydrogen economy are hydrogen production and use. These features are illustrated by the electrolyzer and fuel cell. The constraints of convenience and feasible technical sophistication for mobile storage and classroom use rule out the demonstration of hydrogen compression, liquefaction, and absorption into a metal hydride. Thus, these technical aspects of hydrogen storage are left out of the demonstration. The source of electrical power for hydrogen production is not part of the hydrogen economy per se and so it is no limitation to not have a model renewable source of electricity integrated with the electrolyzer. The electrolyzer and fuel cell are the exact same technology used in real-world systems and fortunately these technologies scale down very well and therefore offer students a thorough and illustrative demonstration of the hydrogen economy for experimentation and analysis.

## *Experiments*

### Electrolyzer

Four experiments were performed with the demonstration electrolyzer. Various electric input values were used with the results obtained and displayed in Table 2.

**Table 2 Electrolyzer experimental results.**

| Electrolyzer Run # | Time (min) | Inputs | | Outputs | |
|---|---|---|---|---|---|
| | | Volts (V) | Current (Amps) | Final O2 (ml) | Final H2 (ml) |
| 1 | 6.00 | 1.61 | 0.167 | 5.25 | 10.5 |
| 2 | 2.00 | 1.8 | 0.588 | 5.00 | 10.0 |
| 3 | 2.00 | 1.8 | 0.608 | 5.00 | 10.0 |
| 4 | 7.00 | 1.62 | 0.130 | 4.45 | 8.9 |

Using the energy balance developed above, work, heat, and efficiency terms were calculated based on the experimental data in Table 2 and are shown Table 3.

**Table 3 Electrolyzer experiment analysis results.**

| Electrolyzer Run # | Time (min) | Volts (V) | Current (Amps) | $W_{elec}$ (J) | Q (J) | $\eta_{elyzr}$ (HHV) |
|---|---|---|---|---|---|---|
| 1 | 6.00 | 1.61 | 0.167 | 96.79 | -26.7 | 127.6% |
| 2 | 2.00 | 1.8 | 0.588 | 127 | 9.398 | 92.6% |
| 3 | 2.00 | 1.8 | 0.608 | 131.3 | 13.72 | 89.55% |
| 4 | 7.00 | 1.62 | 0.130 | 88.45 | -16.22 | 118.3% |

There must be some experimental error since the efficiency of Run #1 is greater than the theoretical maximum efficiency of 120.5%, but the numbers are fairly reasonable with the equipment used and with so small an electrolyzer at low power. The efficiency results reflect the trend of higher efficiency with lower load levels very clearly. The efficiency values in Table 3 are based on the HHV if $H_2$ since the $H_2O$ reactant was in liquid form. Many applications, however, cannot make use of the HHV so a more practical efficiency equation for these applications can be developed taking this fact into account. An adjusted efficiency can be calculated based on the LHV of $H_2$ as the desired energy product of the electrolyzer operation. The LHV efficiency values are listed in Table 4 below with the efficiency from Table 3 also listed for comparison.

**Table 4 Electrolyzer experiment results with both kinds of efficiency.**

| Electrolyzer Run # | Time (min) | Volts (V) | Current (Amps) | $\eta_{elyzr}$ (HHV) | $\eta_{elyzr}$ (LHV) |
|---|---|---|---|---|---|
| 1 | 6.00 | 1.61 | 0.167 | 127.6% | 108.9% |
| 2 | 2.00 | 1.8 | 0.588 | 92.60% | 79.02% |
| 3 | 2.00 | 1.8 | 0.608 | 89.55% | 76.42% |
| 4 | 7.00 | 1.62 | 0.130 | 118.3% | 101.0% |

Any large-scale production facility would likely be operating at the lower efficiencies (such as Run #'s 2 and 3) because of the high hydrogen output rates desired in commercial operation. Depending on the utilization of the hydrogen products, the efficiency would be

reported based on either the HHV or LHV, so efficiencies in the range of 90-80% seem reasonable from the experiment and are confirmed by other experimentation and industry.[26]

## Fuel Cell

Two experimental runs were performed with different load resistances as shown in Table 5 below.

**Table 5 Fuel cell experimental results.**

| Fuel Cell Run # | Volts (V) | Current (Amps) | $P_{elec}$ (W) (calculated) | $V_{fc}$ (V) | $R_L$ (Ω) | $P_{elec,fc}$ (W) (calculated) |
|---|---|---|---|---|---|---|
| 1 | 1.85 | 0.55 | 1.0175 | 1.577 | 10.5 | 0.237 |
| 2 | 1.85 | 0.55 | 1.0175 | 1.678 | 25.5 | 0.110 |

The combined electrolysis and fuel cell efficiency, $\eta_{comb}$, can be found from the following equation.

$$\eta_{comb} = \frac{P_{elec,fc}}{P_{elec}}$$

**Eq. 3-20**

This combined efficiency can be broken into its parts as follows

$$\eta_{comb} = \eta_{elyzr} \times \eta_{fc} = \frac{P_{fuel}}{P_{elec}} \frac{P_{elec,fc}}{P_{fuel}}$$

**Eq. 3-21**

Where $\eta_{fc}$ is the efficiency of the fuel cell by itself. Depending on how the electrolyzer efficiency is reported (HHV or LHV), the fuel cell efficiency will be lower or higher. Since the operating conditions for the fuel cell experiment are most similar to those of Run #2 from the electrolysis experiments, the Run #2 electrolyzer efficiency will be assumed for $\eta_{elyzr}$ in Eq. 3-21. The efficiencies for the two fuel cell experiment runs are shown in Table 6 below.

[26] For example, F. Barbir, *PEM electrolysis for production of hydrogen from renewable energy sources*, Solar Energy, Volume 78, Issue 5, May 2005, pgs. 661-669.

**Table 6 Fuel cell experiment analysis results with both kinds of efficiency.**

| Fuel Cell Run # | $P_{elec}$ (W) | $V_{fc}$ (V) | $R_L$ (Ω) | $P_{elec,fc}$ (W) | $\eta_{comb}$ | $\eta_{fc}$ (HHV) | $\eta_{fc}$ (LHV) |
|---|---|---|---|---|---|---|---|
| 1 | 1.0175 | 1.577 | 10.5 | 0.237 | 23.28% | 25.14% | 29.47% |
| 2 | 1.0175 | 1.678 | 25.5 | 0.110 | 10.85% | 11.72% | 13.74% |

Full-scale fuel cells in operation are estimated to provide about 0.75 V per cell but can fluctuate based on different loads and operating conditions.[27] The experimental results of slightly over 1.5 V for the two cells in series are therefore expected. The observed trend of increased voltage with increased load is also expected. Fuel cell efficiencies range from mid 30% up to 60% efficiency LHV.[28] PEM fuel cells in particular can have efficiencies between 34% and 36% LHV.[29] As seen in Table 6, the experimental results are comparable to the expected efficiencies. The lower efficiency of the experimental results can possibly be accounted for by leaks in the tubing connecting the electrolyzer to the fuel cell and an over-sized resistance load.

## Accuracy of Demonstration

The efficiencies of both the electrolyzer and fuel operation were very close to those reported in industry and expected from theory. The production of hydrogen and oxygen in the electrolyzer leading directly into their consumption in the fuel cell presents an accurate picture of much of the hydrogen economy. While not demonstrating storage technologies, the need for hydrogen storage can be appreciated given the small amount of power from a relatively large volume of $H_2$. Comparison of the energy output from burning the same volume of gasoline shows how little energy $H_2$ has per unit volume at standard conditions. It is also easy to see how both of these technologies could be vastly scaled up from their demonstration sizes for commercial and practical use in important applications such as automobiles. In this illustrative capacity, this demonstration thus gives students illuminating and valuable experience with key components of the hydrogen economy.

---

[27] Ulf Bossel. *Efficiency of Hydrogen Fuel Cell, Diesel-SOFC-Hybrid and Battery Electric Vehicles*. European Fuel Cell Forum. October 20, 2003. <http://www.efcf.com/reports/E04.pdf> Last accessed August 8, 2007.
[28] Ulf Bossel. *Efficiency of Hydrogen Fuel Cell, Diesel-SOFC-Hybrid and Battery Electric Vehicles*. European Fuel Cell Forum. October 20, 2003. <http://www.efcf.com/reports/E04.pdf> Last accessed August 8, 2007.
[29] U.S. Department of Energy, Office of Fossil Energy. *Fuel Cell Handbook*, Fifth Edition. EG&G Services. October 2000

# Chapter 4 WIND TURBINE

## *Background*

Wind turbines function as a source of useful energy in contrast to the hydrogen economy's goals of efficient energy conveyance, storage, and use. Wind turbines capture energy directly from wind though that energy ultimately comes from the sun. The sun's differential heating and cooling of the Earth's atmosphere cause density differences and through the resulting buoyancy forces cause wind.

Wind turbines have grown to become one of the major sources of renewable energy in the world. In 2005, 0.2% of the U.S. energy production came from wind[30]. The use of wind for electricity production in the U.S. is second only to Germany and Spain and there are plans to double U.S. wind energy capacity by 2009.[31] The goal of the U.S. Department of Energy is for 6% of U.S. electricity to be provided by wind power by the year 2020.[32] Europe grew its wind energy capacity 23% in 2005 to reach a 2006 total capacity of about 48,000 MW.[33] Wind energy uses range from multi-megawatt electricity production for residences and industry all the way down to small battery chargers. Locations of use range from boats to cities to country to the ocean.

Energy in wind, like energy directly from the sun, is a distributed source which presents difficulties in its capture. The balance between cost of capture and concentration of wind energy is one of the major considerations regarding the location of wind turbine placement, and continued research and development towards cheaper and better turbines. A wind turbine is comprised of blades that are caused to rotate by wind. This rotation is mechanically coupled to an electric generator. The electric output of the generator usually must be further conditioned for integration with a grid or to charge a battery or be utilized in some other way. There is a wide variety of wind turbine types and according to their turbine blade orientation fall into two main classes—vertical or horizontal. Figure 4-1 shows both a horizontal and vertical axis wind turbine with the major parts labeled and Figure 4-2 shows three vertical axis designs.

---

[30] Energy Production by Source, 1949-2005. Energy Information Administration, Department of Energy. <http://www.eia.doe.gov/emeu/aer/txt/stb0102.xls> Last accessed May 17, 2007

[31] *Wind Energy Statistics*. American Wind Energy Association. <http://www.awea.org/faq/wwt_statistics.html> Last accessed May 17, 2007

[32] *Wind Energy Statistics*. American Wind Energy Association. <http://www.awea.org/faq/wwt_statistics.html> Last accessed May 17, 2007

[33] *Statistics*. European Wind Energy Association. <http://www.ewea.org/index.php?id=180> Last accessed May 17, 2007.

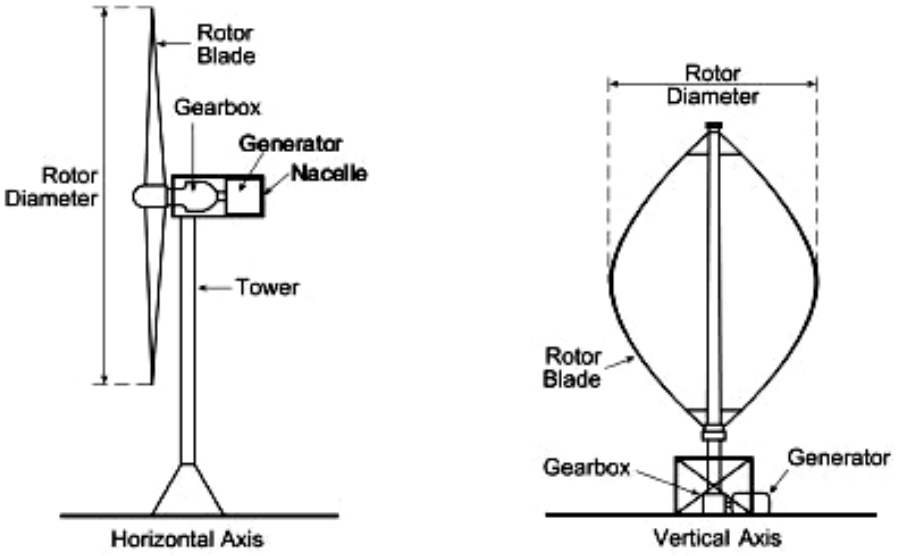


**Figure 4-1 Examples of a horizontal and vertical blade wind turbine**[34]

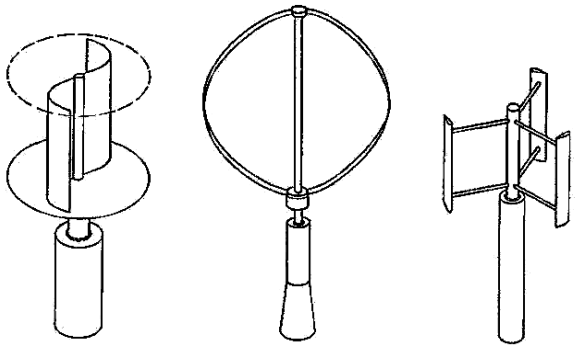

**Figure 4-2 In order from left to right, a Savonius rotor, a Darrieus rotor, and an H-Darrieus rotor.**[35]

There are many design variations within each type of turbine. These designs vary in performance, economics, optimum locations, etc. Worldwide, horizontal axis turbines predominate. This is due to many factors: lower efficiency of vertical axis turbines, the inability to self-start, and the relative lack of industry experience. Vertical axis turbines do have some advantages such as lower maintenance, lower vibration, and the ability to have the generator at ground level. There is research and development being done on them and one company, TMA Wind, claims to have developed a vertical axis wind turbine that out-

[34] Resource. Scottish Executive. <http://www.scotland.gov.uk/Resource/Img/112453/0033548.jpg> Last accessed August 8, 2007.
[35] Renewable Energy Business World. <http://www.iwr.de/> Last accessed August 8, 2007.

performs horizontal axis turbines and has the respect of representatives from the Idaho National Energy Lab.[36]

## *Theory*

### Energy in Wind

Once moving air exists, there also exists a potential to convert its kinetic energy into electricity. Physical laws govern the maximum amount of kinetic energy that can be extracted and various other characteristics of wind turbines determining their optimum performance. The kinetic energy of moving air per volume is

$$KE = \frac{1}{2}\rho V^2$$

**Eq. 4-1**

where $\rho$ is the density of air and V is velocity. Considering a stationary turbine with a given area swept by its rotating blades, the amount of kinetic energy entering this area per unit time, in other words the power in the moving air, $P_{air}$ is

$$P_{air} = \frac{1}{2}\rho V^2 \times A \times V = \frac{1}{2}\rho A V^3$$

**Eq. 4-2**

where A is the swept area. This is the total power in the airstream through the area the turbine blade sweeps. However, not all of this power is able to be extracted. There is a limit to the extractable energy in moving air.

### The Betz Limit

The basic reason that not all of the energy in moving air can be extracted by a turbine is that if it was, the air coming out of the turbine would be at zero velocity. If the exiting air was not moving, additional air could not flow through the turbine to bring more energy. Therefore there is some limiting balance between the percentage of power extracted and the flowrate of air through the turbine bringing additional energy. This can be quantified by the Betz limit. The main assumption made is that the velocity through the turbine is the average

[36] Sterling D. Allen, *Will TMA Wind Blow Away the Competition?* Pure Energy Systems News. <http://pesn.com/2007/02/01/9500453_TMA_Wind_going_commercial/> Last accessed August 8, 2007.

of the velocity in front of the turbine and behind the turbine. Figure 4-3 shows these two velocities.

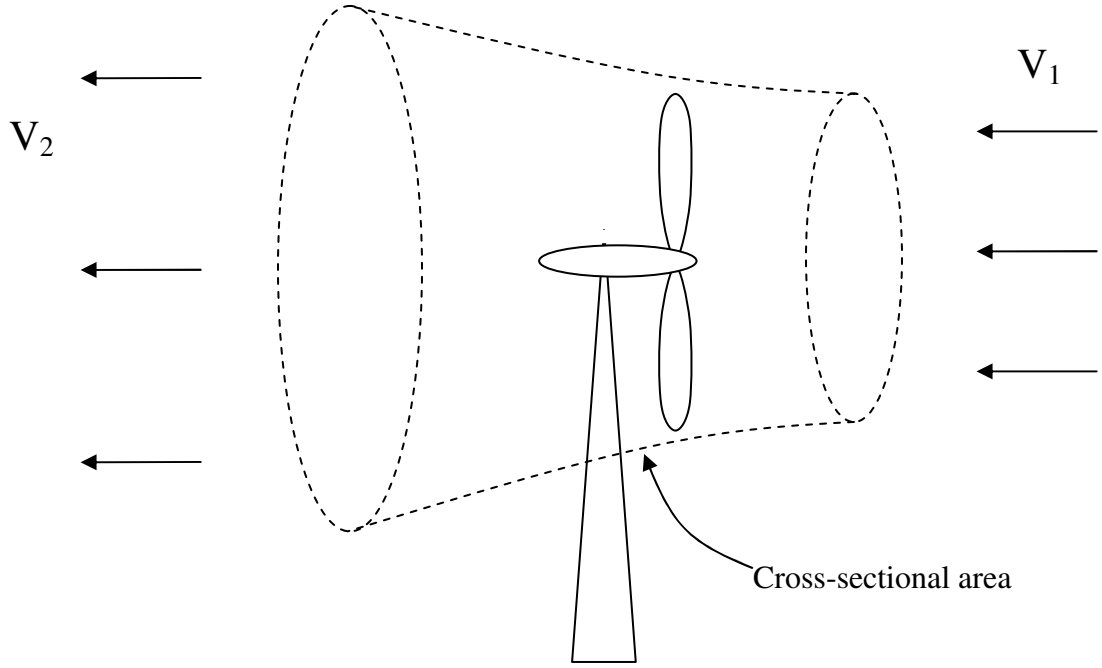


**Figure 4-3 Diagram for the derivation of Betz' limit.**

The reason the cross-sectional area of the airstream through the turbine changes from the upwind to the downwind side of the turbine is because kinetic energy from the air is captured. This can only happen if the air slows down so according to the conservation of mass and the relatively constant pressure of the air, the flow's cross-sectional area must increase. Therefore, the average velocity through the turbine blades is

$$V_t = \frac{V_1 + V_2}{2}$$

**Eq. 4-3**

Using this velocity, the mass flow rate, m, through the turbine area is

$$m = \rho A\left(\frac{V_1 + V_2}{2}\right)$$

**Eq. 4-4**

The power extracted, $P_{ex}$, from the wind by the turbine is the difference between the kinetic energy of the air in front of and behind the turbine.

$$P_{ex} = \frac{mV_1^2}{2} - \frac{mV_2^2}{2} = \frac{m}{2}\left(V_1^2 - V_2^2\right)$$

**Eq. 4-5**

Substituting the equation for mass flow rate into this equation yields

$$P_{ex} = \frac{\rho A}{4}\left(V_1 + V_2\right)\left(V_1^2 - V_2^2\right)$$

**Eq. 4-6**

To obtain efficiency the power extracted is to be compared with how much kinetic energy is in the airstream. So comparing the power extracted with the equation for the total kinetic energy in the wind from above

$$P_{air} = \frac{1}{2}\rho A V_1^3$$

**Eq. 4-7**

gives a ratio or efficiency of

$$\frac{P_{ex}}{P_{air}} = \frac{1}{2}\left(1 + \left(\frac{V_2}{V_1}\right) - \left(\frac{V_2}{V_1}\right)^2 - \left(\frac{V_2}{V_1}\right)^3\right)$$

**Eq. 4-8**

Plotting this power ratio as a function of the velocity ratio yields the curve shown in Figure 4-4.

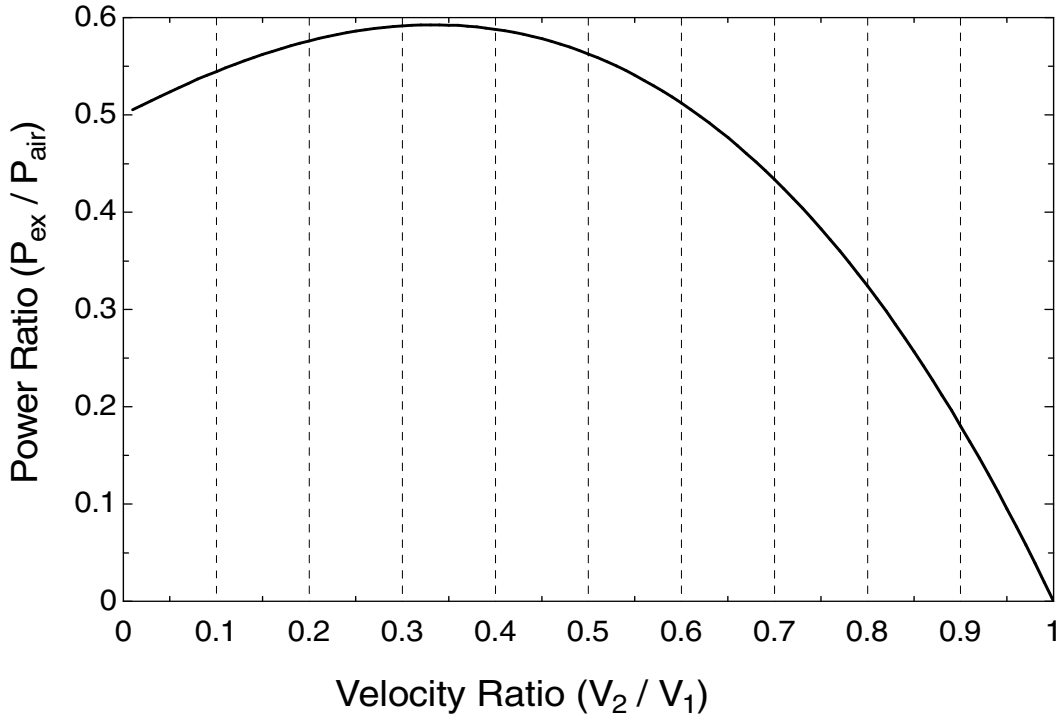


**Figure 4-4 Power ratio as a function of velocity ratio**

This shows that the maximum power able to be extracted from a given airstream, or maximum efficiency in other words, happens when the air is slowed down by 2/3. Putting this value back into the power ratio equation gives a maximum efficiency of

$$\frac{P_{ex}}{P_{air}} = \frac{1}{2}\left(1+\left(\frac{2}{3}\right)-\left(\frac{2}{3}\right)^2-\left(\frac{2}{3}\right)^3\right) = \frac{16}{27} \text{ or } 59.3\%$$

**Eq. 4-9**

This fraction, 16/27, is called Betz' limit. This is a fairly simplified analysis and the assumptions made are not extremely valid. Further investigation of the question of maximum power extraction takes more of the curvature of the airstream into consideration and a more accurate maximum efficiency of closer to 30% has been argued for by A.N. Gorban' et al.[37] This is more in accordance with actual practice of wind turbines which typically reports efficiencies of around 20%.[38]

[37] A.N. Gorban', A.M. Gorlov and V.M. Silantyev, *Limits of the turbine efficiency for free fluid flow*, ASME Journal of Energy Resources Technology, (December 2001).
[38] *The Power Coefficient*. Danish Wind Industry Association. <http://www.windpower.org/en/tour/wres/cp.htm> Last accessed May 17, 2007

## Wind Turbine Components

A horizontal axis turbine will be the type used for the laboratory demonstration so that will be the focus of the remainder of the theory section. Figure 4-5 shows a horizontal axis wind turbine with a three-bladed rotor.

**Figure 4-5 Three-bladed horizontal axis wind turbine**[39]

Figure 4-6 shows a closer view of the main parts of a large-scale horizontal axis turbine. As shown, the turbine is facing wind coming from the left and half of the housing is cut away to show the inside.

[39] *Wind Energy Capacity Grows*. KWTX. <http://www.kwtx.com/home/headlines/2229761.html> Last accessed August 8, 2007.

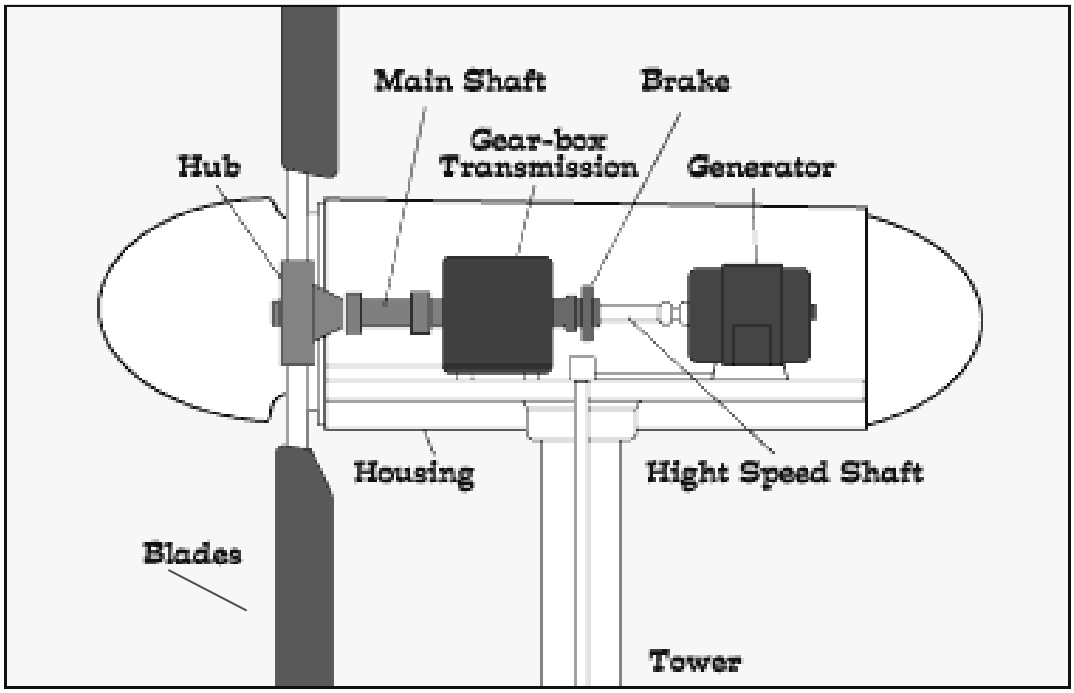


**Figure 4-6 Turbine mechanical diagram.**[40]

The blades are the component responsible for the conversion of kinetic energy in the air to mechanical energy in the turbine. The blades are connected at the hub to rotate the main shaft. Especially with larger turbines, the large radius of the blades results in a relatively low rate of revolution of the main shaft. To effectively drive the generator, this low revolution rate must be increased using a gear-box. The high-speed shaft coming out of the gear-box is sometimes equipped with a brake for control in extremely high wind speeds. For large-scale electricity production usually tens or even hundreds of turbines are installed in a certain relatively small region with common spacing practice of five turbine diameters between adjacent turbines. These large scale "wind farms" are integrated with an established electric grid to which each turbine ultimately connects. For a grid-connected turbine, the electricity generated needs to be conditioned to match the electricity of the grid. The increase of shaft speed can help in this conditioning by making the rpm suitable for an economical generator to output 50 or 60 Hz AC electricity, which is necessary for a European or American electric grid, respectively.

---

[40] Image adapted from Energex.
<http://www.energex.com.au/switched_on/images/project_info/electricity_production/33.gif> Last accessed August 9, 2007.

## Turbine Response and Control

In addition to electrical conditioning, response of the turbine to the wind and control of the turbine in undesired winds is necessary. Wind turbines have a speed at which they start rotating which is called the cut-in speed and a speed called the cut-out speed above which the turbine ceases operation because of the inability to maintain control. Turbines are built for a certain wind speed called the rated wind speed which is in between the cut-in and cut-out speed and is typically around 15 m/s[41]. Between the rated speed and the cut-out speed the turbine rotational speed needs to be controlled (constrained) for the turbine's protection. Though the wind at times attains higher speeds than the rated wind speed, those times are so rare it is economically not worth designing a turbine to be capable of making full use of those high speeds. Since the wind speed a turbine may occasionally experience is greater that its rated wind speed, some measure needs to control the turbine under these high-speed wind circumstances. If some measure is not taken to constrain the turbine in case the wind exceeds the rated speed, the turbine's excess rotational speed could cause damage to the blades, generator, or other turbine components. The two main methods to constrain turbine rotational speed in wind speeds exceeding the rated speed are pitch control and stall control.

Pitch control adds much complexity to the design of a turbine because instead of a turbine blade being rigidly fixed to the hub, it is able to rotate along its length, altering its angle relative to the wind. This allows for very precise control of the rotational speed in high winds and can also improve overall efficiency by adjusting the blade to the best pitch for any wind speed. Figure 4-7 shows the power curve for pitch control. It shows very accurate control of extracted power which never goes above the rated power. Stall control is also shown in Figure 4-7 and is seen to be less accurate. It works automatically because of the shape of the blades. The blades are designed to progressively stall from one end of the blade to the other as the wind speed increases above the rated speed.[42] Stalling describes the state in which the lift of a wind turbine blade disappears which in turn reduces power extraction, rotational speed, and generator output. The advantage of this method of control is that it avoids the complexity of the pitch control by being completely passive. No changes occur in the blade for stall control to take effect. The disadvantage is the lessened accuracy or control as shown in the figure which results in the turbine not only going above rated power and

[41] *Power Control of Wind Turbines*. Danish Wind Industry Association. <http://www.windpower.org/en/tour/wtrb/powerreg.htm> Last accessed May 17, 2007
[42] *Power Control of Wind Turbines*. Danish Wind Industry Association. <http://www.windpower.org/en/tour/wtrb/powerreg.htm> Last accessed May 17, 2007

potentially harming components, but going below rated speed and wasting power that would have otherwise been extracted.

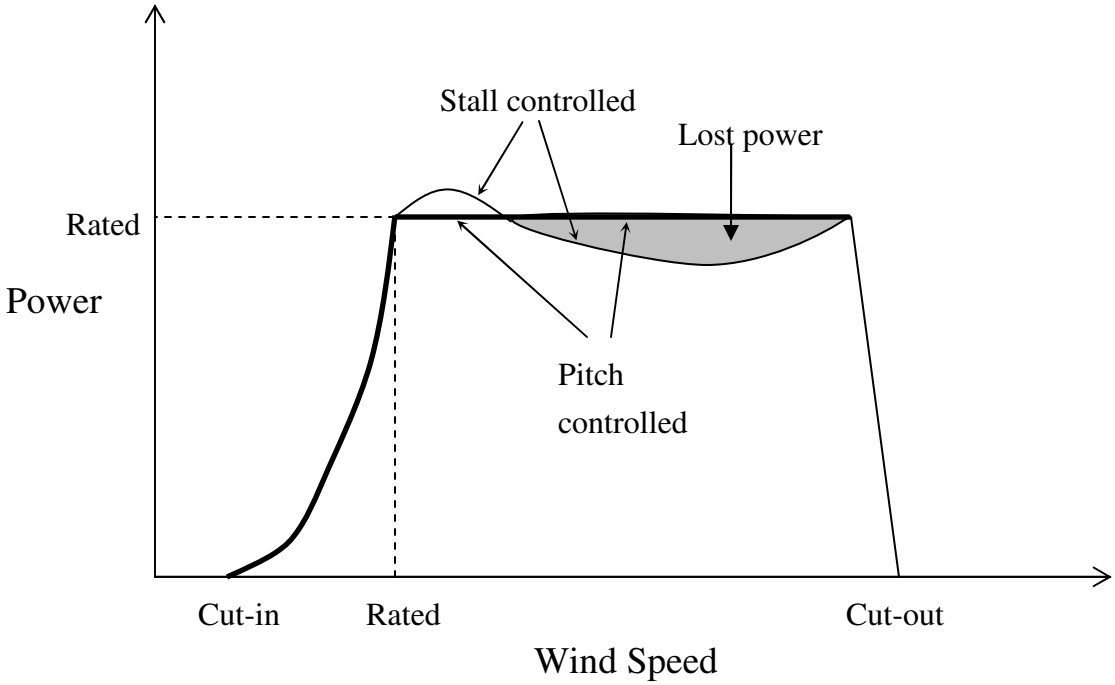


**Figure 4-7 Power curve for pitch and stall controlled wind turbine**[43]

Once the cut-out speed is reached, several methods exist for stopping the rotation of the turbine rotor. One is the brakes seen in Figure 4-6 above. A second is centrifugal brakes that release once the blades are rotating above a certain rotational speed. These centrifugal brakes are reset either manually or automatically. Pitch controlled turbines can simply pitch blades enough to stop rotation.

### *Demonstration*

For the demonstration of wind turbine technology a small-scale horizontal axis turbine attached to an electric generator mounted on a stand was chosen. The turbine generator is shown below in Figure 4-8.

[43] Adapted from *Wind Energy Training Course*, De Montfort University. Module 3, Section 2: Aerodynamics and Power Control. <http://www.iesd.dmu.ac.uk/wind_energy/m32extex.html> Last accessed August 8, 2007.

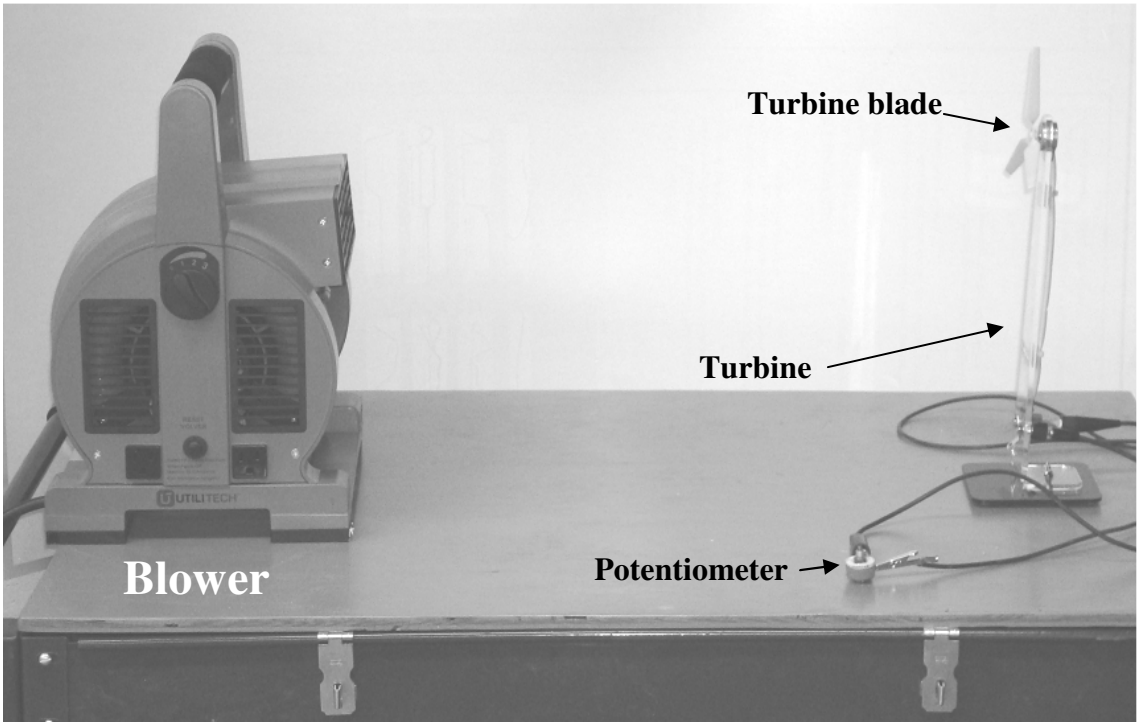


**Figure 4-8 The turbine demonstration set-up**

To give greater understanding of wind turbine technology and for more opportunity for engineering analysis, two different turbine rotors will be used. One is a truncated version of the other down to one-half the swept area. They therefore have the same shape and pitch but different blade lengths. They mount onto the generator via friction for easy switching of rotors.

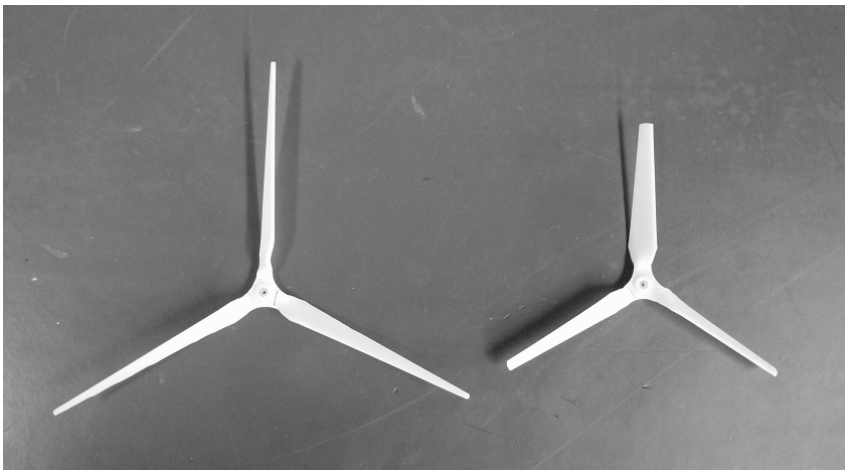

**Figure 4-9 Turbine rotors.**

To generate high velocity wind an electric blower will be used as can be seen above in Figure 4-8. A three-speed control is integrated with the blower and additional velocity control is possible through changing the distance from the turbine to the blower and by partially blocking the blower's intake opening.

In the theory section above efficiency was determined by dividing power extracted by power in the air. In practice, however, the concern is not as much with the power extracted from the wind, but with the power output as electricity which includes the additional conversion from mechanical power to electricity. Therefore an additional efficiency besides the turbine efficiency considered in the theory section above can be identified. This additional efficiency is that of the extracted power being converted into electricity. The first has to do with the turbine itself and the latter with the efficiency of the electric generator. When designing wind turbine systems each of these can be analyzed and optimized individually. In practice, though, it is useful to consider the overall efficiency of wind power-to-electricity since wind is the relevant input and electricity is the relevant product. In the demonstration set-up for wind energy included in the lab, the generator's efficiency is not known and given the instrumentation available, neither it nor the efficiency of the turbine by itself can be determined, so the overall efficiency will be the focus. This efficiency in equation form is as follows.

$$\eta_{overall} = \frac{P_{out}}{P_{air}}$$

**Eq. 4-10**

From the wind speed and the electrical output, $P_{out}$, this overall efficiency can be determined. Wind speed, V, can be found using an anemometer held in the turbine position though with the turbine temporarily removed to prevent the turbine's disturbance to the free stream velocity. It should be averaged over area covered by the rotating blades to make sure the velocity distribution is constant. If it is not constant, the blower may need to be moved farther away to flatten out the velocity distribution. Like with the fuel cell the electrical power output can be connected to some resistive load with the resulting voltage, $V_{elec}$, measured using a digital voltmeter. The resistance of the resistive load, R, will be provided by a rheostat which allows for adjustable resistance. The resistance can be measured with an ohmmeter and can be used along with voltage in the following equation to determine electric power output.

$$P_{out} = \frac{V_{elec}^{\ 2}}{R}$$

**Eq. 4-11**

The power in the air can be found with the equation developed and the variables defined above in Eq. 4-7 in the theory section. This equation is repeated below.

$$P_{air} = \frac{1}{2}\rho A V^3$$

**Eq. 4-12**

Power and efficiency measurements can be taken with different load resistances at the same wind speed to optimize the load resistance value for maximizing power at a certain wind speed. From this data power as a function of resistance in the form of $P_{out} = f(R)$ can be developed along with an efficiency as a function of resistance $\eta_{overall} = f(R)$. This efficiency curve as a function of load resistance can be developed by substituting Eq. 4-11 and Eq. 4-12 into efficiency equation Eq. 4-10.

$$\eta_{overall}(R) = \frac{2V_{elec}^{\ 2}}{R\rho A V^3}$$

**Eq. 4-13**

Another independent variable besides load resistance is wind speed. By taking measurements over increasing wind speeds, a power curve of the form $P_{out} = f(V)$ can be plotted. From the power curve an efficiency curve as a function of velocity with the same form as Eq. 4-13 can be also be found. These four curves of power and efficiency versus both load resistance and wind velocity can be determined for each of the two blades for comparison and analysis.

## Reasonableness of Demonstration Developed

There are no significant features or components of wind turbine technology left out of the demonstration chosen. The divergence from full-scale wind turbines is in the turbine and generator sophistication because of the necessity to keep the demonstration significantly scaled down for practical purposes. Sophisticated mechanisms for both turbine control and electrical output conditioning that are integral to full-size turbines as discussed above are not included. In particular gear-box is not included because of the significant friction involved in

its rotation, which probably would be too much for the small turbine rotors to overcome. Neither is pitch control included because of its sophistication and impracticality in a turbine of this size. Stall control is the control mechanism in place, though this is not finely-tuned, but rather is simply the unintentional by-product of the turbine blade shape and size. Despite the absence of these features, the main aspects of wind turbine operation and performance in the conversion of energy from wind to electricity are displayed in this demonstration and aid in student understanding of this alternative energy technology.

## *Experiments*

Three speeds were chosen for the varying load resistance experiment. These speeds were 3.9. 6.1, and 8.1 m/s. The resistance was varied between about 4 ohms and about 15 ohms for each speed for each blade. Voltage was measured for each combination of velocity and resistance for both the long blade and the short blade. From this, power was calculated according to Eq. 4-11. These results are presented in Figure 4-10 below.

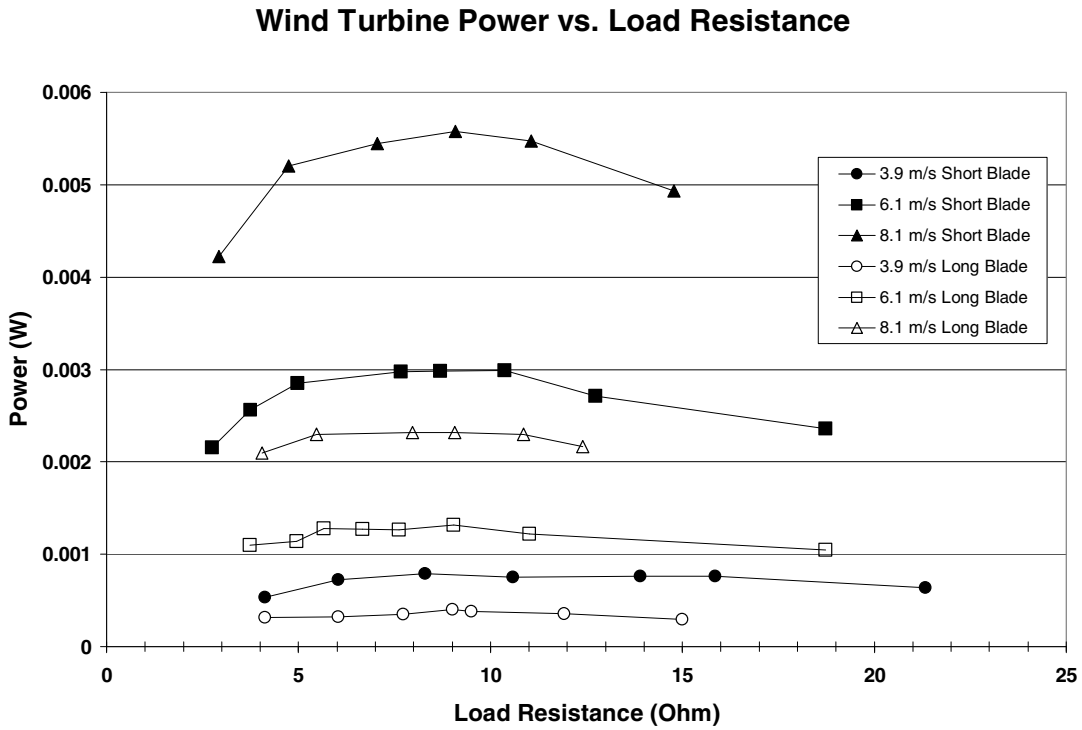


**Figure 4-10 Wind turbine power output as a function of load resistance.**

The general trends with each blade are to be expected. The higher the wind speed, the higher the power. The optimal resistance for power maximization appears to be about 9 ohms for both rotors and at all speeds. The power curves are also flatter for the long blade.

The very surprising result is that the short-bladed rotor has a higher power output than the long-bladed rotor. This is contrary to what would be predicted theoretically, which says that a rotor twice the area of another would have twice the power output. Clearly there is a flaw in the rotor design that results in increased drag with the additional blade length rather than additional area with which to capture wind energy. At the wind speeds used in this experiment, however, the extra blade length was a hindrance to effective wind power capture and conversion. Using Eq. 4-13 the efficiency of the turbine can be calculated under the same conditions as shown in Figure 4-10. These are shown below in Figure 4-11.

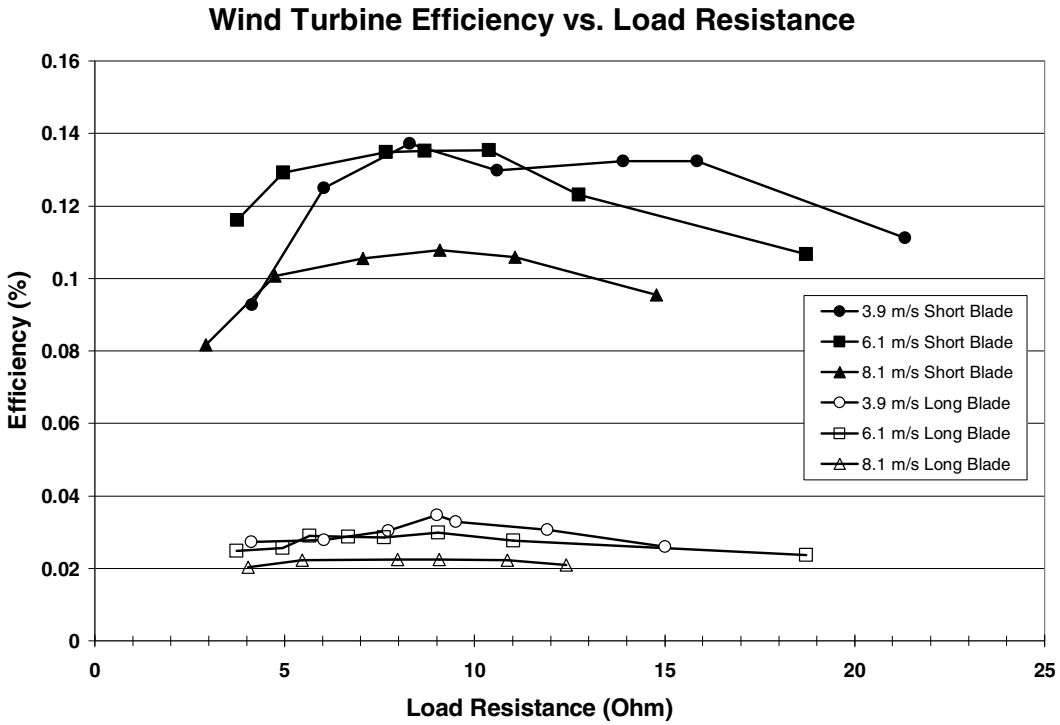


**Figure 4-11 Wind turbine efficiency as a function of load resistance.**

The maximum efficiencies are with a load resistance of around 9 ohms just as it was for maximum power, which is to be expected. What is unexpected, however, is the extremely low efficiency. The efficiencies are well below 1% which is very well below both the theoretical maximum of 53.9% and the real efficiencies of exiting commercial turbines of around 20%. There are numerous possible explanations for this extremely poor performance. The rotor is mounted close to the clear plastic "tower" as shown in Figure 4-8. The tower is fairly wide and likely causes significant disruption in the airstream thus preventing effective capture of the wind energy. Another possible cause of inefficiency is that the pitch of the rotor blades is constant along their length. This is in contrast to commercial turbines whose

rotor blades have varying pitch along the blade length. This varying pitch is designed to account for the difference in blade velocity relative to the air as a function of distance along the blade from the axis of rotation to the blade tip. The demonstration rotor lacks this feature and as a result may have the blade tips actually outputting energy to the air rather than receiving it. This factor may be the explanation of the especially low efficiency of the long-bladed rotor as well as its power output being lower than the short-bladed rotor as was seen in Figure 4-10. A third possible cause of inefficiency is that the rotor blades do not have an airfoil shape. They are of constant thickness with fairly blunt edges. This probably causes turbulence and increases drag which dissipates energy in the wind rather than harnessing it. A fourth possible cause of inefficiency is an improperly sized electric generator. There may be more torque available than the electric generator can effectively use in the production of electric energy. Finally, the small size of this demonstration makes it especially prone to deviate significantly from idealizations which depend on the assumption of 1-D and idealized behavior. With such short blades and small areas, this assumption becomes more and more unreasonable. Motor friction and other inefficiencies become proportionally larger as the turbine becomes smaller. In other words, the economies of scale are lost. Due to all these factors and possible others, the extremely low efficiency is understandable.

An analysis of wind turbine performance as a function of wind speed can shed further light on the wind turbine performance. Wind turbine power output as a function of wind speed is shown below in Figure 4-12.

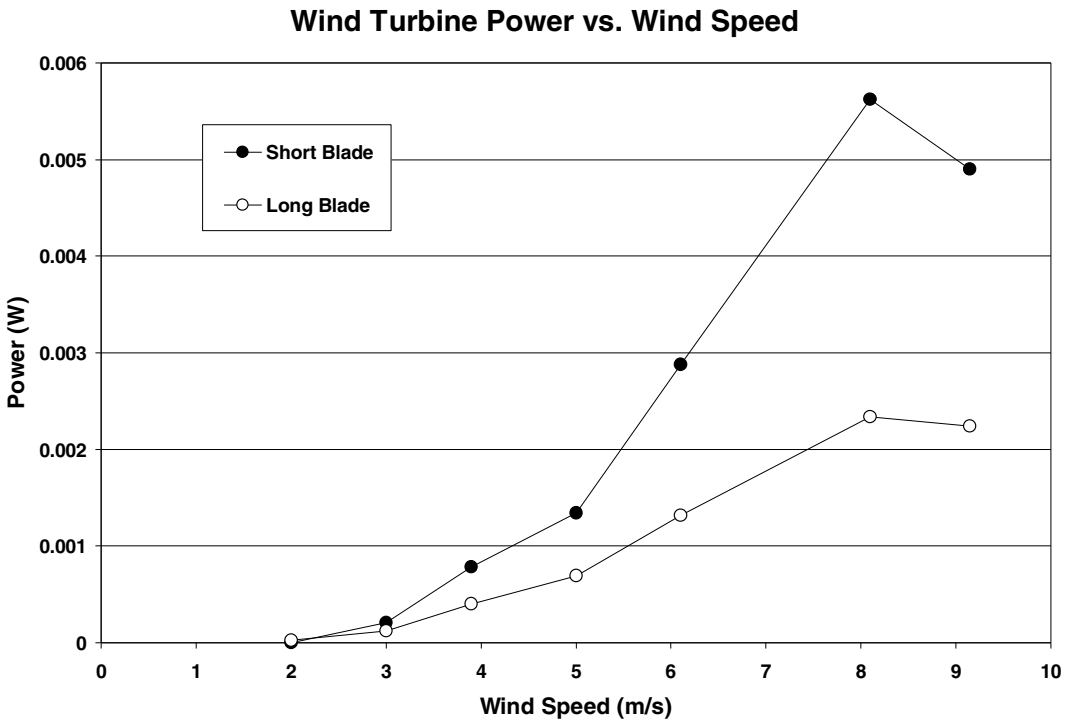


**Figure 4-12 Wind turbine power output as a function of wind speed.**

The shape of these curves is expected and is similar to that shown in Figure 4-7. Wind speeds higher than about 9 m/s were unable to be attained with the equipment used but the power output levels off around 8 m/s. This leveling off would likely continue and would present an example of stall control as explained above. The increasing slope is caused by the velocity-cubed term in the air power equation and matches theoretical predictions. The cut in speed for both rotor blades was about 1.9 m/s. This was unexpected since the larger rotor should be able to move the system at lower speeds than the smaller rotor can since the larger rotor theoretically can harness more energy from the air. This inability of the larger rotor to out-perform the smaller rotor can be explained by the reasons stated above for poor turbine performance, particularly poor blade design.

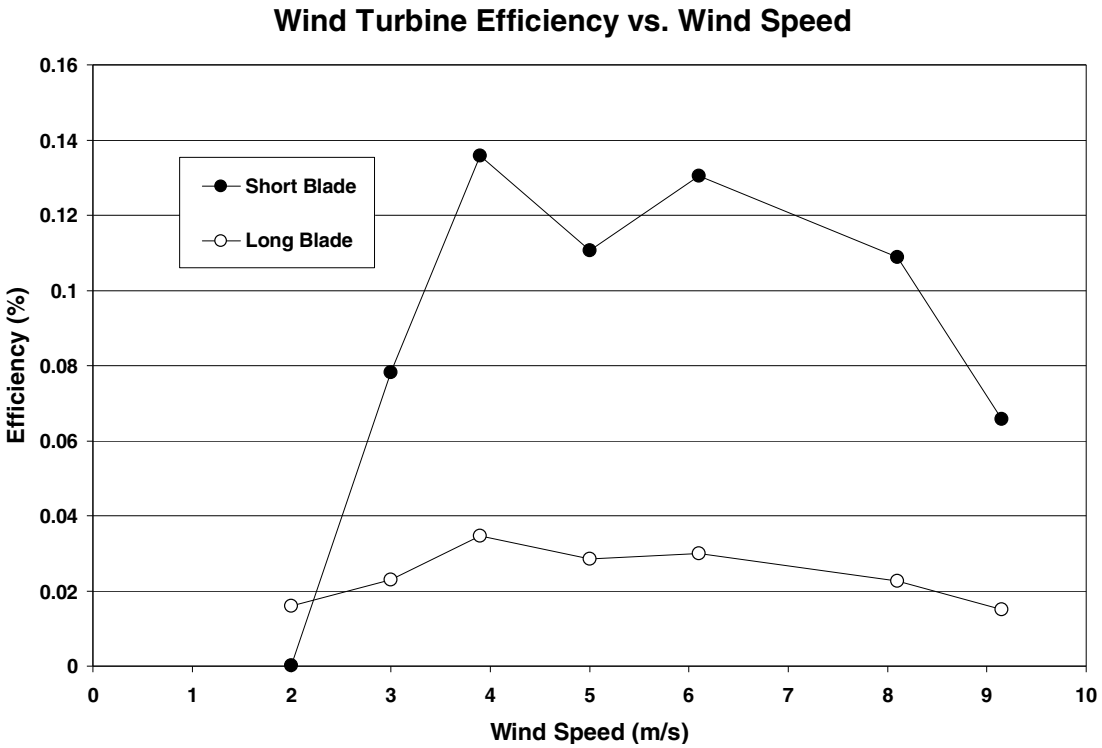


**Figure 4-13 Wind turbine efficiency as a function of wind speed.**

Wind turbine efficiency as a function of wind speed is shown in Figure 4-13 above. This data is consistent with the results that have already been reported. The fact that the efficiency starts to decrease around 5 m/s shows that stall or excess turbulence is starting to take place. Properly designed rotor blades would be designed to have as high efficiency as possible all the way to the rated wind speed, and then start to stall at the rated wind speed. This maximizes power extracted from the wind over all wind speeds. It appears from Figure 4-13, however, that the onset or increase of stall is a gradual transition starting at fairly low wind speeds. This isn't surprising given the unsophisticated design of the demonstration rotors.

## Accuracy of Demonstration

The two turbine combinations considered individually follow theoretical predictions and expectations very well. The efficiencies, while very low, are understandable given the scale. The power curves are very close to the expected shapes and show how power content of wind varies with speed. The power drop-off at the end also illustrates the effect that stall control makes use of and confirms the counter-intuitive fact that power can lessen in higher wind speeds. However, despite these positive aspects of the demonstration, some possible

deficiencies do exist in the unexpected results from this demonstration in the comparative results between the two turbine rotors not confirming or following theoretical predictions. This can be considered a flaw but it can also be considered an asset in that the results do illustrate important considerations in wind turbine operation and design, especially rotor design. The importance of good rotor blade design to make best use of wind energy is seen very clearly and a greater appreciation the aerodynamics of wind turbines can be gleaned. Additionally, the unpredicted results provide an occasion for practicing engineering thought and problem solving. So despite the seeming inaccuracy of the demonstrations performance relative to theoretical predictions, a basic understanding of wind turbine technology operation and performance as well as other valuable insights about the importance of proper wind turbine design, is gained through experimentation with the wind turbine demonstrations used in the laboratory facility.

# Chapter 5 PHOTOVOLTAIC

## *Background*

Like wind turbines, photovoltaic (PV) technology is a source of useful energy. PV technology converts radiative energy into electrical energy. Used in sun light, PV technology converts solar power into electricity as do wind turbines but in a much more direct way.

PV technology has its practical form in a thin panel that is composed of multiple cells connected either in series or in parallel depending on the desired characteristics of the electricity to be supplied. This technology was first developed in the 1950s and had a major application in providing space crafts with electricity[44]. They were especially suited to this application because of their light weight relative to the amount of energy they provided over their desired lifetimes. No weight-adding fuel storage was necessary since solar radiation could reach the space craft almost wherever it was, and then would be converted to electricity by PV technology. A great deal of research and development has gone into photovoltaic panels to make them cheaper, more efficient, and more versatile since their first use and they can now be found all over the world. Few commercial PV power plants exist because of the high cost, but an increasing number of private residences and businesses are making use of significant amounts of PV technology to supplement or replace conventional electricity sources. PV technology also has a niche in remote and off-grid locations and can be seen on many interstate emergency phone stations, for example, and for use charging cell phones and powering other small appliances in the third world. Because it is solid state, PV technology is known for being durable and maintenance-free. This makes it especially suitable in remote, off-grid, and low-technology areas.

PV technology is priced on a per peak Watt basis ($/Wp). That is, dollars per amount of PV panel that will produce one watt of power at maximum sun. This is a more useful measure than dollars per area of panel because of the different efficiencies of different kinds of PV technologies available. Electrical output, rather than area, is the product of interest and so is the basis of the PV technology pricing. Several different kinds of PV technology have been developed and each has different prices per peak Watt and different efficiencies. There is a trade-off between efficiency and area necessary for a certain power output. Depending on the application, a higher efficiency and therefore smaller area PV system may

[44] *Solar Timeline*. Solar Energy Technologies Program. Department of Energy. <http://www1.eere.energy.gov/solar/solar_timeline.html> Last accessed May 21, 2007.

be worth a higher ($/Wp) price, though when area is not a constraint a lower efficiency and larger area system may be suitable. The different kinds of PV technology also have different physical characteristics, such as being flexible or rigid, making them more or less suitable for some applications. Additional performance characteristics such as efficiency as a function of PV cell temperature or solar incident radiation level may be pertinent to a design making certain kinds of PV technology more or less appropriate for a particular application.

The two main kinds of PV technology are distinguished by the form of their silicon. One kind is called crystalline is so called because of the crystalline structure of its silicon, the second kind is called amorphous since its silicon does not have a crystalline structure. Crystalline silicon PV cells are typically more efficient but also of higher cost. Amorphous silicon PV cells are less efficient but of lower cost, and have the unique ability to be flexible which crystalline cells do not. Crystalline cells can be either single-crystal or semi-crystalline. Semi-crystalline cells, also called multi-crystalline, are composed of smaller crystals and are easier to make but have lower efficiency than single-crystal silicon cells. Amorphous cells are a more recent development and other, newer kinds of PV technology are under development with the hope of even higher efficiencies and lower costs. These newer technologies fall under the categories of crystalline or amorphous but have additional distinguishing features. A brief history of the efficiency of various PV technologies over time is shown in Figure 5-1 below.

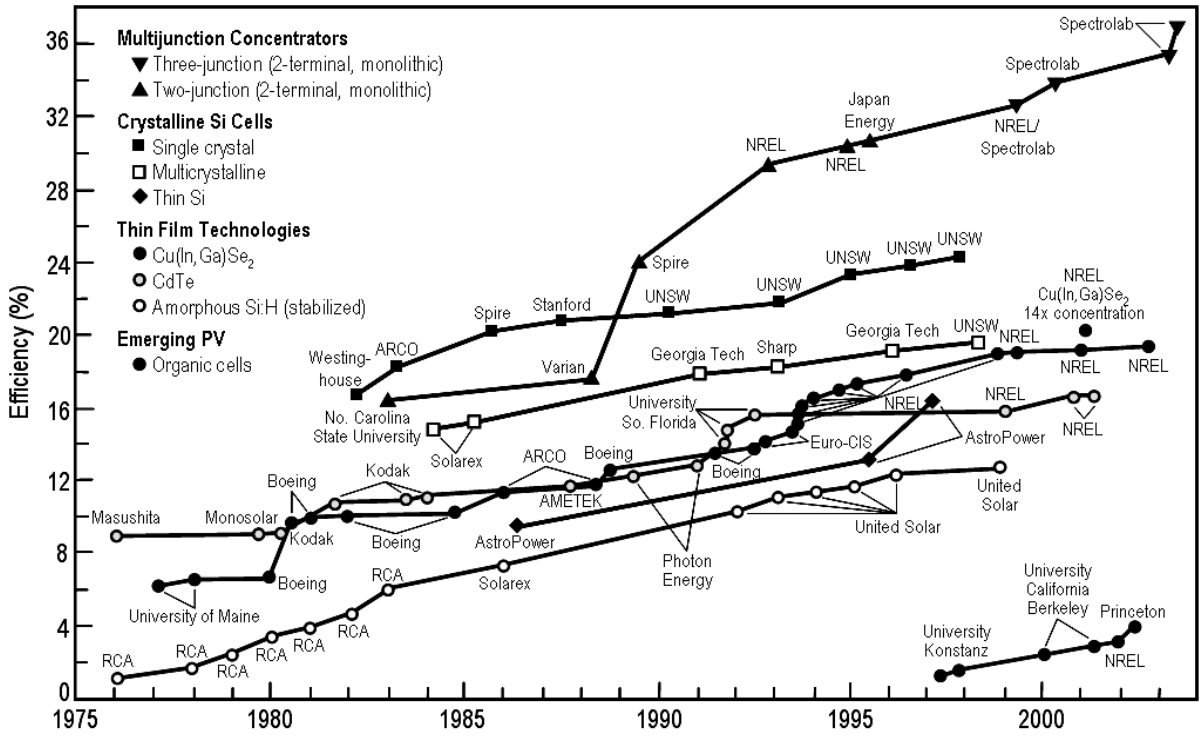


**Figure 5-1 History of efficiencies achieved with various PV technologies.**[45]

## *Theory*

### Energy conversion

Conventional silicon PV technology will be used in the demonstration so the theory behind its operation will be covered here. The basic components making up a PV cell are two layers of silicon doped with two different elements. Doping involves the addition of a slight amount of a foreign substance to an otherwise pure substance to change that substance's properties. One layer is doped with a very small amount of an element that has one more electron than silicon. This silicon is then called n-silicon since it has a negative charge. The second layer of silicon is doped with a small amount of an element with one less electron than silicon. This layer is called p-silicon. Because of the different charges of the two layers, an electric potential exists between the two. When incident radiation, or irradiation, of a proper energy level strikes the silicon, an electron may gain the correct amount of energy to be freed from its atomic bonds in the silicon material. Depending on the materials used and the kind of PV cell, thin conductive contacts may be positioned across the

[45] L. Kazmerski, K. Zweibel. *Best Research Cell Efficiencies*. National Renewable Energy Laboratory, June 2005. <http://www.nrel.gov/pv/thin_film/pn_general_interest.html> Last accessed May 25, 2007.

top layer of the cell to provide electrical contact between the external circuit and the panel. Once the two silicon layers are connected in a complete circuit, the freed electrons can flow through the circuit and produce an electric current capable of work. This is shown in Figure 5-2 below.

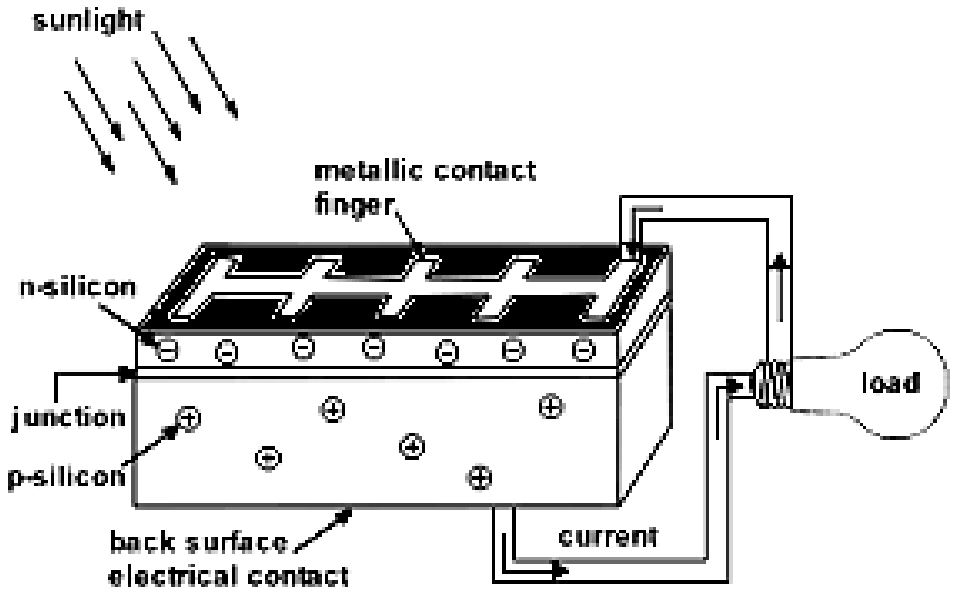


**Figure 5-2 Cross-section of a PV cell showing silicon layers and electric circuit.**[46]

Individual PV cells have a certain voltage that their current travels across determined by the doping material, or dopant, used and other chemical characteristics. These cells can be connected in series or parallel to increase voltage or current, respectively. A group of connected cells compose a PV panel, and many panels are combined to form an array.

Since only some of the irradiation striking a PV panel is at the correct energy level to free an electron, some of the irradiation goes unused. This effect is quantified by the efficiency. The efficiency of the panel is the ratio of the electric power output to irradiative power input. Electric power output can be easily calculated by measuring voltage, V, across a known resistance with a voltmeter. The load resistance, R, for maximum power can be experimentally determined by varying the load resistance until maximum power is achieved. The electric power out, $P_{elec}$, can be calculated as follows.

[46] Sundance Technology. <https://www.sundancepowerinc.com/images/cross-section.bmp> Last accessed August 8, 2007.

$$P_{elec} = \frac{V^2}{R}$$

**Eq. 5-1**

The irradiative power input is the product of the irradiation, $I$, and the projected area, A. Projected area will be discussed below. The irradiation, $I$, can be measured with a radiometer. Efficiency is the ratio of electric power output to radiative power input and can be formulated as follows.

$$\eta = \frac{V^2}{R \times I \times A}$$

**Eq. 5-2**

## Storage and Sizing

Depending on the usual period of the radiation source, the size of the panel needs to be large enough to collect enough energy during one period to supply the application with its needed power throughout a full period. The period typically is 24 hours, and the time span in which energy can be collected is around 12 hours, though it can vary greatly depending on the season and latitude on the Earth. The energy collected during that 12 hours needs to supply the application's power for 24 hours, so array design needs to take this into account. Once the array is sized such that it will collect all the energy needed over a particular length of time, energy storage needs to be designed to store energy until it is needed. Solar irradiation is intermittent, so energy storage can be used to decouple irradiation (input) from the power supply (output) so as to be capable of providing a constant energy supply if required by an application. Since the energy output from a PV system is already in electrical form electric battery energy storage is typically used, though for large-scale PV panel systems hydrogen storage may be feasible. Computerized control systems can be used to protect batteries from overcharging and other harmful conditions that will shorten their life. The sizing of the storage depends on the longest possible time without recharge, and the maximum power necessary to be supplied to the load.

## Positioning and Total Electrical Production

While two-axis solar tracking will increase a PV panel's electrical output, many PV applications are small enough that this isn't economically feasible. The total amount of electrical energy produced in a day will be a function of weather, location on the earth, day of the year, efficiency, irradiation, etc. While some of these variables are dependent on geography and the particular PV technology used, some generalizations can be made. Assuming a clear day, the intensity of the solar irradiation reaching a PV panel is firstly a function of the orientation of the panel relative to the sun. 90% of the solar radiation received on the Earth's surface on a clear day is directly from the sun, with the remainder being diffuse irradiation reflected from the sun by the rest of the sky[47]. The direct irradiation is most of interest because it carries much more energy than diffuse irradiation. This is characterized by what is sometimes called the cosine effect and can be seen in Figure 5-3. The cosine effect adjusts the actual area of a PV panel by the cosine of the angle between the normal of that panel and the direction to the sun. This results in a value for the projected area, which is the area of the panel perpendicular to the direction of radiation. This adjustment factor will range from 1, where the panel is perpendicular to and facing the sun, to 0, when the panel is completely sideways and receives no radiation.

[47] Incropera, DeWitt: *Fundamentals of Heat and Mass Transfer*. Wiley, Fifth Edition. p. 749.

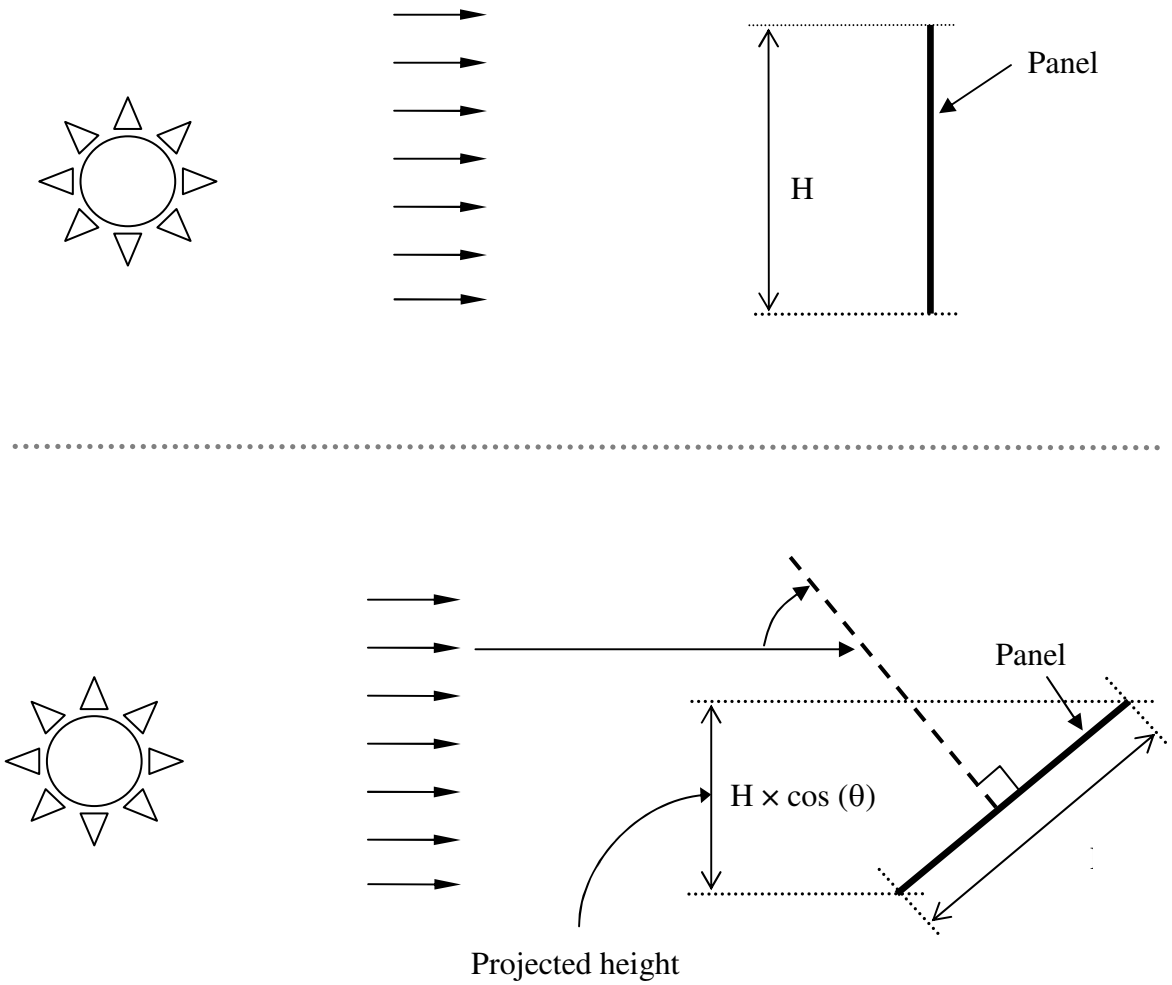


**Figure 5-3 Illustration of projected area.**

With a non-tracking panel, the sun's movement across the sky will result in a θ from Figure 5-3 above that is a function of time. This θ=f(t) can be made explicit if certain factors are known. The panel's latitude and orientation with respect to the rotational axis of the Earth along with the day of the year specify this function of time for a particular day and panel.

Time of day also has an effect because of the amount of air solar radiation must pass through to reach a panel. Air both absorbs and disperses radiation from the sun in accordance with its mass, so the additional length of travel through the atmosphere means more mass to pass through and therefore a decreased intensity of radiation reaching the surface[48]. Air mass 1.0 is defined as the mass of air radiation must travel through to reach

[48] William B. Stine and Michael Geyer, *Power from the Sun,* 2001. Chapter 2. <http://www.powerfromthesun.net/book.htm> Last accessed August 8, 2007.

the ground at sea level if the sun is directly overhead. The air mass value can be adjusted in proportion to the additional length of atmosphere through which radiation must travel if the sun is not directly overhead. At sunrise and sunset the air mass value is around 38[49]. The length of travel and therefore the air mass value can be determined from the position of the sun in the sky. Figure 5-4 below illustrates this concept.

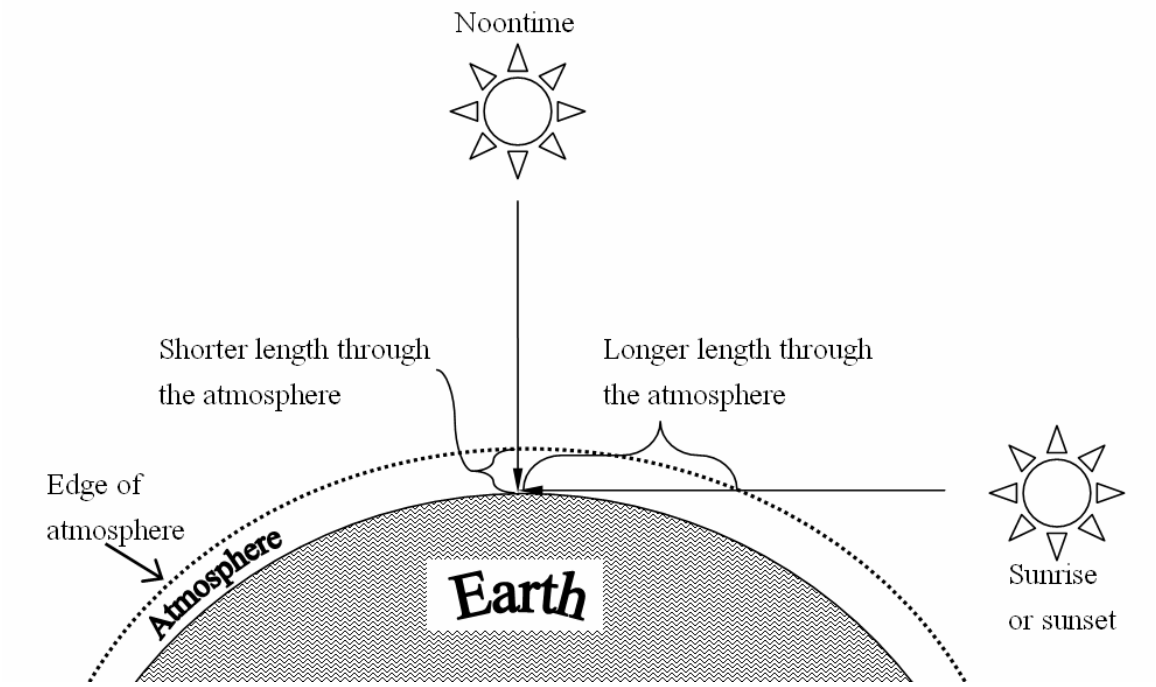


**Figure 5-4 Air mass illustration. The longer distance radiation travels through the atmosphere, the more it is attenuated.**

The concept of air mass can aid in more accurately determining the intensity of solar irradiation at the surface of the Earth, but there are other variables that also affect radiation intensity that are more dependent on local conditions. The amount of water vapor in the air depending on the time of year, various weather conditions or wind patterns that bring more or less dust particles into the atmosphere and pollution can all cause significant deviation in the effective air mass for a particular place. Using very clear, sea level air the air mass values result in the corresponding irradiation levels as shown in Table 5-1.

[49] William B. Stine and Michael Geyer, *Power from the Sun,* 2001. Chapter 2. <http://www.powerfromthesun.net/book.htm> Last accessed August 8, 2007.

**Table 5-1 Irradiation as a function of air mass.[50]**

| Air mass | Irradiation ($W/m^2$) |
|---|---|
| 0 | 1353 |
| 1 | 956.2 |
| 4 | 595.2 |
| 7 | 413.6 |
| 10 | 302.5 |

The cosine effect and the air mass effect are the most predictable factors that affect radiation intensity at ground level. With the explicit $\theta=f(t)$ equation discussed above along with an equation for air mass=$f(\theta)$, the total radiative energy striking a surface can be found by integration over some period of time. However, weather and other factors particular to geography are very significant consequently in real-world design sizing must make use of historical data. Solar irradiation charts and tables are available with data presented usually in average monthly or annual energy per unit area. The unit area for which solar irradiation is reported is usually either horizontal area or area tilted to the angle of the latitude of the location. This data aids in sizing by providing an expected amount of energy per unit area so with a needed amount of electricity, the required area can be calculated accordingly. It is clear upon some reflection that if a non-tracking panel is used, the best orientation is to have the panel normal perpendicular to the surface of the Earth relative to West and East directions, and perpendicular to the axis of rotation of the Earth relative to North and South directions. This orientation maximizes the projected area when the air mass is least on a daily basis. It also maximizes projected area annually by being midway between the summer and winter position of the sun. Certain design criteria, however, may make a different orientation more desirable even though it will collect less energy annually. A panel oriented exactly at the sun in the winter will (thus the panel normal is not perpendicular to the Earth's rotational axis) collect less energy annually since at that orientation the projected area in the summer will be much less than if the panel was perpendicular to the rotational axis of the Earth, resulting in a lower average annual projected area. This may still be the best orientation for a particular application if it happens that in the summer less power is required. Another deviation from the general rule of a panel being oriented perpendicular to the

[50] William B. Stine and Michael Geyer, *Power from the Sun,* 2001. Chapter 2. <http://www.powerfromthesun.net/book.htm> Last accessed August 8, 2007.

rotational axis of the Earth is if some location has a lot of cloud cover during certain times of the year. It is not beneficial to be oriented as close to the sun as possible if there is cloud cover, so orientation closer to the sun for one season over another may result in maximum annual collected energy. Overall, however, orientation perpendicular to the Earth's rotational axis is best unless overriding design or weather factors are present.

### *Demonstration*

Both semi-crystalline and amorphous thin-film silicon cells will be used for the demonstration. The load resistance will be provided by a number of potentiometers. The semi-crystalline panel is integrated with an aluminum frame to which the stands will be attached. The thin-film panel is flexible and will use the semi-crystalline panel for a frame and for positioning. The thin-film panel is affixed to the semi-crystalline panel by elastic bands. The thin-film panel attached to the semi-crystalline panel is shown in Figure 5-5 below.


**Figure 5-5 Thin-film solar panel attached to the semi-crystalline frame as used in the demonstration.**

Because of the requirement for indoor operation of the laboratory demonstration, an alternative radiation source to the sun will be necessary for the PV technology demonstration.

This alternative radiation source will be a bank of six 250 watt halogen lights giving a total of 1500 watts. Figure 5-6 below shows the light bank. Not all of this energy is converted into radiative energy and not all the radiative energy reaches the panel, so the radiative power level will have to be measured experimentally and an average level for the entire area of the panel will have to be determined. A radiometer will be used for this measurement.

**Figure 5-6 Bank of halogen lights used for the demonstration.**

The PV panels are mounted in a stand that provides an axis of rotation around which the panel can rotate and be fixed at any orientation. The angle between the normal of the panel and the direction of radiation from the light bank can be set as desired for experimentation. This feature means that the panel output and efficiency at various angles and radiation intensities can be measured. A picture and diagram of this is shown in Figure 5-7 below.

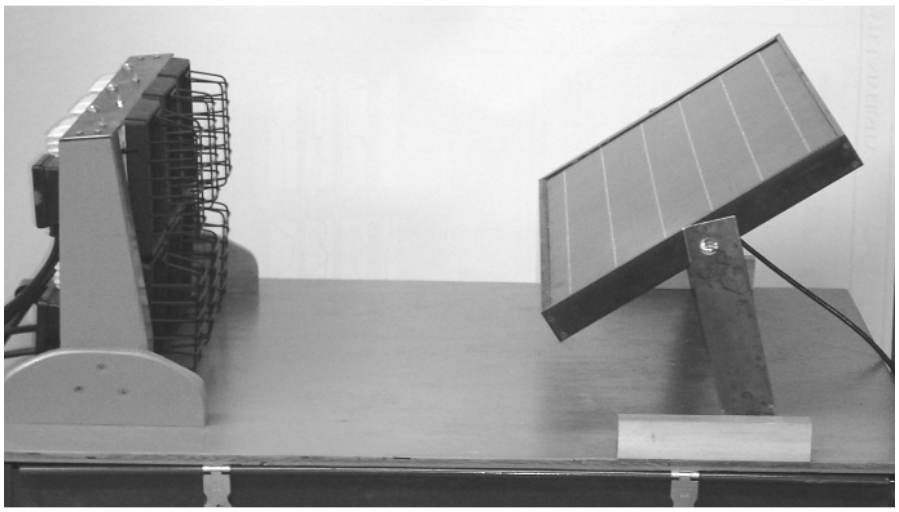

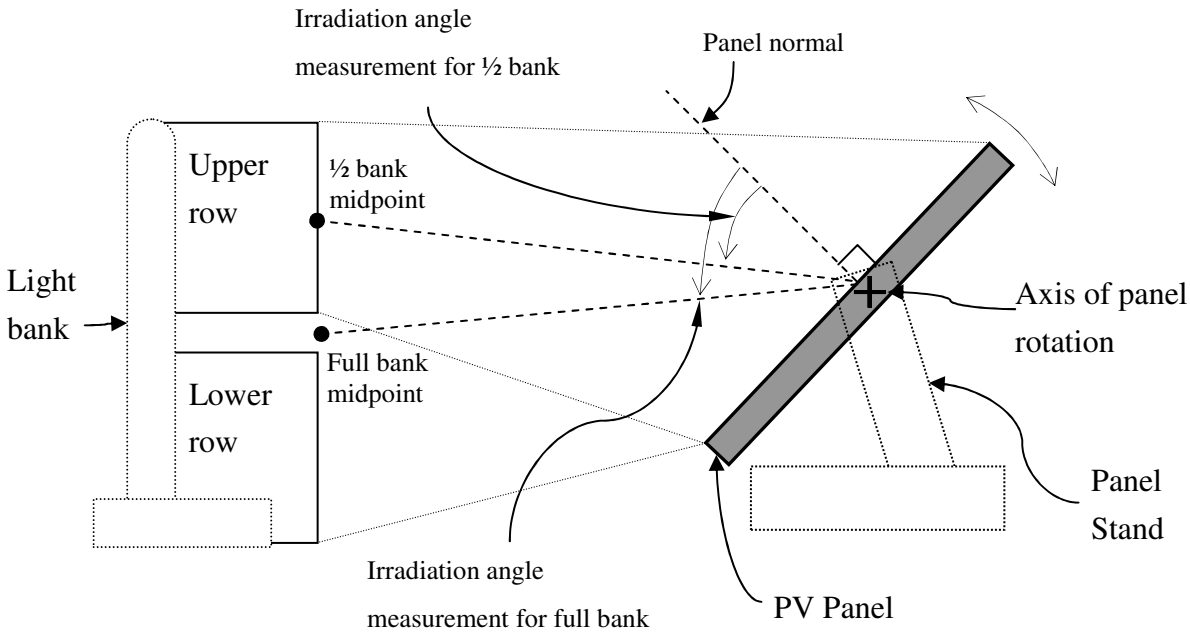


**Figure 5-7 Panel stand showing orientation of panel relative to light bank and the irradiation angle measurement method.**

Because six lights are necessary to provide a relatively intense irradiation level, the resemblance to a point source is not nearly as close as it is with radiation from the sun. The angle between lines from Earth to points on either side of a diameter of the sun is around only 0.5º. Since the majority of solar irradiation comes from this narrow angle, the sun can reasonably be approximated as a point source. Therefore, the direction of all solar irradiation

is parallel and the angle between a solar panel and all irradiation striking it is uniform, neglecting diffuse radiation from the sky. This radiative direction uniformity cannot be achieved with the light bank because of its size and proximity to the panel. There is not another light source option that satisfies the constraints of mobility and classroom use. Therefore, the angle between the normal of the panel and the midpoint of the radiation source height will be used for experimentation as Figure 5-7 shows. The midpoint of the radiation source height will be different depending on the experiment being performed. For the low irradiation intensity experiment, only three of the six halogen lights will be turned on and these three will be the lights on the upper row of the light bank. The midpoint of the radiation source height from which the irradiation angle is measured for this ½ bank situation as well as that for the full bank of six lights is specified Figure 5-7.

The efficiency equation Eq. 5-2 includes a projected area that can be distinguished into the actual panel area, $A_{act}$, and the irradiation angle, $\theta$, as follows.

$$\eta = \frac{V^2}{R \times I \times A_{act} \times \cos(\theta)}$$

**Eq. 5-3**

To investigate PV panel performance, both electric power output and efficiency can be found as functions of irradiation angle, $\theta$, by changing the panel orientation and irradiation intensity by changing the amount of the light bank under power. From this kind of knowledge, total PV electric output over time can be determined by integration and various PV panels can be compared.

## Reasonableness of Demonstration Developed

This demonstration captures the important PV technologies of semi-crystalline and amorphous silicon thin-film. Some factors relevant to PV performance are not included due to necessary simplifications required because of the laboratory facility constraints. One of these neglected factors is the measurement of performance in response to diffuse irradiation. Under real world conditions, periods of diffuse-only irradiation may exist and the differing efficiencies under these conditions would be of use in determining the optimal kind of panel for a particular application[51]. Though there is no feasible way to create a controlled diffuse

[51] M. van Cleef et al., *Superior Energy Yields of UNI-SOLAR® Triple Junction Thin Film Silicon Solar Cells compared to Crystalline Silicon Solar Cells under Real Outdoor Conditions in Western Europe*. Proc. 17th EU PV Solar Energy Conf., Munich, 2001.

radiation source for this laboratory facility resulting in this aspect of PV performance being left out, the more important principles of PV technology's performance in response to beam irradiation will be seen and the significance of the cosine effect will be able to be investigated.

A second limitation of this demonstration is the use of halogen lights instead of sunlight. However, even though the spectrum of the halogen lights will not be identical to the sun, the principles involved will all still have effect and will provide an occasion for investigation of PV technology. As was discussed in the theory section above, only a certain range of radiation is at the correct energy level to be converted into electricity by a PV panel. The actual efficiency, however, is calculated based on the *total* amount of radiation reaching a panel including the fraction of radiation that cannot be converted. Since the spectrum of the sun and the spectrum of the halogen lights are different, the panel's efficiency under halogen light illumination will be different than the nominal efficiency reported above for each panel, since the nominal efficiency assumed the sun as the radiation source. This can be taken into account when considering experimental results and is not a serious problem for learning about PV technology.

A third limitation that was mentioned above is the fact that the light bank does not resemble a point source very accurately so the measurement of irradiation angle will of necessity be an approximation. The way the approximate angle will be measured is shown above in Figure 5-7. While not being overly precise, this measurement method will still enable student investigation and analysis of the cosine effect.

Even with the aforementioned limitations, an accurate understanding of and experience with PV technology will be gained by students through the use of this demonstration. The demonstration incorporates the main important features of PV technology. The various kinds of PV technology available with different advantages and disadvantages in terms of efficiency, low-level radiation response, physical characteristics, etc. are reflected in the two choices of panels for the demonstration. The rotational freedom of the panel stand allows for the important investigation of the effect of orientation on panel performance. The multi-level irradiation possible from the light source permits the effect of irradiation level to be analyzed. These features give students an opportunity to accomplish experiments and investigations of important features of PV technology.

## *Experiments*

Two of the major performance differences between these kinds of PV cells are power and efficiency at different irradiation angles and levels so the two panels' performance in each of these areas will be characterized and compared. Though cell performance is affected by temperature as well, this is less significant under normal conditions than irradiation level and irradiation angle. It would also be difficult at classroom scale to control panel temperature accurately. The radiometer was used and with it was found an average radiation flux at the distance of the panels of 360W/m$^2$ with a ½ bank of lights. The radiometer was out of range much above this flux level so the flux was assumed to be double with a full bank. The thin-film panel was exposed to ½ and full bank irradiation at 0º, 30º, and 60º as measured according to Figure 5-7 above. The results are presented graphically in Figure 5-8 below.

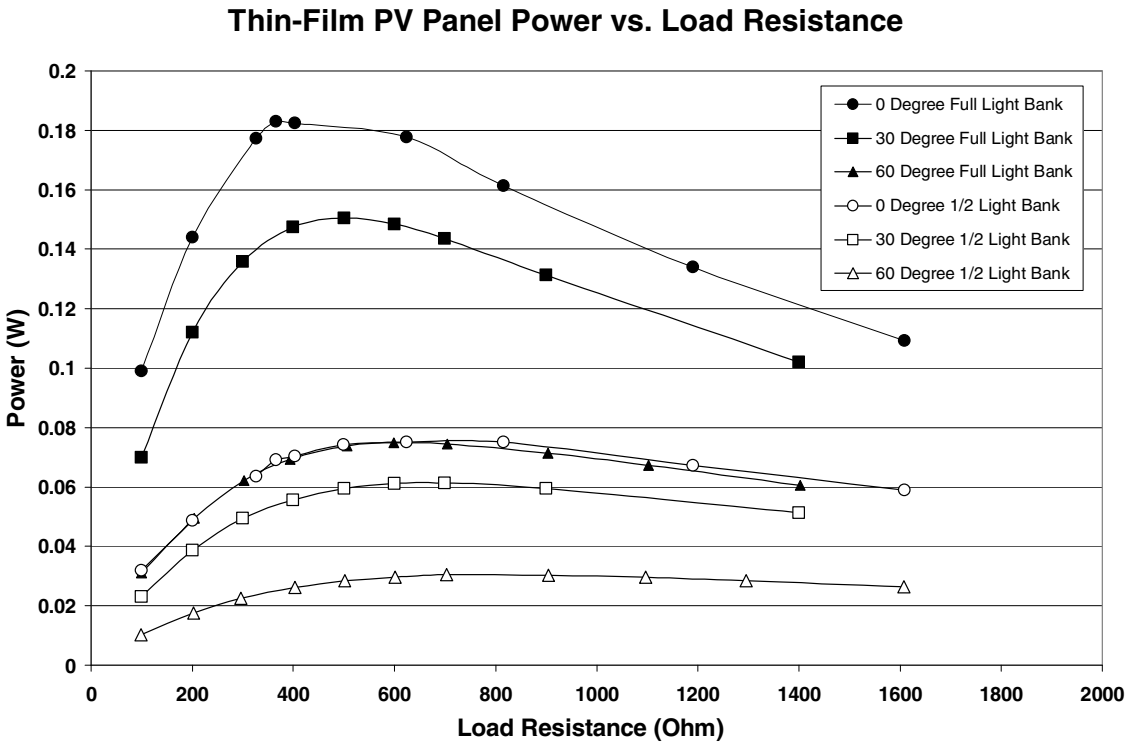


**Figure 5-8 Thin-film Panel Power vs. Load Resistance**

The trends shown in Figure 5-8 are very much as expected from theoretical predictions. Under full bank irradiation there was a higher power output for each orientation than at ½

bank illumination. The higher the difference between the panel normal and the direction of the irradiation, the lower the power—as is described by the cosine effect. The load resistance for maximum power follows a clear curve that would be important for a control system trying to maximize power for a battery, for instance. The near identical curve for the 60º orientation under full bank irradiation and the 0º orientation under ½ bank irradiation is very interesting and is predicted by theory. This is because the cosine of 60º is 0.5, so the overlapping curves are expected given that the full bank provides double the irradiation as the ½ bank and that the efficiency is not a function of irradiation angle. Thin-film PV panels, and especially the model used for the demonstration, are known for not decreasing in efficiency at irradiation angles, so this result makes sense. The ratio of maximum power at ½ bank irradiation to the maximum power at full bank irradiation, however, is not exactly ½ which leads to a consideration of efficiency, specifically as a function of irradiation level. Efficiency as a function of load resistance calculated using the data from Figure 5-8, irradiation levels known from radiometer measurements, and panel area is shown in Figure 5-9 below.

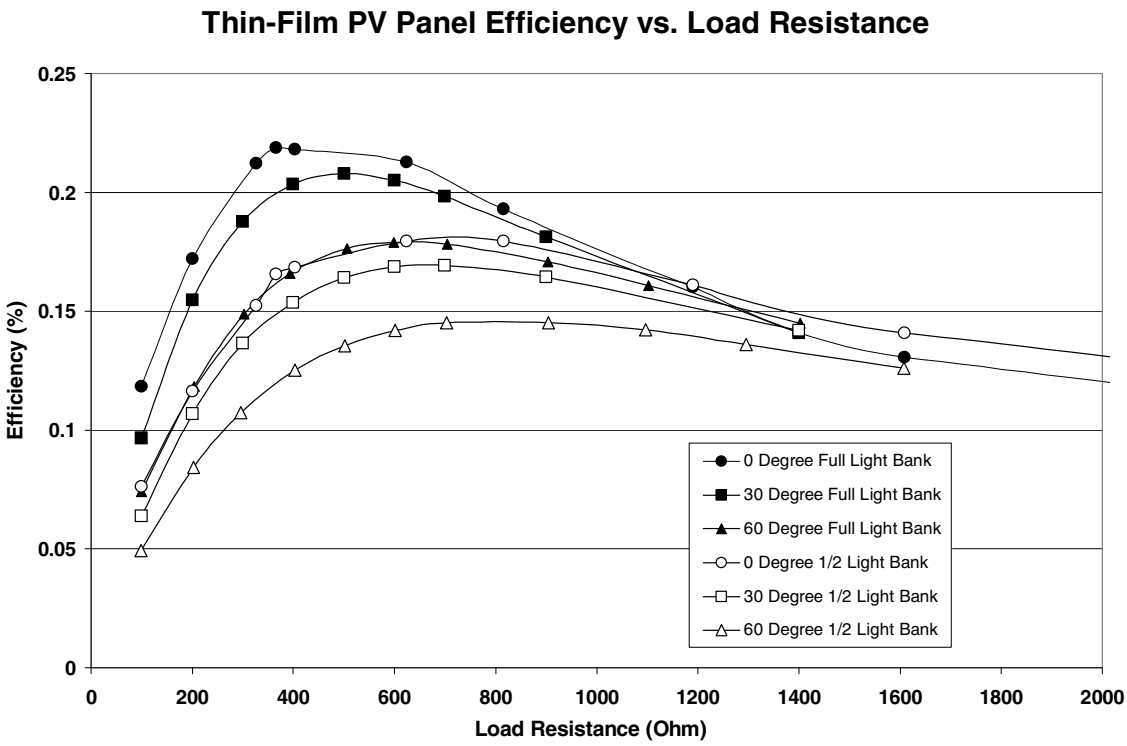


**Figure 5-9 Thin-film Panel Efficiency vs. Load Resistance**

From Figure 5-9 it can be seen that efficiencies vary widely with higher efficiencies are attained with higher irradiation levels. The angle of incidence of the irradiation is seen to have very little bearing on efficiency. This can be concluded because of the near identical efficiency of the full bank at 60º and the ½ bank at 0º. These have equal irradiative power per panel area despite the difference in irradiation angle. This is experimental evidence to support the claim that thin-film panels have little efficiency dependence on irradiation angle. This feature allows thin-film panels to work well in the morning and evening and even though they have lower efficiencies overall, can provide more energy under certain circumstances than other kinds of PV technologies.

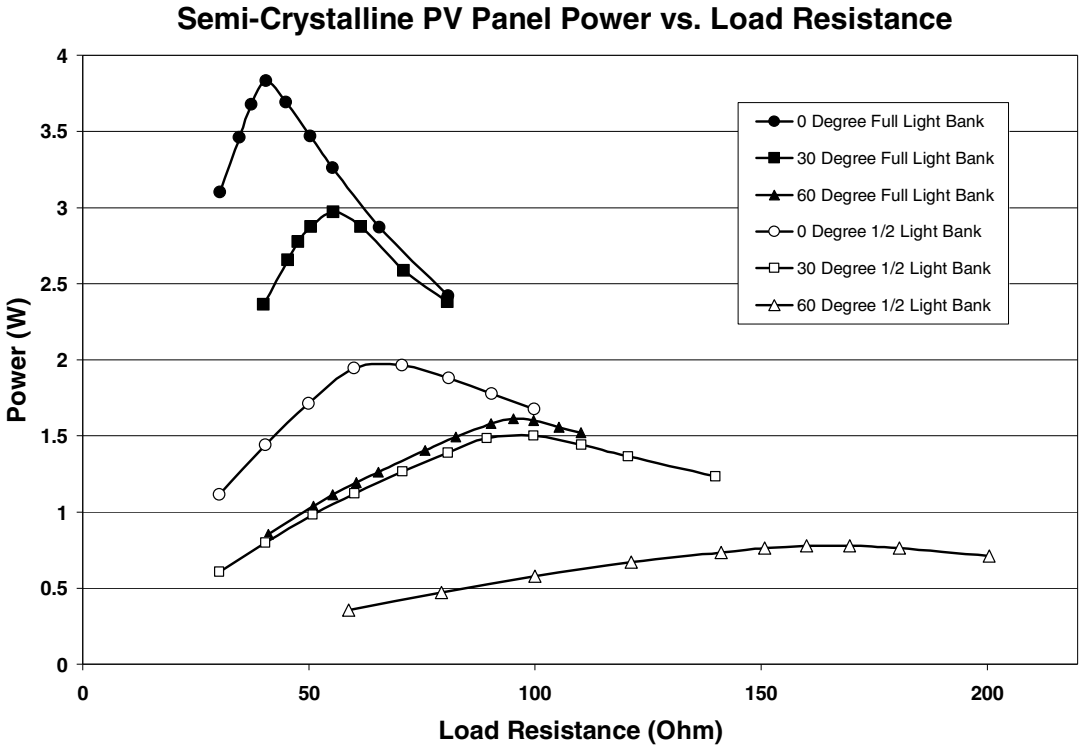


**Figure 5-10 Semi-crystalline Power vs. Load Resistance.**

The semi-crystalline PV panel clearly has much higher power output than the thin-film panel. It follows the same as did the thin-film panel and as theory predicts of decreased power with decreased irradiation and increased incident angle of radiation. The two curves that overlapped in the thin-film experiment—the 60º orientation under full bank irradiation and the 0º orientation under ½ bank irradiation—do not overlap for the semi-crystalline panel. This indicates that not only is irradiation important for power conversion by the semi-crystalline panel, but a low incident irradiation angle. It may be that the cover of the semi-

crystalline panel or the solar cells has high reflectivity at high incident irradiation angles, thus losing much energy in reflection to the surroundings. The trend that was seen in the thin-film experiment of the ½ bank irradiation not producing fully ½ the power of the full bank irradiation is not the case with the semi-crystalline panel. Comparing the ½ bank irradiation to the full bank irradiation at each orientation reveals they are it is nearly exactly ½ the power. Closer examination can be had with the efficiency information, but this initial observation suggests the semi-crystalline efficiency is not as much dependent on irradiation level as is the thin-film panel. The graph showing efficiency as a function of load resistance is shown in Figure 5-11 below.

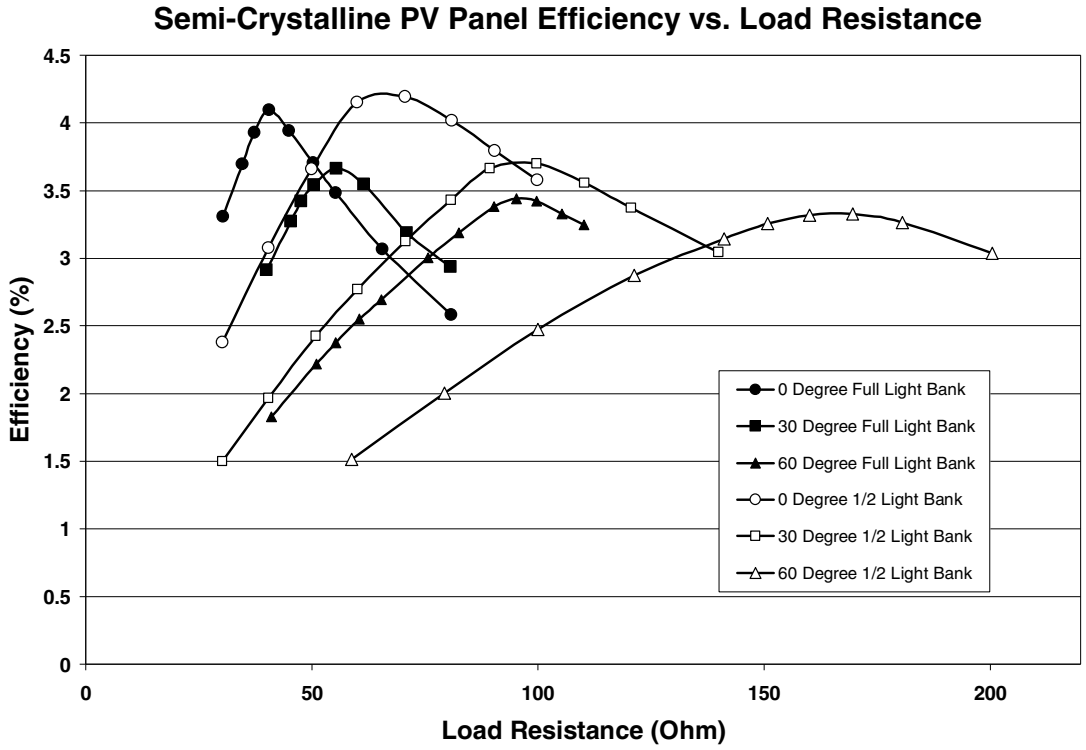


**Figure 5-11 Semi-crystalline Panel Efficiency vs. Load Resistance**

It is clear that efficiency does not depend on irradiation level since the full bank and half bank irradiation experiments have the same efficiency. Comparing the runs with the full bank at 60º and the ½ bank at 0º, shows that despite having the same irradiative level per panel area, there is a lower efficiency with the panel tilted at an angle. This shows that the efficiency of this kind of PV panel is dependent on irradiation angle. Thus, irradiation level does not significantly affect panel efficiency while irradiation angle does. The semi-

crystalline and the thin-film panels have opposite attributes in what they are and are not dependent on for their efficiencies.

## Accuracy of Demonstration

The performance of different PV technologies as a function of the two most significant factors affecting them, irradiation level and irradiation angle is thoroughly investigated in these experiments. The differences in various aspects of performance between two different PV technologies exposes the advantages and disadvantages of them and gives information for choosing a PV technology for a certain application. The different power output levels attained as a function of load resistance highlights the additional components of a full PV system needed such as power control. The output and efficiency values obtained are very reasonable given the PV technologies used and the halogen light substitute for solar irradiation. Overall the experiments performed on this demonstration give valuable familiarity with the operation and performance of real-world PV systems.

# Chapter 6 CONCENTRATING SOLAR THERMAL POWER

## *Background*

The conversion of energy from solar radiation directly into electricity in a photovoltaic cell was covered in the previous chapter. Another means of this conversion from solar energy to electricity is not direct, but is indirect through a thermal cycle. Solar radiation can be used as the heat source for a thermal cycle through which mechanical energy can be developed and from mechanical energy in turn electrical energy can be generated. Because solar radiation is fairly dilute, some way of increasing its concentration is necessary to generate a high enough temperature to be efficiently used in a thermal cycle. Concentration of radiation is only feasible for radiation coming from a point source, or at least a source approximating a point. For this reason, only *beam* or *direct* radiation can be utilized in concentrating solar power technologies. This kind of radiation is in contrast to *dilute* or *scattered* radiation, which is radiation coming from all directions besides directly from the sun such as is supplied by clouds or a dusty atmosphere. To use this beam radiation for the generation of electricity, two main components of a concentrating solar thermal power technology are necessary.

The first component is a concentrator which collects beam solar irradiation and concentrates it many times to some focus. The concentrating is usually done by the use of mirrors. Once the sunlight has been concentrated the second main component, the power conversion unit, converts this high concentration radiation into electricity. The major concentrating solar thermal power (CSP) technologies are distinguished mainly by their method of concentration, though depending on the method of concentration certain types of power conversion units make the most sense as will be seen below. The power conversion units have three main subcomponents which include the receiver which received the solar power, the engine which maintains the thermal power cycle, and the electric generator which produces electricity from the mechanical power. There are three major concentrating solar thermal power technologies: parabolic dish concentrators, parabolic trough concentrators, and central receivers (also known as power tower) or distributed heliostat concentrators.

### Parabolic Dish

Concentrator

Dish concentrators are parabolic dishes which track the sun throughout each day along two axis of rotation. A diagram of a dish concentrator is shown in Figure 6-1 below.

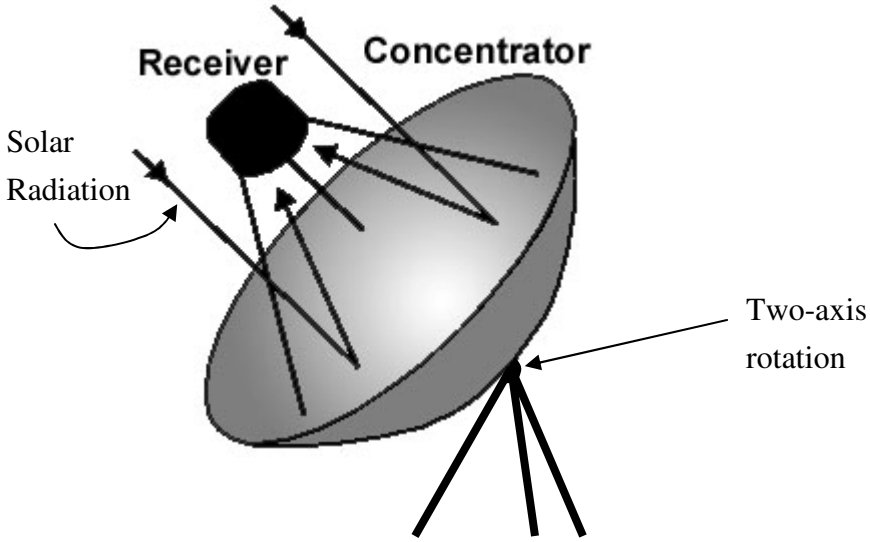


**Figure 6-1 Parabolic dish concentrator showing mirror and receiver.**[52]

Commercial dishes range in size between about 10 and 12m in diameter with capacities of around 25 kW but can vary depending on the type of power conversion unit used. The main structure of the dish system is a rigid frame to which is attached a parabolic dish-shaped mirror. For economic and practical reasons, the mirror is usually composed of many smaller mirrors to make up the total dish diameter as shown in Figure 6-2 below.

**Figure 6-2 Dish concentrator made up of individual mirror components.**[53]

[52] Adapted from *High Temperature Solar Thermal*. Information Portal. Research Institute for Sustainable Energy. <www.rise.org.au/info/Tech/hightemp/image007.jpg> Last accessed May 4, 2007.

The direct solar radiation striking the dish is reflected to a focal point because of the parabolic shape of the mirror. The system's receiver is situated at this focal point and, depending on the type of power conversion unit used, the temperature of the working gas flowing through the receiver can reach temperatures of about 1300ºC[54] with radiation fluxes of over 2000 suns, or approximately 2 ($MW/m^2$) [55]. Two kinds of tracking technologies exist to provide the crucial ability to accurately track the sun through the course of a day. Azimuth-elevation tracking rotates along an axis normal to the surface of the ground and along another axis which is tangent to the ground. The first is responsible for tracking the sun from east to west; the second is responsible for tracking the sun's elevation in the sky, which would go from low to higher to low throughout each day. The second kind of tracking is called polar tracking. Polar tracking maintains one axis parallel to the Earth's axis about which the collector rotates 15º/hr, matching the rotational speed of the Earth. The second axis is parallel to this axis and varies yearly according to the tilt of the Earth's axis relative to the sun which ranges plus or minus about 23.5º. The first kind of tracking is more common among bigger dish systems and the latter among smaller systems[56]. Some concentrators are able to turn to face downward in severe weather to protect the mirrors and structural components from damage. Various kinds of mirrors have been developed for use in dish concentrators with low cost of manufacturing, durability, and high reflectivity being the main goals. Mirrors traditionally are made of glass coated with silver or aluminum. The use of specially designed glass can result in a solar reflectance of 90-94%[57]. A newer design for mirrors involves a reflective membrane stretched over a hoop with a partial vacuum maintained behind the membrane to stretch the membrane into a parabolic shape. Many of these mirrors then are arranged to form a larger parabola, similar to the dish shown in Figure 6-2 above. Once the concentrator is complete, the next component required for the production of electric energy is the power conversion unit. Several kinds of thermal power cycles can be integrated with a dish concentrator for converting thermal to mechanical energy Brayton, Rankine, and Stirling cycles will be investigated below.

---

[53] Image Gallery. Stirling Energy Systems. <http://www.stirlingenergy.com> Last accessed April 30, 2007
[54] William B. Stine and Michael Geyer, *Power from the Sun,* 2001. Chapter 12. <http://www.powerfromthesun.net/book.htm> Last accessed August 8, 2007.
[55] *Solar Dish Engine*. CSP Technologies Overview. SunLab. <http://www.energylan.sandia.gov/sunlab/PDFs/solar_dish.pdf> Last accessed August 8, 2007.
[56] *Solar Dish Engine*. CSP Technologies Overview. SunLab. <http://www.energylan.sandia.gov/sunlab/PDFs/solar_dish.pdf> Last accessed August 8, 2007.
[57] *Solar Dish Engine*. CSP Technologies Overview. SunLab. <http://www.energylan.sandia.gov/sunlab/PDFs/solar_dish.pdf> Last accessed August 8, 2007.

Power Cycles

A less frequently used and currently less developed thermal cycle for use with a dish concentrator is the Brayton cycle. A Brayton cycle uses solar energy to heat air for use in a gas turbine. Air is first compressed and run through a receiver which heats the air with solar energy from the concentrator. The air then is either supplemented with burning of fuel or is used as it is in a gas turbine. There are particular difficulties with the use of this thermal cycle surrounding the transfer of heat into the air at a sufficient rate without causing an excessive pressure drop in the receiver. Since conduction of heat through the receiver walls into the air is the limiting feature in this scheme, alternatives to conduction through a wall have been developed. Volumetric absorption has been developed in the using a porous matrix behind a window in the form of a ceramic foam or honeycomb structure[58]. This can solve some of the unique problems associated with heat transfer from a radiative source. Once high pressure air is available, it is run through a gas turbine which supplies power to the compressor and excess power to run an electric generator. The exhaust from the turbine can be used to pre-heat incoming air. A schematic of a Brayton cycle used with a dish concentrator is shown below in Figure 6-3.

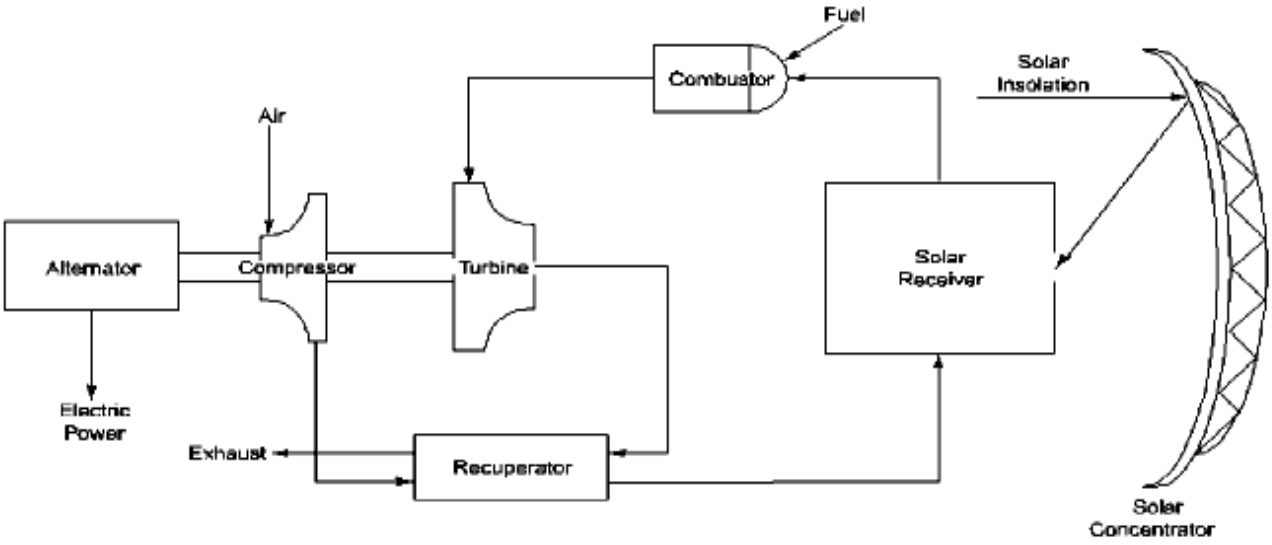


**Figure 6-3 Brayton cycle design with integrated dish concentrator.[59]**

[58] *Solar Dish Engine*. CSP Technologies Overview. SunLab. <http://www.energylan.sandia.gov/sunlab/PDFs/solar_dish.pdf> Last accessed August 8, 2007.

[59] *Solar Dish Engine*. CSP Technologies Overview. SunLab. <http://www.energylan.sandia.gov/sunlab/PDFs/solar_dish.pdf> Last accessed August 8, 2007.

Brayton cycles can be open or closed, with some closed cycles designed for use with some sub-atmospheric pressures within the cycle. Peak efficiencies for electric generation with this design have reached 27% and another open cycle design is expected to have a peak efficiency of 47%. This type of power conversion unit is currently less developed but holds promise for concentrated solar thermal power generation.[60]

Rankine cycles can also be used with dish concentrators with steam being raised for a steam turbine either directly in the receiver or by some intermediate thermal fluid like oil. The fluid is run through a receiver that is located at the focal point of the dish raising its temperature. Many dishes can be used in series for raising the temperature of the fluid higher than would be possible with single dish concentrators or for a higher power[61]. A picture of dishes connected in series is shown in Figure 6-4.

**Figure 6-4 Artist's rendition of a solar field with dishes connected in series for centralized power production.[62]**

If an intermediary fluid is used in the receiver this fluid is used in a heat exchanger to raise steam otherwise steam is raised directly in the receiver and makes its way to a steam

[60] *Solar Dish Engine*. CSP Technologies Overview. SunLab. <http://www.energylan.sandia.gov/sunlab/PDFs/solar_dish.pdf> Last accessed August 8, 2007.
[61] Keith Lovegrove, et al. *Paraboloidal Dish Solar Concentrators for Multimegawatt Power generation*, International Solar Energy Society, Solar World Congress, Gothenberg Sweden, June 2003. <http://engnet.anu.edu.au/DEresearch/solarthermal/pages/pubs/Swed03.pdf> Last accessed August 8, 2007.
[62] *Wizard Power.* Wizard Power Solar Technology. Australian Solar Power Company. <http://www.wizardpower.com.au/solar_technology.html> Last accessed May 1, 2007.

turbine before being cooled to restart the cycle. This cycle is used more with parabolic trough collectors and will be considered in more detail below.

The third and most popular cycle for use with dish concentrators is the Stirling cycle as it exists in a Stirling engine. This is a closed cycle usually employing high-pressure hydrogen as a working fluid. It differs practically from the previous two types of power conversion units in that it cannot practically take advantage of many dishes in series. This results in a stand-alone power generation technology that can provide around 25kW of power for a roughly $88m^2$ dish[63]. Peak conversion efficiency from solar energy to electricity can be about 24-29%[64]. It also has less maintenance requirements than the other two cycles so has peaked interest for development projects in the developing world. A Stirling engine works by being mounted above the concentrating dish such that its hot side is located at the focal point. This is shown in above in Figure 6-2. The concentrated radiation is absorbed by the receiver through which the working fluid flows and develops power to run an integrated generator. One of the difficulties unique to Stirling engines is keeping the high-pressure working fluid from leaking out of the engine. One of the ways to solve this problem is by completely sealing the engine but this presents a challenge to power extraction from the cycle. Several solutions exist to this problem. One type of Stirling engine provides oscillatory motion from which power is captured by a linear generator, and conveyed outside the engine casing through electrically conductive but air-tight components. Electricity can then be conducted directly through the engine casing with no fear of leakage. Another option is applicable if the Stirling engine outputs rotary mechanical power. If this is the case, the generator can be included within the sealed casing and then, like with the previous option, output electric power right through the casing. Finally, a third option is the use of magnetic couplings have been developed which allow mechanical power to be conveyed through a sealed casing so mechanical power could be delivered to a generator without leakage. Since a Stirling engine is used for the demonstration, further discussion and more detail will be included in a section to follow.

---

[63] *Boeing/SES 25-KW Dish/Engine Critical Component System*. Major CSP Projects. SunLab. <http://www.energylan.sandia.gov/sunlab/PDFs/boeing.pdf> Last accessed April 30, 2007

[64] Distributed Power. Major Projects. SunLab. <http://www.energylan.sandia.gov/sunlab/projects.htm> Last accessed April 30, 2007

## Parabolic Trough

Concentrator

The second main type of concentrating solar thermal power technology is parabolic troughs. The concentrator for this technology is long and trough-shaped which means that there is not a focal point, but a focal line. This is shown in below Figure 6-5.

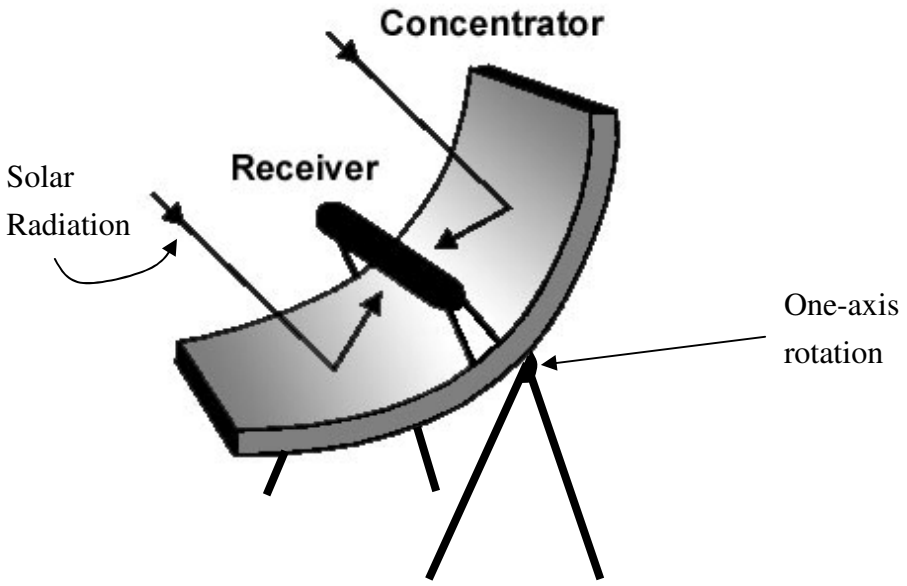


**Figure 6-5 Parabolic trough concentrator showing mirror and receiver.**[65]

This also means that only one axis of rotation is needed to track the sun. Typical aperture widths of the trough are between 4 and 6m with modules roughly 12m long[66]. These modules can be connected in series with limitations only from the land on which the solar collectors are situated. These troughs can be faced down in severe weather to prevent damage. While the dish concentrators are typically composed of many smaller mirrors, the full parabola of a trough module is typically one continuous mirror with a module composed of several mirrors. An entire trough is composed of many modules coupled in parallel and series to form a solar field as shown in Figure 6-6 below.

---

[65] Adapted from *High Temperature Solar Thermal*. Information Portal. Research Institute for Sustainable Energy. <www.rise.org.au/info/Tech/hightemp/image007.jpg> Last accessed May 4, 2007.

[66] Dr. David W. Kearney. *Parabolic Trough Collector Overview*. Parabolic Trough Workshop 2007. National Renewable Energy Laboratory, Golden, CO. <http://www.nrel.gov/csp/troughnet/pdfs/2007/kearney_collector_technology.pdf> Last accessed on May 4, 2007.

**Figure 6-6 Parabolic trough field showing modules attached together in series.[67] This solar thermal plant is located in Kramer Junction, California.**

The shape of the parabolic trough dictates the geometry of the receiver which will clearly have to be different than receivers designed for use with dish concentrators with their focal *point* as opposed to focal line. To make use of the solar irradiation concentrated along a line a linear receiver will need to be used and this lends itself best to the Rankine cycle. Solar irradiation concentrated by a trough is less concentrated than with a dish because there is concentration in one dimension rather than two dimensions. This results in a lower heat flux and better suitability to higher thermal mass flow with lower temperature applications than lower thermal mass flow with high temperature applications. Rankine cycles work perfectly with this because a pipe with either the working fluid itself or an intermediary heat transfer fluid can be mounted right along the focal line and the fluid pumped through it for continual heating. This is shown in the Figure 6-7 below with a single module shown in the upper left. A solar field is composed of many of these modules connected together in series and in parallel with cold fluid entering and hot liquid exiting.

[67] *Concentrating Solar Power*. National Renewable Energy Laboratory. <http://www.nrel.gov/learning/re_csp.html> Last accessed on May 4, 2007

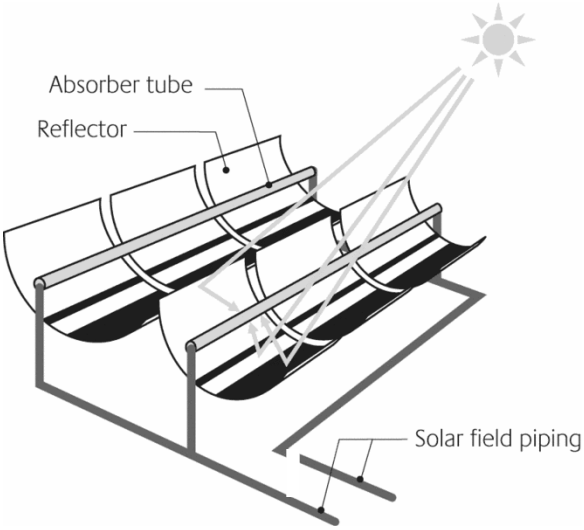


**Figure 6-7 A field of parabolic troughs.**[68]

Receiver

Because there is so much more surface area with a long, linear receiver than with a point receiver, more attention must be paid to preventing heat losses from the receiver itself. An entire industry has developed for the production of insulated pipe receivers that have application both in CSP as discussed here as well as solar water heating as will be discussed in another section. The basic technology is the use of a coating on the receiver pipe that is highly absorptive of solar radiation and minimally emissive of radiation of its own temperature. This minimizes radiative losses. Convective losses are addressed by the use of an anti-reflective glass tube which maintains a vacuum around the receiver pipe. This greatly reduces convective losses and allows the fluid to absorb more and more energy as it travels through the pipe. Receiver pipes can be made of stainless steel with a diameter of about 70 mm, with surrounding glass tube of 115 mm diameter.[69] The end of a receiver pipe is shown in Figure 6-8 below.

---

[68] *The German Solar Thermal Power Plant Industry*. Renewables Made in Germany. <http://www.renewables-made-in-germany.com/en/solar-thermal-power-plants/> Last accessed August 8, 2007.

[69] *Parabolic Trough Solar Power Network*. TroughNet. National Renewable Energy Laboratory. <http://www.nrel.gov/csp/troughnet/> Last accessed May 5, 2007.

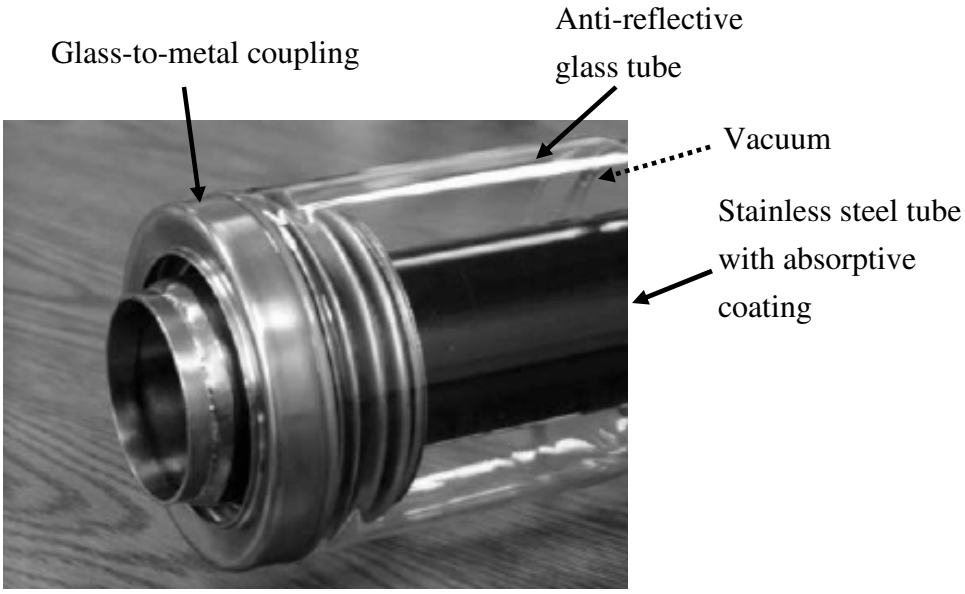


**Figure 6-8 Receiver pipe end showing various components.**[70]

The continual absorption of energy with minimal losses results in a higher temperature working fluid, thus increasing the thermal efficiency of the power cycle. The excellent insulation provided by the vacuum allows for temperatures of around 400ºC to be reached without significant losses, increasing overall efficiency. [71] From this hot liquid, steam can be raised and used to run a turbine. One technical difficulty with the insulated receiver pipes is the issue of differential thermal expansion. Glass and stainless steel expand different amounts in response to temperature changes. With receiver section lengths of around 4 m, this presents large difficulties in maintaining the vacuum seal between the receiver pipe and the surrounding glass. Various approaches to solving this problem exist including the development of a glass with the same coefficient of thermal expansion as the receiver pipe material and improved couplings between the glass and the receiver pipe.[72] Aside from this issue related to a particular receiver pipe section, another challenge is the coupling of one section to another. As will be recalled from above, mirror module lengths are about 4 m, and the receiver sections are made to the same length. Each of these mirror modules tracks the sun independently around an axis that is some distance from the receiver pipe. Practically,

[70] *Parabolic Trough Receiver Thermal Performance.* Parabolic Trough Workshop. Golden, Colorado March 9, 2007. Sandia National Laboratories. <http://www.nrel.gov/csp/troughnet/pdfs/2007/41423.pdf> Last accessed May 10, 2007.
[71] *Solar Parabolic Trough.* CSP Technologies Overview. SunLab. <http://www.energylan.sandia.gov/sunlab/PDFs/solar_trough.pdf> Last accessed August 8, 2007
[72] Schott PTR Receiver Details. Schott Solar, Inc. <http://www.us.schott.com/solarthermal/english/products/receiver/details.html> Last accessed August 8, 2007.

this results in the sections of receiver pipe not necessarily being collinear at all times. A coupling between the sections of receiver pipe that allows for independent movement of each receiver pipe section is necessary for independent tracking and to convey heat transfer fluid from one receiver section to the next.[73] A flexible tube has been tried but found to be unreliable and to add too much pumping loss to the system, so a new kind of coupling currently has been designed and is under testing. The new design is a ball joint coupling that is rigid but has an axis of rotation that is collinear with the tracking axis. So far it has proven better in terms of both reliability and pumping loss. A picture of this is shown in Figure 6-9 below.

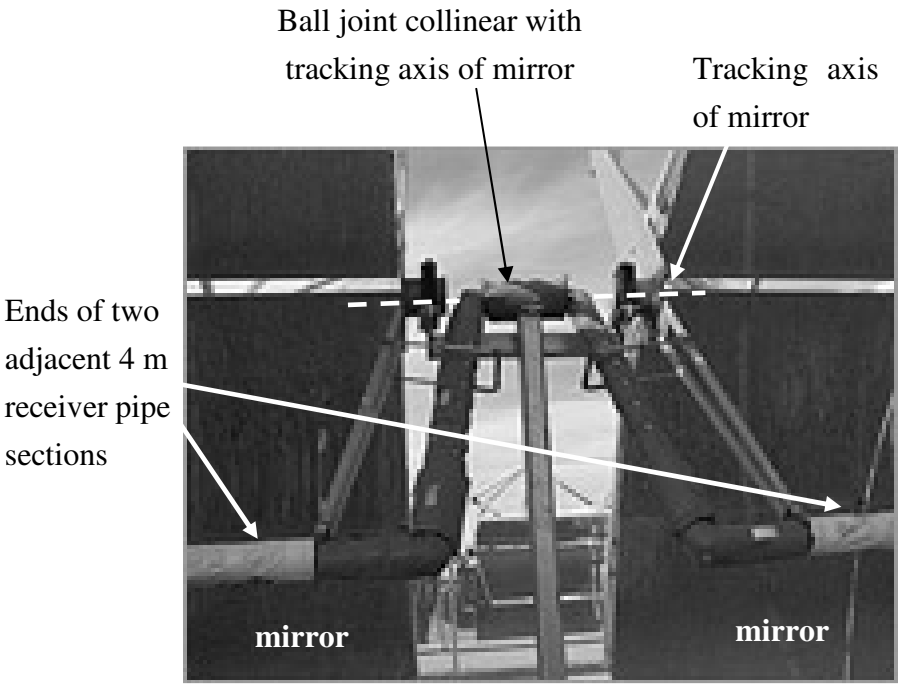


**Figure 6-9 Picture of sectional coupling device.[74]**

Storage

One of the setbacks of solar power in general is its intermittency. There are two different approaches to dealing with this issue with the first being to store solar energy for use when it isn't immediately available and the second to supplement solar energy with fossil-fuel

[73] *Parabolic Trough Solar Power Network*. TroughNet. National Renewable Energy Laboratory. <http://www.nrel.gov/csp/troughnet/> Last accessed May 5, 2007.

[74] *Parabolic Trough Solar Power Network*. TroughNet. National Renewable Energy Laboratory. <http://www.nrel.gov/csp/troughnet/> Last accessed May 5, 2007.

energy. The fossil-fuel supplement approach is fairly simple with conventional fossil technology like boilers or combustors being installed in-line with solar CSP technology. For example, the receivers for a parabolic dish Stirling system can be modified to include the possibility of being heated by natural gas instead of solar radiation. Natural gas can also be easily used to supplement solar heat in Brayton cycles. A coal-fired boiler can be used to supplement heat in a Rankine cycle. The non-fossil-fuel approach which relies exclusively on solar (renewable) energy, however, has a very well suited technology in parabolic trough Rankine cycle technology. The heat received into the heat transfer fluid through the receiver is very well insulated, so the thermal energy is very versatile. It can either be used immediately in generating steam, or it can be stored in a thermal storage unit for later use. Thermal storage utilizes a variety of heat storage mediums including concrete, water, organic oil, and high-temperature salt phase-changes. The energy stored in these mediums can be utilized as a high-temperature heat source for overnight or cloudy operation of the turbine and generator. With thermal storage, not only is the problem of intermittent sun mitigated, but there are significant economic benefits from using thermal energy storage. If a plant is sized according to the incoming solar radiative power available at noon, it will be underutilized the majority of every 24 hour day. If instead it can be sized according to the average energy received from the sun over that same 24 hours, it can be operated near its capacity all the time and therefore make much more economical use of capital costs. Figure 6-10 below illustrates visually the hourly energy supply distribution over one day and how energy storage allows for the supply of energy at a constant rate from an intermittent energy source.

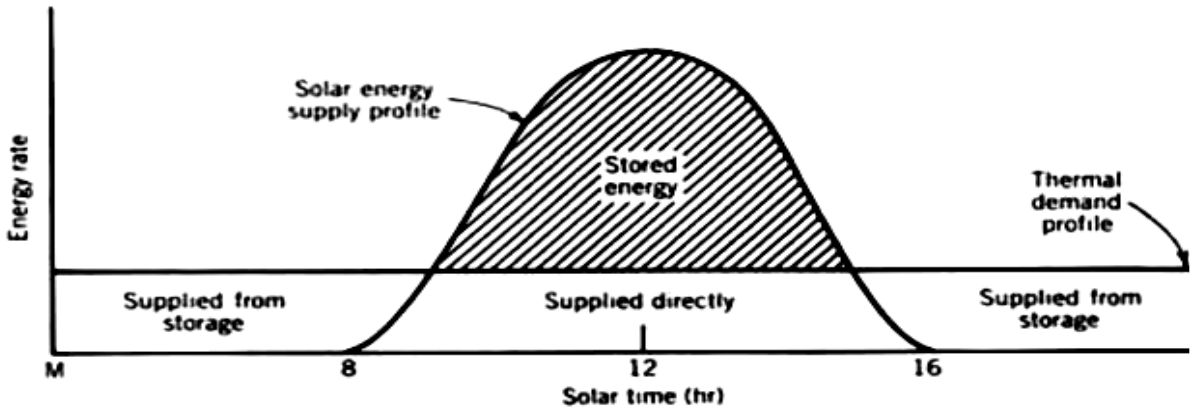


**Figure 6-10 Energy supply, storage, and distribution over one day.**[75]

[75] William B. Stine and Michael Geyer, *Power from the Sun,* 2001. Chapter 11. <http://www.powerfromthesun.net/book.htm> Last accessed August 8, 2007.

Thermal storage is also useful with the CSP technology to be discussed next which is power tower CSP technology.

## Power Tower

Power tower CSP technology consists of many mirrors called heliostats all of which are independently adjustable around two axes of rotation. These heliostats are about 6 m by 6 m each and many are optimally located over a large area. Their function is to remain oriented such that the solar radiation reaching them is reflected onto a receiver at the top of a tower which is called the "power tower" throughout the course of a day. An individual heliostat is shown in Figure 6-11 and a heliostat field with a power tower in the center is shown in Figure 6-12 below.

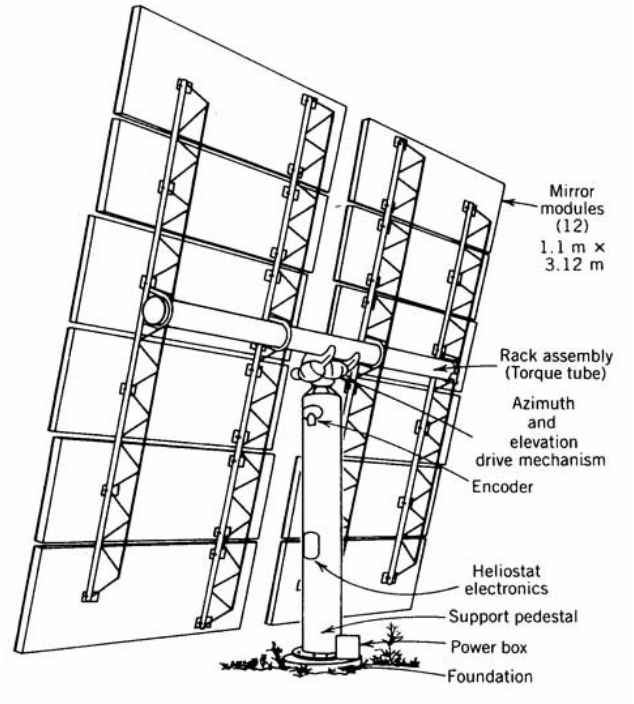


**Figure 6-11 Individual heliostat showing mirror sections and support structure.[76]**

[76] William B. Stine and Michael Geyer, *Power from the Sun,* 2001. Chapter 10. <http://www.powerfromthesun.net/book.htm> Last accessed August 8, 2007.

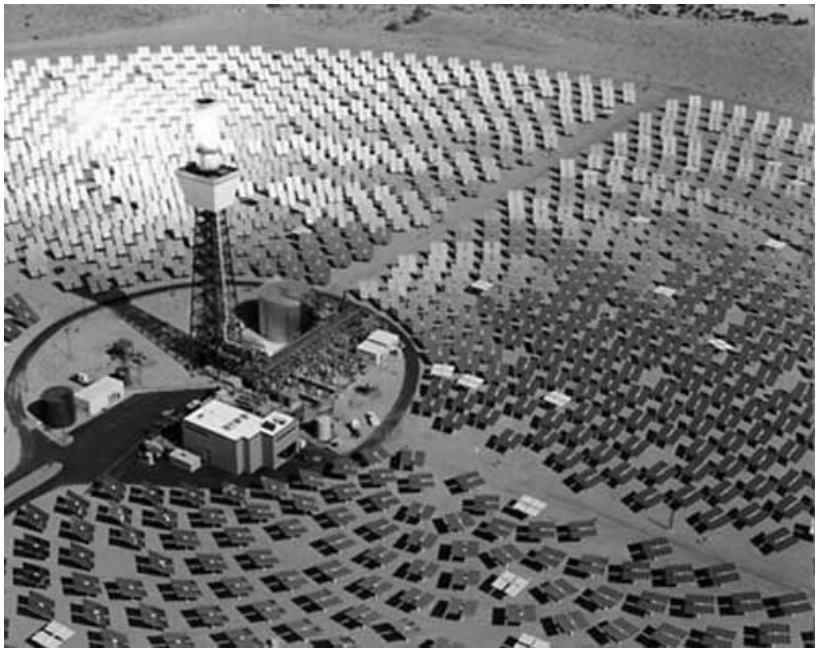

**Figure 6-12 Heliostat field with 10-megawatt central receiver (power tower) in the middle.**[77]

Heliostat mirror sections are slightly concave to focus their reflected radiation on the receiver, and each mirror section can be independently adjusted—though only the structure is tracked and adjusted throughout the day. The heliostat is designed for strength to maintain accurate control of reflected radiation even in high winds, when it would tend to bend and twist, sending the radiation far from the receiver. Because of the enormous reflective area of the heliostat field, extremely high temperatures and heat fluxes are achievable at the receiver. The geometry of the heliostat field and the power tower relative to each other and relative to the sun present a practical limit to how many heliostats can be economically used for a single power tower. One of the experimental power tower systems that have been tested had a total heliostat area of 72,000 $m^2$ over a total land area of 291,000 $m^2$ (72 acres).[78]

Power tower technology has a power conversion unit similar to the parabolic trough technology. A receiver is located atop a tall tower to maximize the projected area from the receiver to the heliostat field. On one of the existing power tower plants the tower is 77.1 m tall.[79] A fluid to receive the solar energy is pumped through the receiver and is then used to raise steam or charge up a thermal storage reservoir. There are two types of receivers;

[77] *Solar History Timeline*. Solar Energy Technologies Program. Department of Energy. <http://www1.eere.energy.gov/solar/solar_time_1900.html> accessed May 7, 2007

[78] William B. Stine and Michael Geyer, *Power from the Sun,* 2001. Chapter 10. <http://www.powerfromthesun.net/book.htm> Last accessed August 8, 2007.

[79] William B. Stine and Michael Geyer, *Power from the Sun,* 2001. Chapter 10. <http://www.powerfromthesun.net/book.htm> Last accessed August 8, 2007.

external and cavity. External receivers are composed of many small tubes welded together to form a large cylinder. A schematic is shown in Figure 6-13 below.

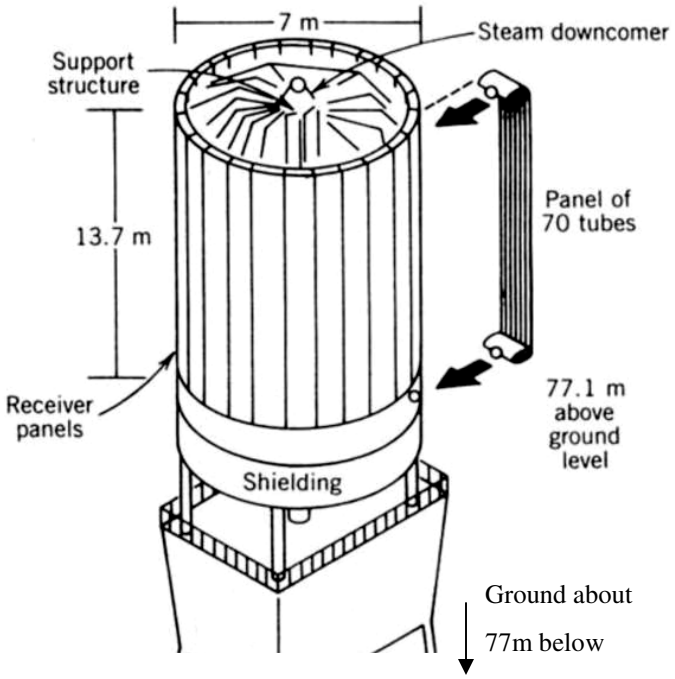


**Figure 6-13 Power Tower receiver that is positioned on top of a tower.**[80]

Cavity receivers are designed to enclose the receiving surface in a cavity to help prevent convection losses. There are other loss modes besides convection and measures are taken to minimize these as well. A diagram of various loss modes is shown in Figure 6-14 below.

[80] William B. Stine and Michael Geyer, *Power from the Sun,* 2001. Chapter 10. <http://www.powerfromthesun.net/book.htm> Last accessed August 8, 2007.

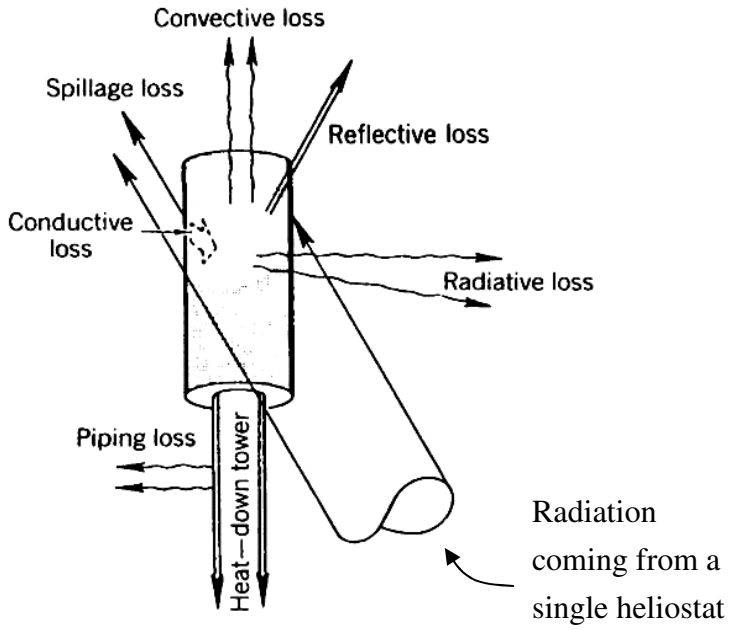


**Figure 6-14 Receiver heat loss modes.**[81]

Receiver design is a current area of research and development. From this point on, the power conversion unit is similar to the parabolic trough with thermal energy being used to either raise steam to run a turbine or being stored for later use.

## *Theory*

### Parabolic Dish Concentrator

The laboratory demonstration is a Stirling engine dish concentrator model so the focus of this theory section will be on parabolic dish concentrators and Stirling engines. Parabolas are lines with a unique shape that has significance for concentrating solar power. The practical import of this shape is that all radiation parallel to a reflective parabolic surface's line of symmetry that strikes that surface will be reflected to a single point, called the focus. This is illustrated in Figure 6-15 below.

[81] William B. Stine and Michael Geyer, *Power from the Sun,* 2001. Chapter 10. <http://www.powerfromthesun.net/book.htm> Last accessed August 8, 2007.

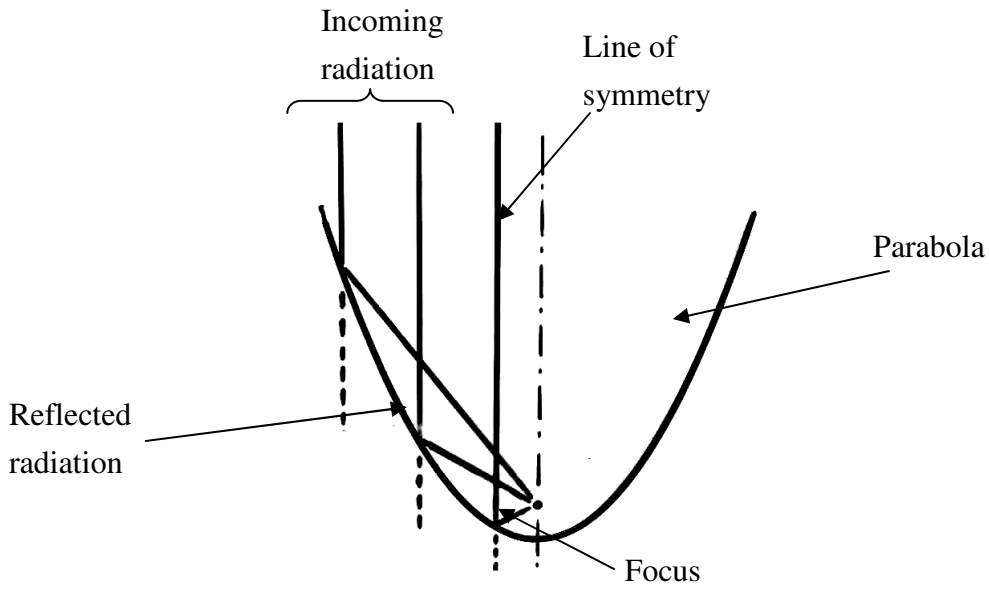


**Figure 6-15 Parabola**[82]

This characteristic of parabolic curves allows the rate of solar energy collection at the focus to be much higher than without concentration. This results in far more efficient energy collection, higher temperatures, and better economy. The parabolic shape can be extended in one direction to form a parabolic trough as has been discussed above, but it can also be rotated around its line of symmetry to form a parabolic dish. Parabolic dishes for solar energy collection have a parabolic shape that is much shallower than the parabola depicted in Figure 6-15. This shallower shape means that the focal point will be a lot farther from the mirror surface and eases the job of the receiver by decreasing the necessary acceptance angle of radiation. As can be observed in Figure 6-2, its acceptance angle looks to be close to 45º whereas the example parabola in Figure 6-15 looks to be somewhat higher than 270º. For the prevention of convective losses, a much narrower acceptance angle range is better, so solar energy can be absorbed in an enclosed, covered space rather than exposed to the environment.

[82] Adapted from <http://kmr.nada.kth.se/files/pointfocus/PointFocus/Parabola-rays.jpg> Last accessed August 8, 2007.

Parabolic dish efficiency

The efficiency of a parabolic dish powering a thermal cycle is found by the amount of useful heat absorbed divided by the total amount of solar energy falling on the aperture area. This equation is shown below

$$\eta = \frac{\dot{Q}_{useful}}{I_b A}$$

**Eq. 6-1**

Where $\dot{Q}_{useful}$ is the useful heat absorbed (i.e. heat absorbed by the working fluid), irradiation, $I_b$, for concentrating collectors is the beam radiation, and $A$ is the collector aperture area. Since it is assumed that the collector tracks the sun, the aperture area is constant. This efficiency will not necessarily be constant, however, because thermal losses increase as temperature increases, so collector efficiency will decrease with temperature. Two aspects of the collector efficiency can therefore be distinguished. The first aspect characterizes the energy reaching the heat transfer fluid and contributing positively to $\dot{Q}_{useful}$. The second aspect is thermal loss of a portion of that energy through conduction, radiation, etc. The first aspect can be termed the optical efficiency, since it neglects thermal considerations. It can be quantified as shown in Eq. 6-2 below with four factors all less than unity.[83]

$$\eta_{opt} = \Gamma \rho \tau \alpha$$

**Eq. 6-2**

[83] William B. Stine and Michael Geyer, *Power from the Sun,* 2001. Chapter 5. <http://www.powerfromthesun.net/book.htm> Last accessed August 8, 2007.

$\Gamma$ is the capture fraction which is the fraction of reflected energy entering or impinging on receiver. This quantifies both the accuracy of the concentrator shape to reflect the most possible incoming radiation to the receiver as well as the appropriateness of the receiver size to collect all the reflected radiation. $\rho$ is a measure of the reflectance of the mirror, $\tau$ quantifies the transmittance of any intermediary materials the solar radiation must travel through, and $\alpha$ measures the fraction of impinging radiation absorbed by the receiver. Table 2 below gives some rough estimates of the values of each of these parameters.

**Table 2 Typical ranges of optical efficiency parameters.**[84]

| Parameter | Value | Description |
|---|---|---|
| $\Gamma$ | 0.95-?? | Properly designed concentrators can reach this but it can be much lower with deflection, poor shape, etc. |
| $\rho$ | 0.94-0.86 | Silver/glass mirrors can attain the high end of the range while new aluminum mirrors are closer to the low end. |
| $\tau$ | 0.97-0.92 | The high range is for glass with special coating while the lower range is for uncoated glass. |
| $\alpha$ | 0.95-0.90 | The high of this range is from specialized coatings while some kinds of black paint are toward the lower end. |

One note should be made about transmittance and absorptivity. These values are given for the wavelengths of maximum solar power. At longer wavelengths (e.g. radiation from a receiver at 400ºC) these numbers can and should be as low as possible. Their value would contribute to the constant described below and found in Eq. 6-3.

The thermal aspect of the collector efficiency is fairly simple for a dish Stirling engine because it is designed to run at a constant temperature. This allows for an experimental constant to be determined that quantifies the thermal loss degradation of the collector

[84] William B. Stine and Michael Geyer, *Power from the Sun,* 2001. Chapter 5. <http://www.powerfromthesun.net/book.htm> Last accessed August 8, 2007 and Nikolaus Benz, *Next Generation Receivers Workshop,* Schott. NREL March 8-9, 2007. <http://www.nrel.gov/csp/troughnet/pdfs/2007/benz_next_generation_receivers.pdf> Last accessed on May 10, 2007.

efficiency in inverse proportion with the solar radiation.[85] Combined with the optical efficiency, this becomes the collector efficiency, $\eta_{col}$, as follows.

$$\eta_{col} = \Gamma\rho\tau\alpha - \frac{\text{constant}}{I_b}$$

**Eq. 6-3**

As will be discussed in more detail below, Stirling engines are closely integrated with their receivers so a combined efficiency makes more sense than separate collector and engine efficiencies. This introduces an additional term to the two already in efficiency equation Eq. 6-3. This engine term is a function of incoming solar radiation, environment, and engine design and would need experimental data for its specification. This total efficiency is the product of the collector and engine efficiency and is shown below.

$$\eta = \left(\Gamma\rho\tau\alpha - \frac{\text{constant}}{I_b}\right) \times \eta_{eng}\left(I_b, Environment, Design\right)$$

**Eq. 6-4**

## Stirling Engine

Because Stirling/Dish systems are a prominent CSP technology and the one chosen for the laboratory demonstration, the theory of Stirling engine operation will be discussed. A Stirling thermodynamic cycle is a closed cycle so the same working fluid is used over and over. Successive heating and cooling of this same fluid causes successive pressure variations that can be tapped for power. This is much different than, for example, a typical gasoline car engine which uses new fluid for each cycle, ejecting the previously used fluid out of the system. A Stirling cycle can be analyzed with varying degrees of idealization and simplicity. An overview of the cycle will be given along with some idealized analyses.

Overview of ideal cycle—Discontinuous

A Stirling engine can have one of several configurations. One of them, called the alpha configuration, is shown in Figure 6-16 below. The main components are two spaces, a compression space and an expansion space, connected by a regenerator. On each side of the regenerator there is a heat exchanger that either cools or heats the air. A complete cycle is

[85] William B. Stine and Michael Geyer, *Power from the Sun,* 2001. Chapter 5. <http://www.powerfromthesun.net/book.htm> Last accessed August 8, 2007.

composed of four processes each of which is described below. These processes are considered in isolation though in real engines they are not discontinuous as this explanation portrays.

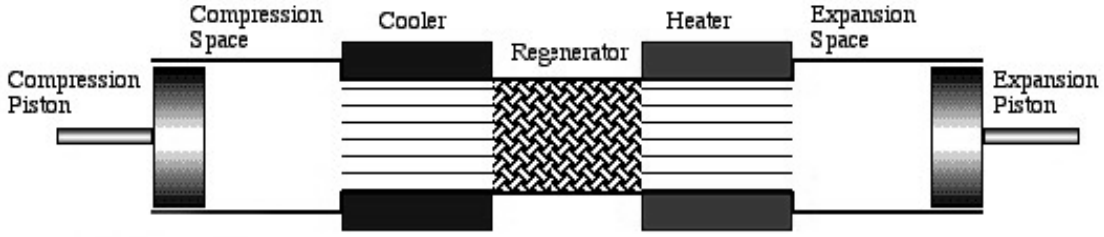


**Figure 6-16 Components of a Stirling engine**[86]

The first state (shown in Figure 6-17 below) will be taken to be the one where all of the working fluid is in the compression (cold) space and at the cold temperature $T_k$. The volume of the working fluid is at a maximum at this state.

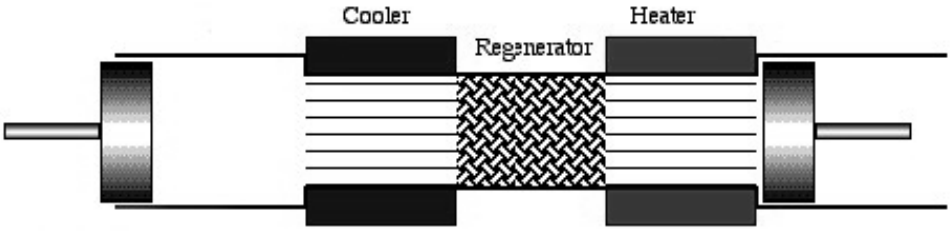


**Figure 6-17 State 1 where all fluid is in the compression (cold) space and volume is at a maximum.**

The process from state 1 to state 2 is an isothermal compression. All of the fluid remains in the compression (cold) space and at $T_k$ but the volume is smaller and is now at a minimum for the cycle. State 2 is shown in Figure 6-18.

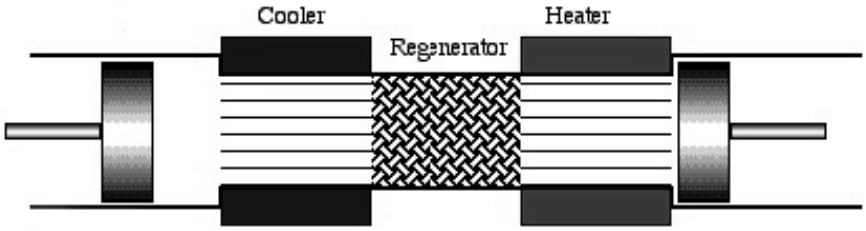


**Figure 6-18 State 2 where all fluid is in the compression (cold) space and volume is at a minimum.**

[86] The illustrations in this section unless otherwise noted are based on those from a website by Dr. Israel Urieli, *Stirling Cycle Machine Analysis.* Ohio University. <http://www.ent.ohiou.edu/~urieli/stirling/me422.html> Last accessed August 8, 2007.

The process from state 2 to state 3 is an isochoric process in which the fluid at the minimum volume stays at that volume as it shifts to the expansion (hot) space and is heated to the hot temperature, $T_h$. State 3 is shown in Figure 6-19 below.

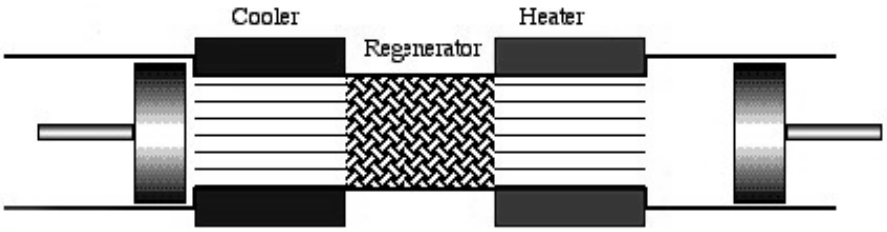


**Figure 6-19 State 3 where all fluid is in the expansion (hot) space and volume is at a minimum.**

In the process from state 3 to state 4, the hot fluid expands back to the maximum volume isothermally. All of the fluid remains in the expansion (hot) space and at $T_h$ but the volume is back to the maximum volume for the cycle. State 4 is shown in Figure 6-20.

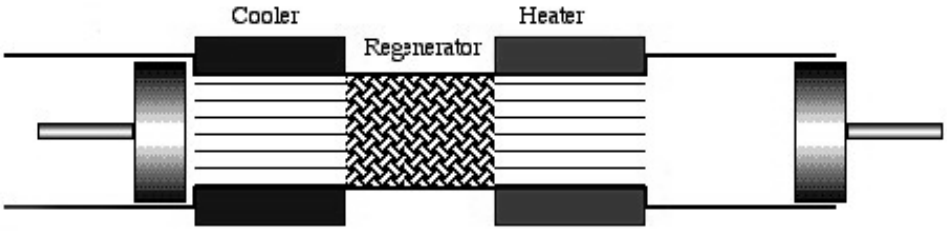


**Figure 6-20 State 4 where all fluid is in the expansion (hot) space and volume is at a maximum.**

The process from state 4 back to state 1 to complete the cycle involves an isochoric process shifting all of the gas, at the maximum volume, back to the compression (cold) space where it cools to $T_k$.

These four processes make up the ideal Stirling cycle. It can be diagramed as shown in Figure 6-21 below. Note the alternating isothermal and isochoric processes.

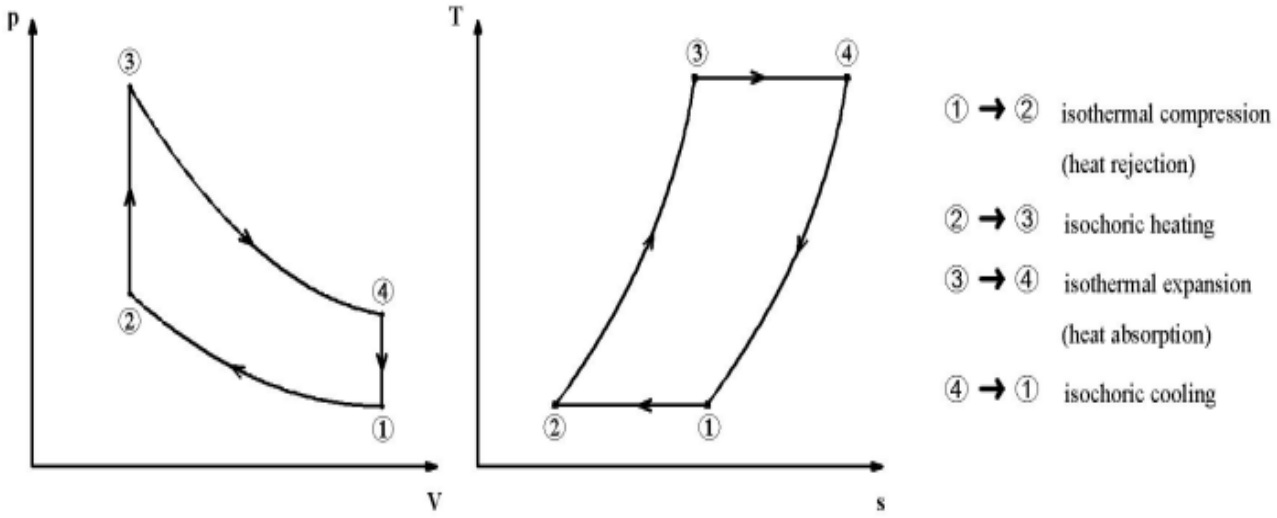


**Figure 6-21 P-V and T-s diagram of Stirling cycle.**[87]

This ideal cycle can be realized with more or less exactly in different Stirling engines. Most engines have sinusoidal motion so the isothermal and isochoric processes somewhat blend into one another. Like all thermal cycles, the ideal efficiency is the Carnot efficiency which is shown in Eq. 6-5.

$$\eta_{carnot} = \frac{T_H - T_C}{T_H}$$

**Eq. 6-5**

With mechanical, thermal, and hydraulic losses, the actual efficiency, $\eta$, is lower than the Carnot efficiency and can be calculated as follows.

$$\eta = \frac{P_{out}}{Q_{in}}$$

**Eq. 6-6**

where $P_{out}$ is the mechanical power from the engine.

The efficiency of the collector and Stirling engine have been discuss separately, but they are usually operated together along with an integrated electric generator. The input of this

[87] This illustration taken from *Investigation of concepts for high power Stirling engines*, Universität Karlsruhe. <http://www-ifkm.mach.uni-karlsruhe.de/Html-e/Project/Stirling/stirling.html> Last accessed August 9, 2007.

integrated system is radiative energy, and the output is electrical energy. Accordingly, the overall solar to electric, $\eta_{s-e}$, efficiency is as follows.

$$\eta_{s-e} = \frac{P_{elec}}{I_b A}$$

**Eq. 6-7**

This solar to electric efficiency is the product of the collector efficiency, the Stirling engine efficiency, and the electric generator efficiency. Stirling engines used with concentrated solar power can achieve solar-to-electric efficiencies of up to 29.4% which includes collector, Stirling engine, and electric generator efficiencies combined.[88]

## *Demonstration*

Stirling/dish technology was the CSP technology chosen for inclusion in the laboratory facility. The first reason is that Stirling thermal-to-mechanical conversion is much simpler than the Rankine cycles used in parabolic and power tower technologies. Secondly, Stirling/dish CSP technology has achieved the highest solar-to-electric conversion efficiency on a commercial scale and continue to be the subject of research and development in governmental, industrial, and academic institutions. Stirling/dish technology has widespread potential impact and use because of their simple, stand-alone, and modular nature. A small-scale Stirling/dish model was chosen to demonstrate the CSP technology as part of the laboratory facility. A picture of the model is shown in Figure 6-22 below.

[88] *Solar Dish Engine*. CSP Technologies Overview. SunLab. <http://www.energylan.sandia.gov/sunlab/PDFs/solar_dish.pdf> Last accessed August 8, 2007.

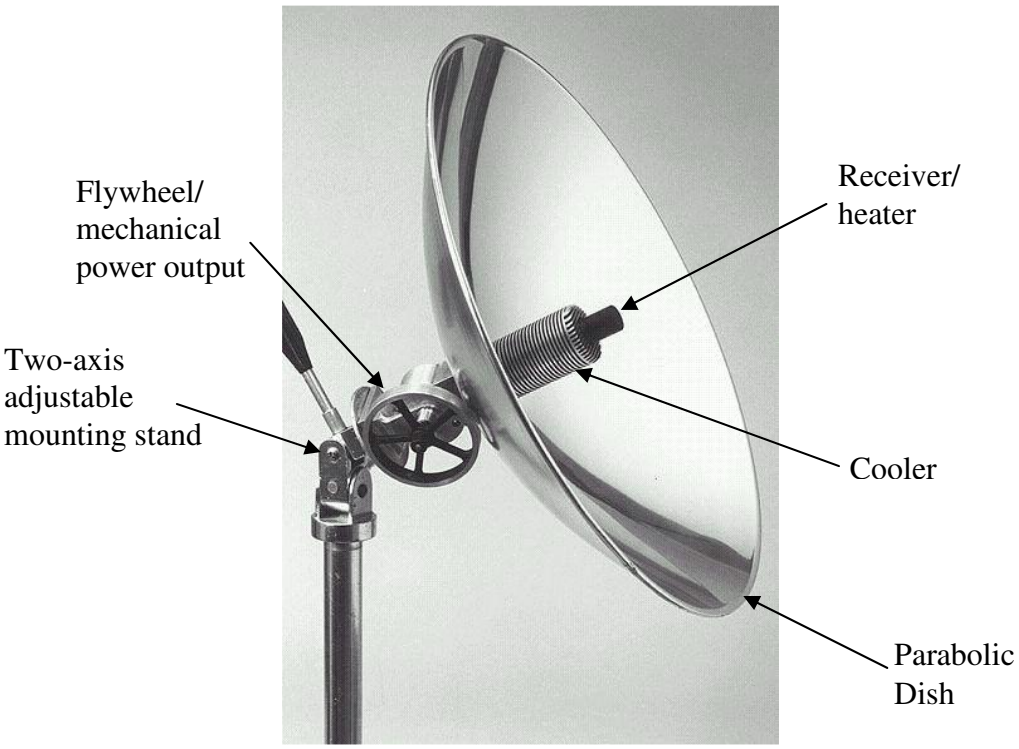


**Figure 6-22 Stirling/dish CSP model chosen for the laboratory facility.**[89]

Since there is no way to provide radiation that resembled beam radiation close enough for effective concentration, the concentration portion of this technology will remain theoretical. The area of the concentrator is known and by assuming a radiation level and optical efficiency the heat input to the engine can be calculated. Eq. 6-2 for optical efficiency will be reproduced below.

$$\eta_{opt} = \Gamma \rho \tau \alpha$$

**Eq. 6-8**

By assuming reasonable values for capture fraction, $\Gamma$, mirror reflectance, $\rho$, and receiver absorptivity, $\alpha$, a reasonable receiver heat input equivalent to that from solar radiation, $Q_{solequiv}$, can be found. Transmissivity, $\tau$, is 1 since there are no intermediary materials between a radiation source and the receiver. The constant in Eq. 6-3 will not be able to be quantified so will be assumed to be negligible but this assumption will be kept in mind during experimental results analysis. Therefore, the optical efficiency, $\eta_{opt}$, is

[89] Bullnet. <www.bullnet.co.uk/shops/test/images/solar4.jpg> Last accessed August 9, 2007.

equivalent to the collector efficiency, $\eta_{col}$. The two other efficiency values besides the collector efficiency that makeup the overall solar to electric efficiency are the Stirling engine and electric generator efficiency. No means of measuring either of these individually will be used since their combined value is more of interest for characterizing and analyzing system performance.

To obtain the combined engine-generator efficiency, $\eta_{eng-gen}$, the theoretically calculated heat input, $Q_{solequiv}$, from the collector under a certain amount of irradiation will be supplied directly to the Stirling receiver by a resistive heater as shown in below.

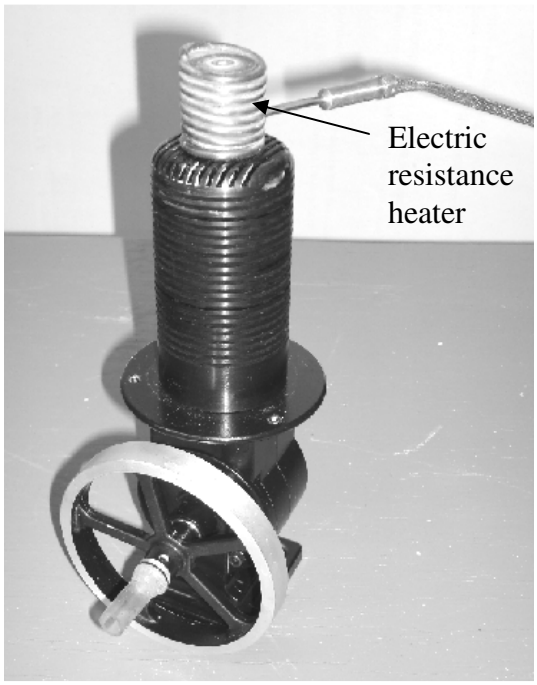


**Figure 6-23 Electric resistance heater for Stirling engine.**

This heater will remain uncovered resembling the fact that the receiver in real operating conditions is exposed to the environment resulting in a significant portion of the received solar energy being lost by convection. If the heater was insulated, forcing most of the electric power into the engine with minimal convective losses, no characterization would be obtained of the convective losses which would take place in actual operation. Another problem with using insulation is that it is unrealistic because no radiation could reach the receiver in real-world operation if the receiver was insulated. Without insulation, a more accurate measure of the engine's performance, including the relative amounts of convective loss and productive use in the engine, is obtained. However, since convective loss is a factor

decreasing efficiency and since convective loss is dependent on wind and other environmental conditions, some inclusion of these variables into the experimentation would be valuable. To incorporate these effects into the demonstration, two set-ups will be used when finding the Stirling engine's performance as a function of heater input. One will involve no receiver/heater wind guard and no draft. The other will use a thin metallic wind guard to both minimize convective losses and protect from a draft that will be directed across the engine cooler. The expectation is that the draft will result in a lower cooler temperature and the wind guard will prevent convective losses. Both of these effects will result in higher engine efficiency.

Heat that is not lost in convection will drive the engine and result in mechanical power. The mechanical output of the Stirling engine will be coupled to an electric generator and the electrical generator will convert mechanical power to electrical power. The generator is shown in Figure 6-24 below.

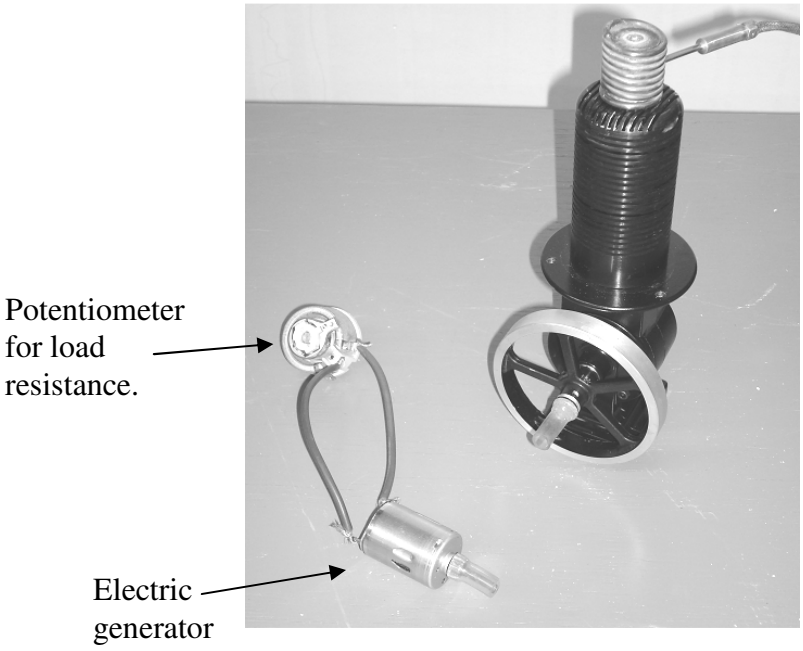


**Figure 6-24 Stirling engine and electric generator.**

The electric power can be calculated by measuring voltage, V, across a known load resistance, R, according to the following equation:

$$P_{elec} = \frac{V^2}{R}$$

**Eq. 6-9**

With the heat supplied to the engine, $Q_{solequiv}$, and electric output, $P_{elec}$, both known, the combined engine-generator efficiency can be calculated according to Eq. 6-10

$$\eta_{eng-gen} = \frac{Q_{solequiv}}{P_{elec}}$$

**Eq. 6-10**

The overall solar to electric efficiency can be calculated by multiplying the engine-generator efficiency found from Eq. 6-10 with the assumed collector efficiency, which is assumed to be the same as the optical efficiency, $\eta_{opt}$, calculated according to Eq. 6-8.

The engine-generator and overall solar to electric efficiencies can be calculated based on different assumptions of the solar radiation level to resemble levels found in different locations and different times of day.

## Reasonableness of Demonstration Developed

The demonstration for CSP technology is subject to major difficulties because of its need to be operable indoors and at any time. A small parabolic dish Stirling system clearly models the principles of Stirling/Dish technology but no means of replicating solar radiation indoors in a way that would render the model operable would be feasible given the constraints of mobility and classroom use. All feasible indoor radiation sources have too much area to resemble a point source of radiation. The proximity of the cooler to the receiver/heater in the Stirling design used (see Figure 6-22) also makes a non-point source of radiation unusable because much of the radiation would spill onto the cooler. The choice to overcome this difficulty by the use of a electric resistive heater as a substitute for solar radiation is the best option because of the electric heater's ability to precisely control heat input. Though the concentration portion of this technology will thus remain theoretical, the visual inspection of the parabolic reflector and the use of assumed values for various parameters will give as good an experience with concentrated radiation as possible without actual solar concentration. Additionally, qualitative experience with concentration could be gained by the use of a laser pointer to experiment with parabolic reflection before the quantitative experimentation begins.

Since total efficiency is composed of collector, Stirling engine, and generator efficiency, students will be able to do quantitative experimentation on the majority of this technology as it exists in real-world operation. A Stirling engine in combination with an electric generator are the most distinctive components of this technology and they will be fully experimented,

investigated, and analyzed with this demonstration giving students as full an experience with Stirling/dish CSP technology as is allowed by the constraints of the laboratory facility.

### *Experiments*

Using the ranges of values for various collector parameters given above in Table 2, estimated values for the parameters to be used in the optical efficiency equation for the demonstration can be chosen. The following parameter values were chosen and optical efficiency calculated as shown in Eq. 6-11 below.

$$\eta_{opt} = \Gamma\rho\tau\alpha = 0.80 \times 0.86 \times 1 \times 0.9 = 0.6192$$

**Eq. 6-11**

This optical efficiency quantifies the fraction of incident beam radiation that strikes the receiver of the engine. Once an irradiation level to be assumed is decided upon, the area of the collector and the optical efficiency can all be multiplied to determine the amount of heat to be provided to the receiver by the electric heater to model a solar heat source. The collector area is $0.1642m^2$ so with an assumed irradiation level of $900W/m^2$, for example, the electric heat to be supplied would be 91.5W. Some discrepancy will naturally exist between the engine output from equal amounts of energy input from the electric heater or radiation. This is because the convective losses will be less for heat received as radiation directly striking the receiver than with the electric heater and its less-than-perfect contact with the receiver, and because of possible error in estimated optical efficiency parameters. However, reasonably close values can be obtained and the calculation of heat input into the receiver yields a rough connection between solar irradiation and indoor operation of the demonstration. Because quantification of the convective loss is beyond the scope of this demonstration, the exact quantity of the energy entering the engine is unknown, so overall efficiency will be focused on using the input from the electric heater and electric generator output.

The experimentation involved measuring the electric generator power output as a function of electric heater input, and the results are shown in Figure 6-25 below. The combined efficiency of the receiver, engine, and electric generator is shown on the secondary axis.

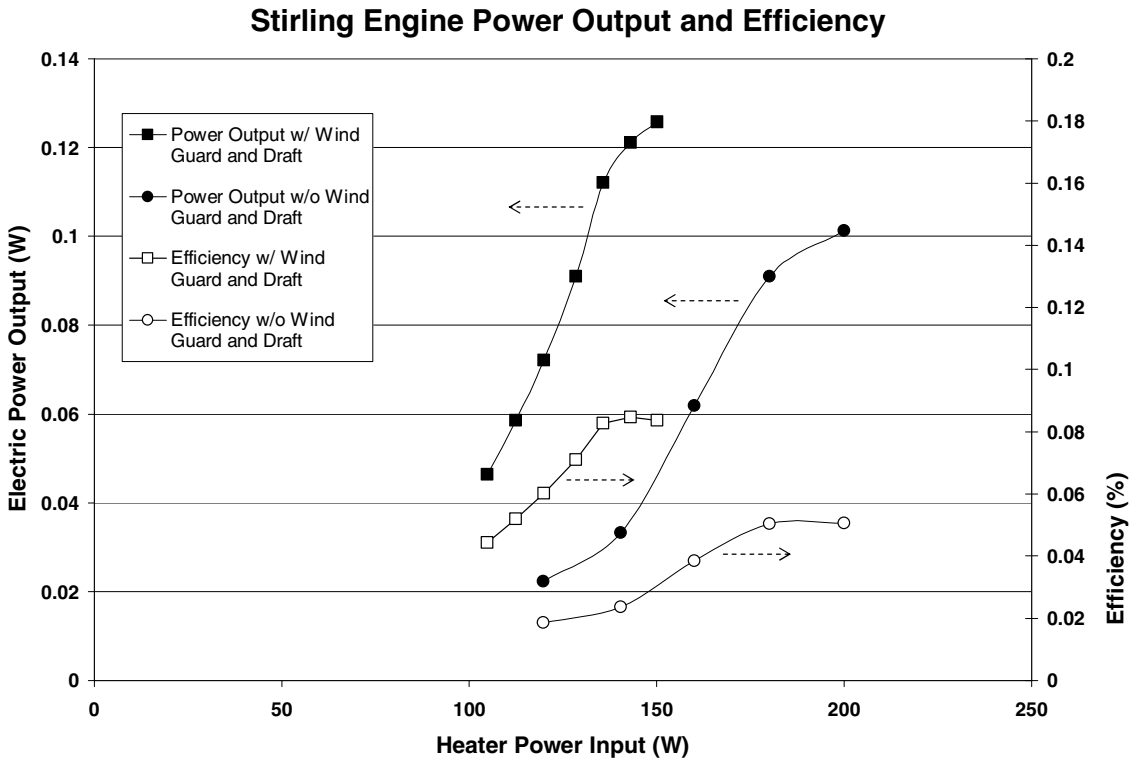


**Figure 6-25 Experimental power output and efficiency results.**

With the assumed collector parameters, the solar irradiation level required to achieve a 150W input would be about 1500W/m$^2$ which is clearly not attainable on the Earth's surface. Therefore the range of heat inputs used in the experimentation exceeds realistic values. Where the power output curves stop on their lower ends is where the engine would not run continuously. Further experimentation showed that it would run fine at these lower levels without the generator as a mechanical load. Therefore the output curves theoretically continue lower into the power input range that would be obtainable with realistic solar irradiation conditions (0-100W), but frictional or other mechanical effects prevent engine operation. This should not be unexpected because the engine was designed for non-generating, pure operational demonstration purposes. There would be nothing preventing the use of a larger solar collector, however, which could provide power inputs in the range used in experimentation. Collector issues aside, then, the engines curve is as expected, with increasing power output resulting from increasing power input. The operating range spans from the low end where the engine would run continuously to the high end where the heater was turning cherry red and reaching the limit of its operating temperature. The flattening of the curve toward the top is expected as frictional and heat losses increase with an increasing

rate to eventually result in no net benefit. The difference between the curves from the two operating conditions (with and without wind guard and draft) makes sense given an understanding of Stirling engine operation. The temperature difference between the hot and cold side is the driver of output power, so any means of increasing this or maintaining it with lower power input will result in a higher output at a lower input (higher efficiency). Because the temperature limit for the hot side of the engine was limited by the heater, the only way to increase maximum power is by lowering the cold side temperature. This was accomplished via the draft blowing across the fins of the cooler and is reflected in the fact that this experimental run has a higher maximum power output than the other experimental run. The wind guard ensured that this higher output power would be attained at a lower input power by minimizing convective loss from the receiver. By these two factors—the wind guard and the draft—the difference between the curves for each experimental run is explained. The exact quantities and shapes of the curves are dependent on various geometric, fluid, and operational characteristics of the engine and its surroundings.

Figure 6-25 also shows engine efficiency values as a function of heater input power. As can be seen, the highest efficiency was about 0.08%. This is clearly not a remarkable value, especially given the fact that Stirling engines in solar applications are known for relatively high efficiencies. But it really shouldn't be surprising given the components of the demonstration. The receiver is as exposed as it can be and even with the wind guard convective losses are undoubtedly high. This is in contrast with the cavity-type receivers used with Stirling engines in solar applications that would be much more protective of received heat. The contact between the electric heater and the Stirling receiver impedes heat transfer and contributes to convective loss in comparison with radiative heat transfer directly to the Stirling receiver. Further, the Stirling engine used is not design for any other purpose than demonstration, so optimization likely focused on minimizing cost with little attention paid to high performance. The engines used in commercial solar power technologies use high-pressure hydrogen or helium which can significantly improve efficiency while the demonstration engine uses atmospheric air. The electric generator used is designed for use as a motor and therefore isn't optimized for use as a generator coupled to a Stirling engine. The smaller the generator, the less efficient it will be as well. All of these factors account for the efficiency values observed, and so while the efficiency values are quite low, they are understandable. The efficiency curves follow the same trend as the power outputs, and the curve for each experimental run reveals more clearly the benefit of the wind guard and draft on performance with over a doubling in efficiency for the run including them.

## Accuracy of Demonstration

Despite the limitations of indoor use, Stirling/Dish concentrated solar power technology is presented accurately. Both in all the essential mechanical elements of the system and in the experimental results the demonstration reflects performance of real-world systems. Trends are seen accurately and the values are reasonable given the scale and limitations of classroom use. The effects of design and environmental variables are seen in the difference between the two experimental runs highlighting their importance and significance in real-world systems and giving students experience in many aspects of this prominent CSP technology.

# Chapter 7 ACTIVE SOLAR WATER HEATING

## *Background*

Two technologies for producing useful energy from solar radiation have been considered so far that both have the potential for large-scale electrical production. Active solar water heating is another technology that makes use of solar radiation but does not have electricity production as its aim. The term 'active' in the name for this technology refers to the fact that there is some active control involved in the conversion of energy. The active control for solar water heating can be in the form of pumps, thermostats, temperature sensors, freeze prevention, and tracking mechanisms. Solar energy is collected, sometimes employing concentration, and used to heat water. The small-scale production of hot water for residential and industrial use is the most common form of active solar water heating device operation. Though most devices exemplifying this technology are fairly small-scale, the cumulative effect of their use by many individuals has already had significant impact in China and portions of the United States. The potential to off-set natural gas or electric water heating is great. In China, which produces 60% of the world's solar heated hot water, solar water heaters are used in an estimated 30 million households.[90] In a relatively small city of three million in China, the solar water heater users displace 0.5 megawatts of electrical hot water heating load.[91]

Active solar water heating has been around in primitive form for years in the form of black water storage containers on residential roofs. These could not truly substitute for natural gas or electric waters heaters, however, because they could not get water as hot as fossil fuel powered methods. The biggest change in this technology that has made it more viable, desirable, and popular is the development of cheap and specialized tube solar collectors that can provide water hot enough to compete with natural gas or electric heaters. These kinds of hot water heaters have decreased in price to around $200 in China because of competition and economies of scale.[92] Even though these kinds of collectors with vacuum-tube insulation are so popular, other kinds of solar water heaters exist as well. The collector

[90] Ryan Hodum, *Kunming Heats Up as China's "Solar City."* June 5, 2007. Worldwatch Institute. <http://www.worldwatch.org/node/5105> Last accessed June 6, 2007
[91] Xuemei Bai, *China's Solar-Powered City*. May 22, 2007. Renewable Energy Access. <http://www.renewableenergyaccess.com/rea/news/story?id=48605> Last accessed June 6, 2007
[92] Ryan Hodum, *Kunming Heats Up as China's "Solar City."* June 5, 2007. Worldwatch Institute. <http://www.worldwatch.org/node/5105> Last accessed June 6, 2007

component of an active solar water heating system is its most distinctive part and there are several kinds to be discussed following.

Cheap and specialized tube collectors are the main component of the popular solar water heaters being sold currently. They are very similar to the parabolic trough receivers discussed in Chapter 6 above and consist of a vacuum-sealed out glass tube surrounding a metal pipe. The metal pipe conducts water or heat transfer fluid and is coated with a special material that maximizes absorption of solar energy and minimizes radiation of its own energy. These tubes don't need to be constructed to have the same strength and durability as the parabolic trough receivers since the fluid they carry is at a significantly lower temperature than for parabolic troughs. The mass production of these vacuum-tube solar collectors have resulted in a decrease in price and much improved economics for their use heating water for residential use. They are typically not used with concentrators but multiple tubes are mounted on a roof or another shade-less area to absorb solar radiation from the entire sky. Their insulation is so effective that any natural outside temperature does not prevent the heating of water. They are also sometimes able to effectively heat water on cloudy days.

A less sophisticated kind of collector used for active solar water heating is a grid of copper pipes covered with an absorptive coating. Instead of being surrounded by a vacuum-tube, the pipes are usually housed in an insulated box with a glass cover. The glass cover serves the same purpose as the vacuum-tube in minimizing convective and radiative losses. To minimize production cost, parallel sections of tube have a small gap between them of around several inches spanned by sheet copper or aluminum also covered with the absorptive coating. The added surface area captures more solar energy and aids in heating the water flowing through the pipes. Variations on this glass-covered insulated box exist with varying materials and geometries.

There is another kind of solar water heater that has a different means for collecting radiation. It employs a closed length of pipe covered by a vacuum-tube like other collectors but instead of that pipe being the conduit of water or a heat transfer fluid, it has a two-phase fluid in it.[93] The two-phase fluid is heated by the sun and its vapor rises to a header located at the upper end of the heat pipes. In the header, the vapor condenses giving its latent heat to water or a heat transfer fluid. After condensing, liquid runs back down to the lower end of the heat pipe to be reheated by the sun. A schematic of this design is shown below in Figure 7-1.

[93] Heat Pipe, Technical Info. Apricus Solar Hot Water.
<http://www.apricus.com/html/solar_collector_heat_pipe.htm> Last accessed August 9, 2007.

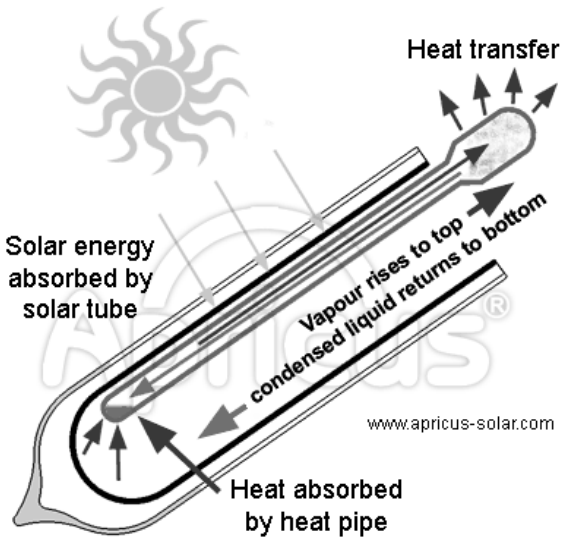


**Figure 7-1 Schematic of two-phase heat pipe.**[94]

The advantage of this arrangement includes resistance to damage from freezing, decreased required pumping power, and increased resiliency in case of damage to one of the collectors. The increased resiliency results from the fact that the vacuum tubes do not carry the water to be heated, but supply the heat to the header so if one of them gets broken or damaged the hot water loop and remaining heat pipes are unaffected.

With any of the three above described collectors, other features of an active solar water heating system are necessary to control it, make it convenient, and integrate it with building water supply. Usually water is the only fluid in the system, but sometimes an intermediate heat transfer fluid is used. With a water-only system, there is a circuit from the tank through the collector and back into the tank. There is another circuit from the tank to a building supply (e.g. shower) to the sewer and eventually back into the tank. The first circuit is the heating circuit and the second circuit is the supply circuit. These two circuits are shown in Figure 7-2 below.

[94] Image from Heat Pipe, Technical Info. Apricus Solar Hot Water. <http://www.apricus.com/html/solar_collector_heat_pipe.htm> Last accessed August 9, 2007.

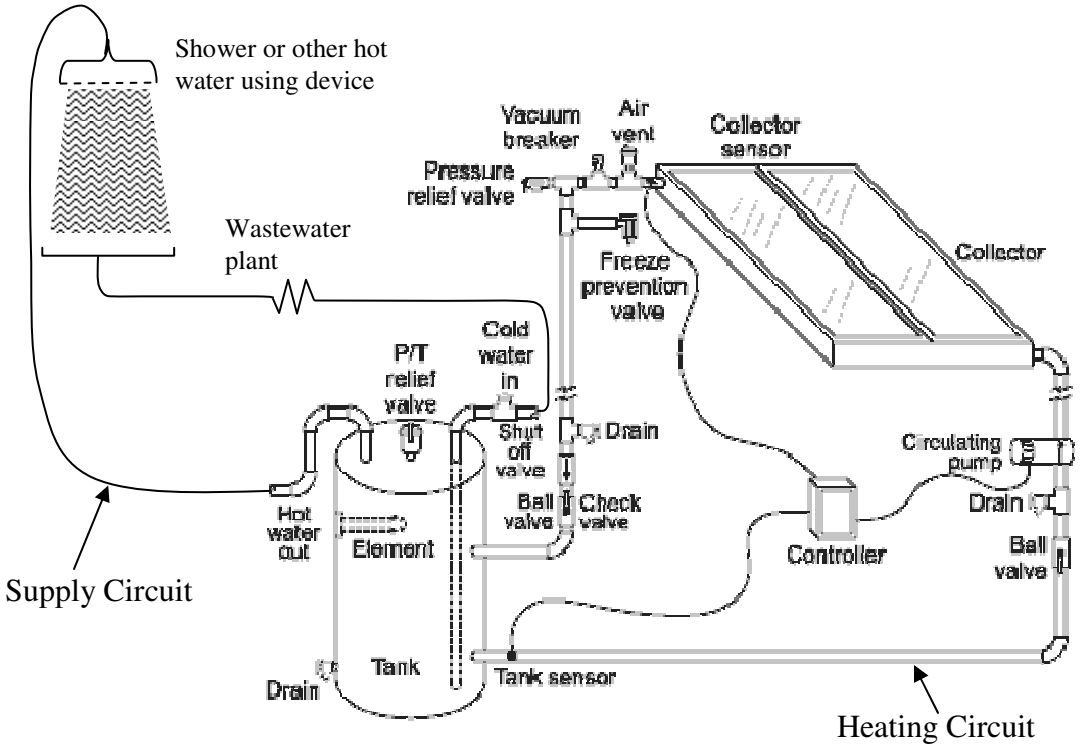


**Figure 7-2 Active solar water heater schematic.**[95]

The features of this integrated system from a hot water storage tank to the rest of a building's plumbing (the supply circuit) are identical to that of a normal hot water heater so its discussion will be neglected here. The parts distinctive to solar water heaters are all those involved in bringing hot water to the tank using the sun's energy (the heating circuit). The control of the heating circuit consists mainly in the regulation of water flow. The change in temperature, $\Delta T$, across the collector can be measured using temperature sensors (shown in Figure 7-2). From a measured $\Delta T$ the pump can be adjusted as necessary. If the $\Delta T$ is positive, the pump will keep running since heat is being gained. If the $\Delta T$ is negative signifying the loss of energy as may be the case on a cold night, then the pump will shut off. One of the temperature sensors may also be linked to a supplemental heater powered by natural gas or electricity to aid in water heating on cloudy days. Control logic would need to take into account the $\Delta T$ and flow rate of water through the solar collector to ensure not to use supplemental heating when it is not needed. Once the water in the storage tank reaches a maximum temperature limit, the kind of system would dictate whether water would be left

[95] Modified from *Solar Hot Water*, For Homes Q & A. Florida Solar Energy Center. <http://www.fsec.ucf.edu/en/consumer/solar_hot_water/homes/q_and_a/index.htm> Last accessed June 6, 2007

stagnant in the collector, whether excess heat would be disposed of in a heat dissipater, or some other option such as home heating.

One potential problem with the above described system is freezing. Freezing can cause serious damage to plumbing and collector tubes and needs to be prevented. One method of prevention is the continual circulation of warm water from the tank through the heater circuit. There would be a negative $\Delta T$ across the collector signifying a loss of heat, but the protection of the heater circuit is worth this loss of energy. Another method of freeze protection is draining water from the heater circuit, or at least the portion of the heater circuit that is subject to outdoor temperatures. A third method is the use of a heat transfer fluid other than water in the heater circuit. The heat transfer fluid could be water mixed with anti-freeze, or organic or synthetic oil. These heat transfer fluids are not in danger of freezing are used permanently in the heater circuit. In this method instead of the heater and supply circuit being open to each other as they are in Figure 7-2, they are closed and independent of one another. To heat water for use in the building, the heater circuit runs through a heat exchanger within the storage tank and transfers its heat to the water stored there.

### *Theory*

Like the other solar technologies discuss in the sections above, active solar water heating has its energy source in solar radiation. The irradiation intensity on the collector and area of the collector specify the total solar resource available. Some of this solar energy when striking the collector will be absorbed and transferred to the water in the collector. At first, there will be a linear increase in the temperature of the water assuming constant irradiation but as the water gets hotter the heat losses will become greater. Conductive, convective, and radiation losses will increase finally to a point when the losses balance out the heat gained from solar irradiation and the system will reach steady state. Depending on the effectiveness of the insulation to minimize losses and the rate of solar energy input, this steady state temperature may be much higher than the maximum temperature limit for the hot water supply, and may even be above the boiling point which will cause difficulties with the system. An energy balance of this situation is shown below in Figure 7-3.

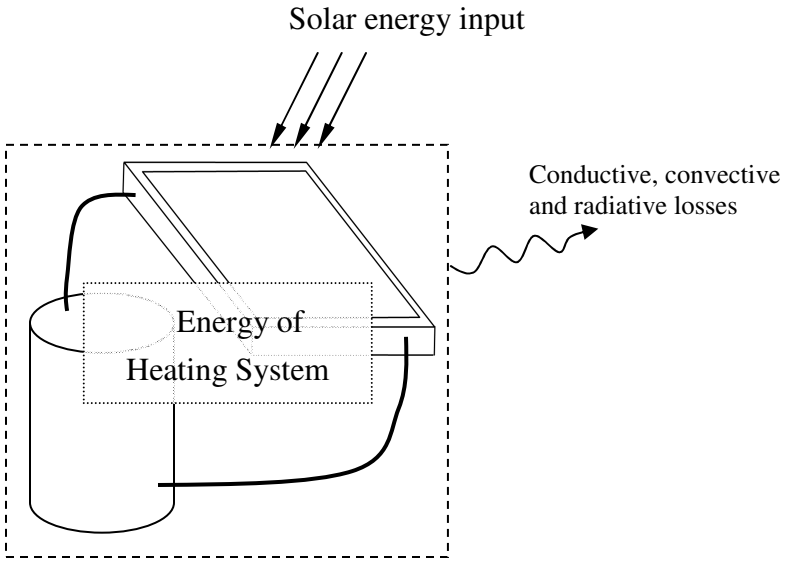


**Figure 7-3 Control volume for solar water heating system.**

The energy balance can be formalized by breaking down the quantities shown in Figure 7-3 into their components. The solar irradiative rate, $q_{irrad}$, is the product of I and A where I is the total (including both beam and direct irradiation) hemispherical irradiation per unit area of the collector at the collector orientation. A is the collector area.

$$q_{irrad} = I \times A$$

**Eq. 7-1**

Though $q_{irrad}$ quantifies the total energy available for heating water, it is not the solar energy actually input into the system because a fraction of $q_{irrad}$ is reflected by the glass cover plate. Thus the value of solar energy actually remaining in the control volume needs to be determined and compared with $q_{irrad}$ to quantify the collector's efficiency. The efficiency will be influenced by reflectivity of the cover or covers and the absorber plates. The rate of heat loss from the control volume of Figure 7-3, $q_{loss,}$ will be assumed to increase linearly with temperature. $q_{loss}$ has many causes: conductive, convective, and radiative heat transfer losses are all occurring simultaneously with various relative significances. Analysis of each of these individually would be extremely and unnecessarily complicated, so the concept of thermal resistance is utilized for simplification. With this assumption the thermal resistance of the system as a whole can be combined into a single resistance term, $R_t$, as follows.

$$R_t = \frac{T - T_\infty}{q_{loss}}$$

**Eq. 7-2**

where $T$ is the temperature of the water and $T_\infty$ is the atmospheric temperature. The assumption of linear heat loss increase with temperature neglects radiative losses but at the temperatures involved with most solar water heaters and the relative areas of the collector and the rest of the system, this assumption is a reasonable starting point. A more complex analysis would need to take into account the materials, geometries, and particularities of a system. The energy of the solar water heater system, E, then changes with respect to time according to the following equation

$$\dot{E} = q_{solar} - q_{loss}$$

**Eq. 7-3**

By rearranging this equation and substituting in the thermal resistance, the overall energy balance becomes

$$\dot{E} = q_{solar} - \frac{T - T_\infty}{R_t}$$

**Eq. 7-4**

If water is assumed to be at a uniform temperature which is reasonable with a small volume of water and relatively high flow rates, the change in internal energy can be broken down further and expressed as

$$\dot{E} = \frac{dE}{dt} = mc_p \frac{dT}{dt}$$

**Eq. 7-5**

Where m is mass of the water and $c_p$ is water's specific heat. Substituting Eq. 7-5 back into Eq. 7-4 gives

$$mc_p \frac{dT}{dt} = q_{solar} - \frac{T - T_\infty}{R_t}$$

**Eq. 7-6**

Eq. 7-6 is helpful because when the temperature reaches a maximum and maintains a steady state the left-hand side of Eq. 7-6 will go to zero. This is when the solar input term and loss term are equal. The maximum temperature can then be solved for as shown below.

$$0 = mc_p \frac{dT}{dt} = q_{solar} - \frac{T_{\max} - T_\infty}{R_t}$$

**Eq. 7-7**

$$T_{\max} = R_t q_{solar} + T_\infty$$

**Eq. 7-8**

Thus as seen in Eq. 7-8, the maximum temperature is increased by the system having a high thermal resistance, high solar radiation input, and high ambient temperature. Only the thermal resistance is a design variable which is why focus is placed on minimizing losses (i.e., increasing resistance).

## Efficiency

The efficiency of a solar water heat is a measure of how well the collector uses the solar energy available to it to heat water. $q_{irrad}$ quantifies the solar energy available to a collector and the change in the energy of the system as discussed above in Eq. 7-5 quantifies the successful use of that energy in heating up water. Eq. 7-5 can be written in a different form for use with a collector in isolation from the rest of the hot water system. This will give a more accurate efficiency for the collector by itself as opposed to the system as a whole. Using this rewritten form, the collector efficiency, $\eta$, can be formulated as follows.

$$\eta = \frac{\dot{m} c_p \left(T_{out} - T_{in}\right)}{q_{irrad}}$$

**Eq. 7-9**

Assuming infinite thermal resistance for the rest of the system besides the collector itself, the water will heat up to a point that the losses from the collector itself equal the radiative energy input. In this case $T_{out}$ and $T_{in}$ will be equal and the efficiency will be zero. However, since there will be some loss in the rest of the system, $T_{in}$ will always be less than $T_{out}$ even though the system as a whole is at steady state.

Efficiency, then, is not quite a clear measure of collector performance because it varies so much over the collector operating range. A more efficient collector at a particular

temperature may have a lower maximum temperature, and vice versa. This difference is captured in the resistivity and $q_{solar}$ terms. More information can be gathered by integrating Eq. 7-6 with respect to time. Assuming that $q_{solar}$ and $T_\infty$ are constant with respect to time the integration results in Eq. 7-10 below.

$$T(t) = \left(R_t q_{solar} + T_\infty - T_o\right)\left(1 - e^{-\left(\frac{1}{R_t m c_p}\right)t}\right) + T_o$$

**Eq. 7-10**

Where t is time and $T_o$ is the initial temperature of the water. Depending on the values of $R_t$ and $q_{solar}$, different rates of temperature rise can occur as well as different maximum temperature achieved as discussed above. Some examples of different curves are shown below in Figure 7-4

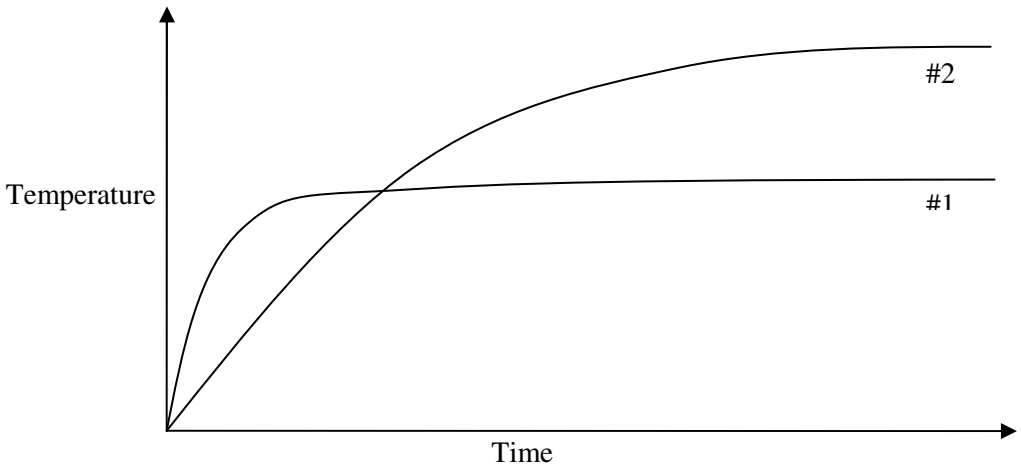


**Figure 7-4 Different efficiency and $T_{max}$ combinations assuming equal irradiation, $q_{irrad}$, and ambient temperature.**

A steeper slope is indicative of a higher efficiency because heat is being added to the system at a faster rate, making more use of the incoming solar energy. To understand the relationship between efficiency and $T_{max}$ better, consider a baseline performance of a collector to be the curve labeled #1 in Figure 7-4. This collector is then modified by the addition of one or more glass cover plates to decrease convection losses and increase $R_t$. However since the cover plates will reflect some more of the incoming irradiation, $q_{solar}$ will be decreased. The product of $R_t$ and $q_{solar}$ though still will be higher than before the cover plates were added. This modification would have two effects. First, the system would have

a higher $T_{max}$ according Eq. 7-8. Secondly, the system would have a slower rise time to that maximum temperature because of the higher $R_t$ term in Eq. 7-10. The result is shown graphically as curve #2 in Figure 7-4. The best balance between and $R_t$ and $q_{solar}$ for an application then is dependent on the needs of the application. If hotter water is more important than a short heating time, then a collector represented by a curve like curve #2 would be desired. If a lower maximum temperature was needed and for an application that needed a lot of it, a collector like that for curve #1 would be a better choice. This characterization will be accomplished with the demonstration chosen and experiments performed.

### *Demonstration*

Vacuum-tube collectors typically come in about four feet long lengths which would not work well for the mobility required by the laboratory facility. A popular but simpler collector technology will be used for the demonstration that consists of a fairly closed grid of copper pipes backed by sheet metal and painted black. This grid is housed in a 0.75 inch plywood box lined with 1.375 inch foam insulation. The collector grid is covered by a single pane of 1/8 inch glass. The insulated water tank is a one gallon thermos. A pump is located within the tank with its outlet connected via insulated tubing to the collector inlet. The outlet of the collector is connected back to the insulated tank completing the hydraulic circuit. The entire system is shown in Figure 7-5.

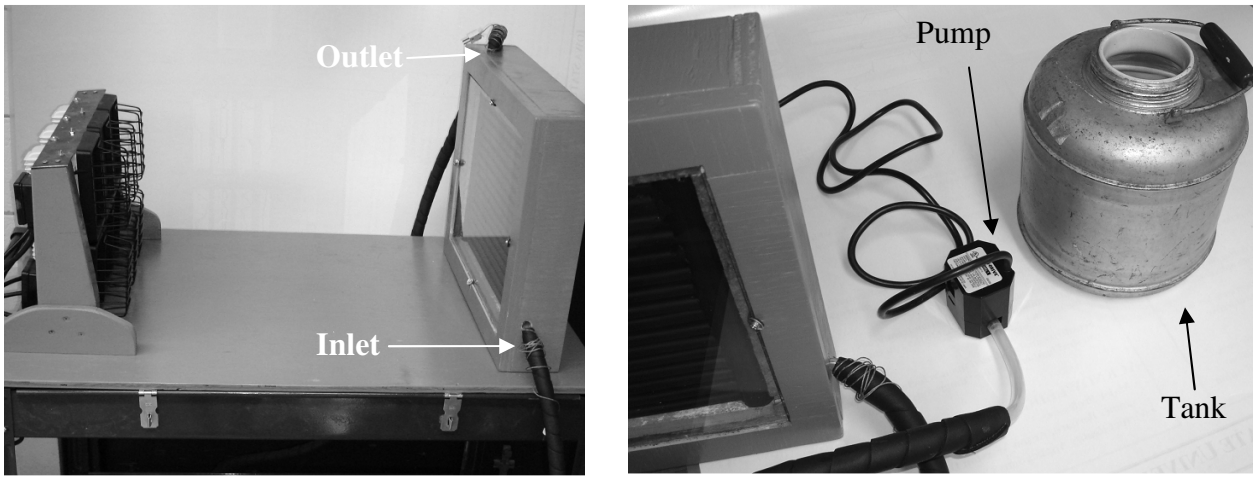


**Figure 7-5 Solar water heater demonstration showing light bank, collector, tubes, tank, and pump.**

The radiation source for the water heating is the bank of six halogen lights described in previous sections. A radiometer will be used to measure irradiation levels giving $q_{irrad}$ and the $q_{solar}$ value will be calculated based off the water temperature rise. To measure system energy change and the water temperature, thermocouples fixed near the inlet and outlet of the collector as well as in the tank will be used. This will allow for measurement of the change in temperature across the collector as well as any losses that occur in piping between the tank and the collector. There will be sufficient mixing so the tank water can be assumed to all be at the same temperature. A temperature as a function of time curve will be found for both ½ bank irradiation and full bank irradiation.

### Reasonableness of Demonstration Developed

The basic black painted copper collector is a typical solar water heater technology. It is somewhat easier to understand because its features can be seen as 2-dimensional units, rather than with the vacuum-tube collectors being seen as many individual components. It also allows for the design and construction of a conveniently sized collector that can perfectly fit into the mobile cart and receive energy from the light banks. All the features of solar water heaters can be discussed including efficiency, maximum temperature, temperature rise time and profile.

$q_{solar}$ variation by the use of different portions of the light bank gives the opportunity to look at different curve for comparison. It also allows for the confirmation of how irradiation affects maximum temperature. Though $q_{solar}$ cannot be measured exactly, its inference from other reasonable assumptions gives a good starting point. Getting a tank of water up to temperature as part of the experiment illustrates how on a larger scale enough water could be heated for a shower or laundry. Many important features of solar water heaters are thus included in this demonstration and the basic ideas and common limitations of water heaters will be seen. A greater appreciation of the characterization of solar water heaters along with the appreciation of alternative designs that address the deficiencies of the demonstration solar heater will give students excellent education of this important alternative energy technology.

## *Experiments*

To characterize the performance of the collector, two experiments were performed with the above described solar water heating system. One gallon of water was added to the system and the pump was started. One run was performed with a half bank of the lights illuminated and the other with the full bank. Both runs started with the water at about room temperature.

The experimental results and curve fit to each experimental run is shown in Figure 7-6 below. The temperature of the solar heater water above the ambient temperature is shown rather than the actual temperature because it is this temperature difference that is most relevant to performance.

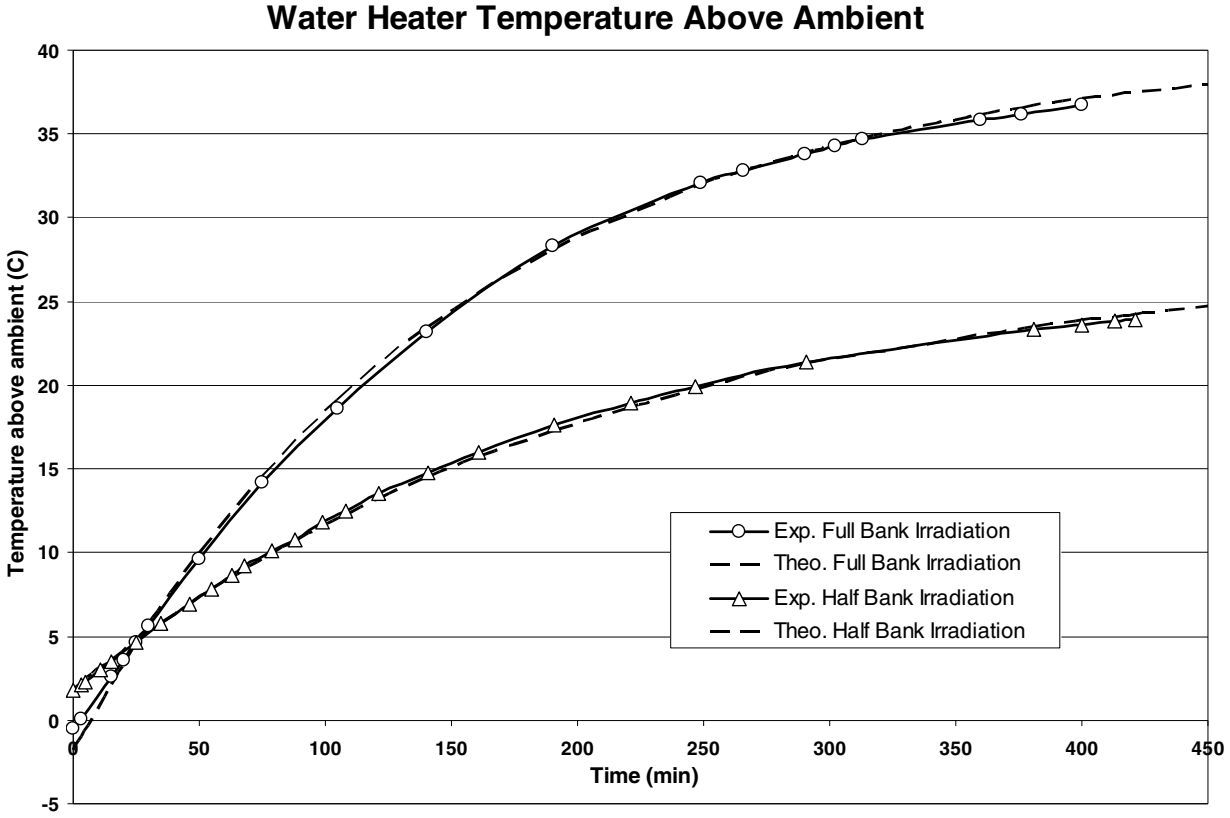


**Figure 7-6 Experimental results and theoretical curve fits to the experimental data.**

The difference between the two experimental results is as expected given the different irradiation levels used in each experimental run. It is clear that steady state would be attained a few hours after the experiment ceased at about seven hours. The maximum temperature for the full bank irradiation experiment was about 58ºC, or 137ºF. This is a very reasonable household hot water temperature. More information about the solar water heater can be gained from curve fitting a line through the experimental data according to Eq. 7-10 and repeated below

$$T(t) = \left(R_t q_{solar} + T_\infty - T_o\right)\left(1 - e^{-\left(\frac{1}{R_t m c_p}\right)t}\right) + T_o$$

The known values of this equation are m and $c_p$ which are found from the gallon volume of water and water's specific heat. Once this is inserted into the equation along with known starting and ambient temperature, thermal resistance $R_t$ and $q_{solar}$ can be adjusted until the curve fits experimental results. The adjusted curve fits are shown in Figure 7-6. The thermal resistances and irradiation values used for the curve fits are shown in Table 7-1 below.

**Table 7-1 Curve fit constants.**

| | Full light bank | Half light bank |
|---|---|---|
| $q_{solar}$ | 74W | 36W |
| $R_t$ | 0.56 K/W | 0.77 K/W |

With radiometer readings of the irradiation levels from the light bank at full and half power along with the solar water heater's collector area of 0.0994 $m^2$, the radiative power, $q_{irrad}$, from Eq. 7-1 can be calculated. The result is 71.5W for the full light bank experiment and 35.8W for the half bank experiment. There is therefore close agreement between $q_{irrad}$ and $q_{solar}$ so according to the same basic relationship shown in Eq. 7-9, the efficiency must be quite high. Though Eq. 7-9 gives an accurate efficiency relationship, this experiment included a high flow rate and small temperature difference which would not offer much accuracy using this equation so the constants from the curve fit were used instead. The high efficiency means that the water heater collected the majority of the radiative power available to it.

The disparity between the thermal resistances between the two experiments is unexpected. Since thermal resistance is a function of the system, not of its operating conditions, they should have been extremely close. Possible explanations include a difference in room draft, difference in how the tank was insulated between experiments, experimental error, and curve fit inaccuracy.

Using Eq. 7-8 and the experimental data, the maximum (steady state) temperature for each experiment can be calculated to be about 41ºC and 28ºC above ambient for the full bank and half bank experiments, respectively. During the summer when ambient conditions may be 20ºC there may be hot enough water, but during the winter if ambient was 0ºC, there would probably not be enough hot water with full illumination and definitely not with half illumination. This is the kind of situation that would show a need for vacuum tube collectors

which have a much higher thermal resistance and therefore can heat water sufficiently even when ambient conditions are very cold.

## Accuracy of Demonstration

These experiments with the solar hot water heater show the viability of even a very basic solar water heating device. Using radiation from a halogen light source, reasonable water temperatures were attained. The relating of theory to experimental results provided deeper understanding of those results while also justifying the theory. The limitations of solar hot water heaters were also seen in the maximum temperatures achieved and in the length of time required to attain them. These two factors are the most important drawbacks to solar water heating as compared with electric or gas heating and offer experience to students of the unique features of this technology.

# Chapter 8 PASSIVE SOLAR BUILDING TECHNOLOGIES

## *Background*

Passive solar building technologies are yet another means of making gainful use of solar energy. It is passive in contrast to active solar technologies because it does not involve active control via the use of additional energy-consuming devices, such as pumps or trackers. Passive solar technologies use intentional design and placement of building features and materials rather than the use of energy-consuming technologies to regulate air temperature, though traditional air temperature regulation technologies are not totally displaced. Regulation of building temperature despite both daily and annual solar cycles is the main challenge of passive solar building technologies. There are many examples of passive solar technologies that employ different strategies for controlling building temperature.

Many passive solar technologies make use of the fact that the sun is in a different position in the sky at different times of the year. Because in the summer buildings usually need to be cooled and in the winter buildings usually need to be heated, building design can make use of the fact that the sun is higher in the sky in the summer and lower in the sky in the winter.

In conjunction with taking advantage of the different positions of the sun, strategically placed thermal mass can be used to absorb and release heat to dampen daily temperature swings. Radiatively absorptive thermal mass takes in solar energy during the day, keeping a building interior cooler than it would be otherwise. Then, during the night the heat is released to heat the building when otherwise it would be cold.

Many variations of these two broad classes of passive technologies exist along with many other individual technologies more difficult to classify into broad categories. Their characteristics and performance is so varied and in many instances heavily dependent on location conditions and factors that generalized theory is impractical.

## *Theory*

Careful placement of landscaping and trees can block the sun from windows in the summer when it is high and let the sun in when it is low during winter. This is illustrated below in Figure 8-1.

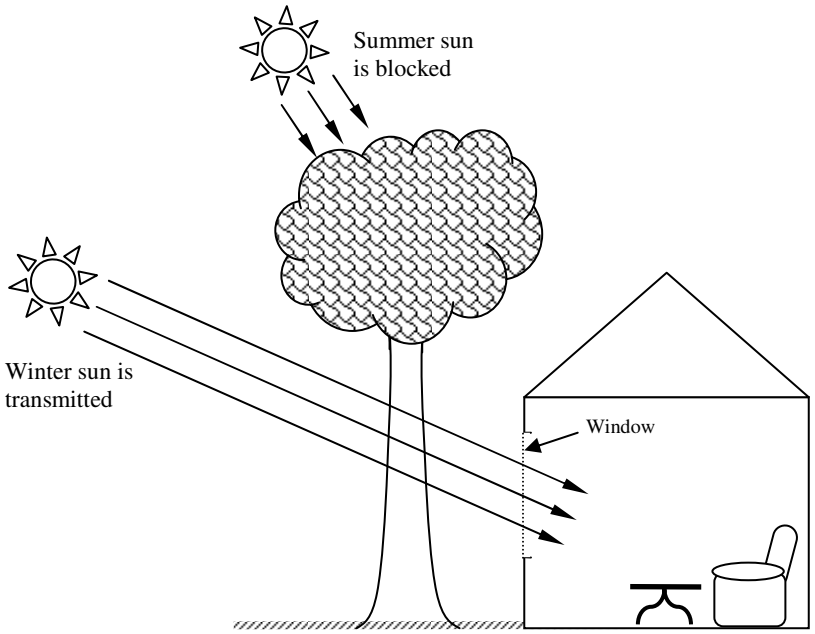


**Figure 8-1 Tree shading passive solar heating and cooling.**

A similar idea is to use overhangs dimensioned such that summer sun is blocked and winter sun is transmitted as shown in Figure 8-2 below.

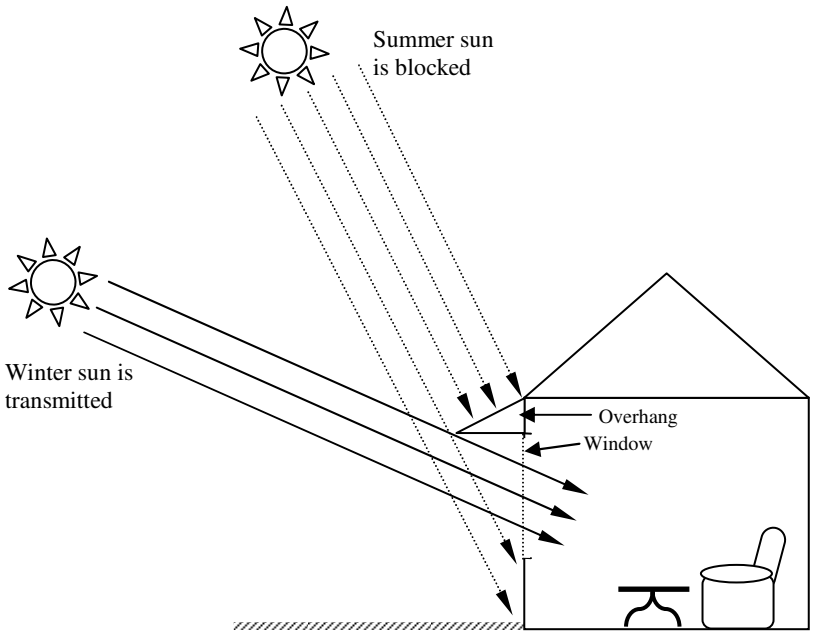


**Figure 8-2 Overhang shading passive heating and cooling.**

Shading strategies can be coupled with another passive solar technology: specially coated glass windows. These can be used especially in south-facing windows (in the northern hemisphere) for temperature regulation. The coatings are selective, that is, they have different transmissivities for wavelengths carry the majority of the energy from the sun than for wavelengths carrying the energy from indoor objects.

The class of strategies utilizing the placement of thermal mass in locations that will absorb heat during the day and release it at night has various examples. The heat absorbed is either to prevent it from entering the building by absorbing it during the day and releasing it back to the atmosphere at night, or is to aid in building heating by absorbing heat during the day for release indoors at night. Thick, thermally massive walls in sun-facing directions can absorb the hot summer sun and release it at night to even out the wide temperature fluctuations that would be present with thin, low thermal mass walls. Thermally massive walls behind glass windows called Trombe walls can absorb solar energy and release it into the building via natural convection at night. A diagram of a Trombe wall is shown in Figure 8-3 below.

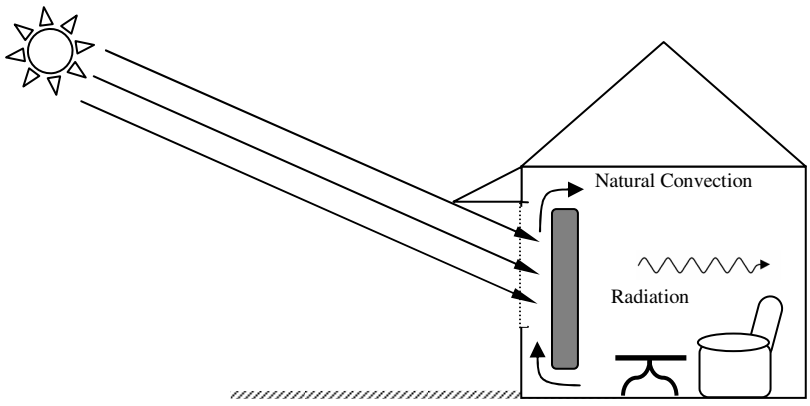


**Figure 8-3 Diagram of Trombe wall.**

Dark, stone (or any thermally massive) flooring can absorb winter sun through windows and release it once the sun has gone down, stabilizing the daily temperature swing. A diagram of this technology is shown in Figure 8-4 below.

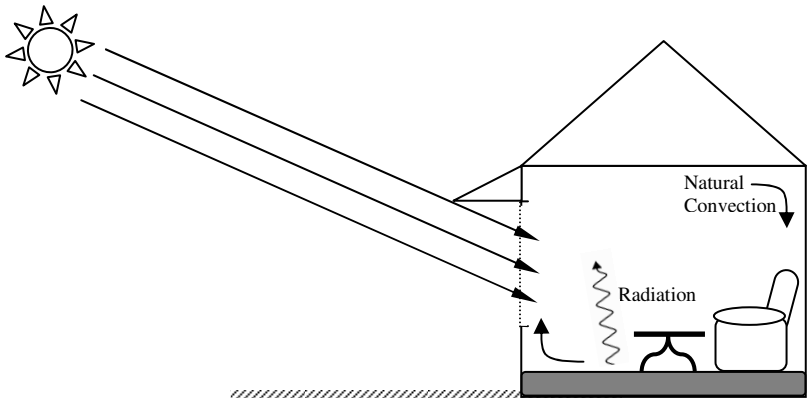


**Figure 8-4 Diagram of thermally massive flooring.**

Sizing calculations for Trombe walls and thermally massive flooring are difficult to generalize because of the various conditions in which they are used and the variety of user desires. Thermal properties of the material and the surrounding building, the geographic location, orientation, time of year, local weather, and other factors are all important. However, the general concepts of having a thermal mass with thermal capacitance enough to hold heat needed for overnight building temperature maintenance, and with enough area given local irradiation levels to collect the necessary heat can guide design.

## *Demonstration*

A model house was constructed for the investigation of passive solar technologies. It consists of a wooden box with an inner space of about 12 inches deep by 18 inches wide by 8 inches tall as seen below. A glass window 5'' by 17'' is located along one side. The model house is shown in Figure 8-5 below.

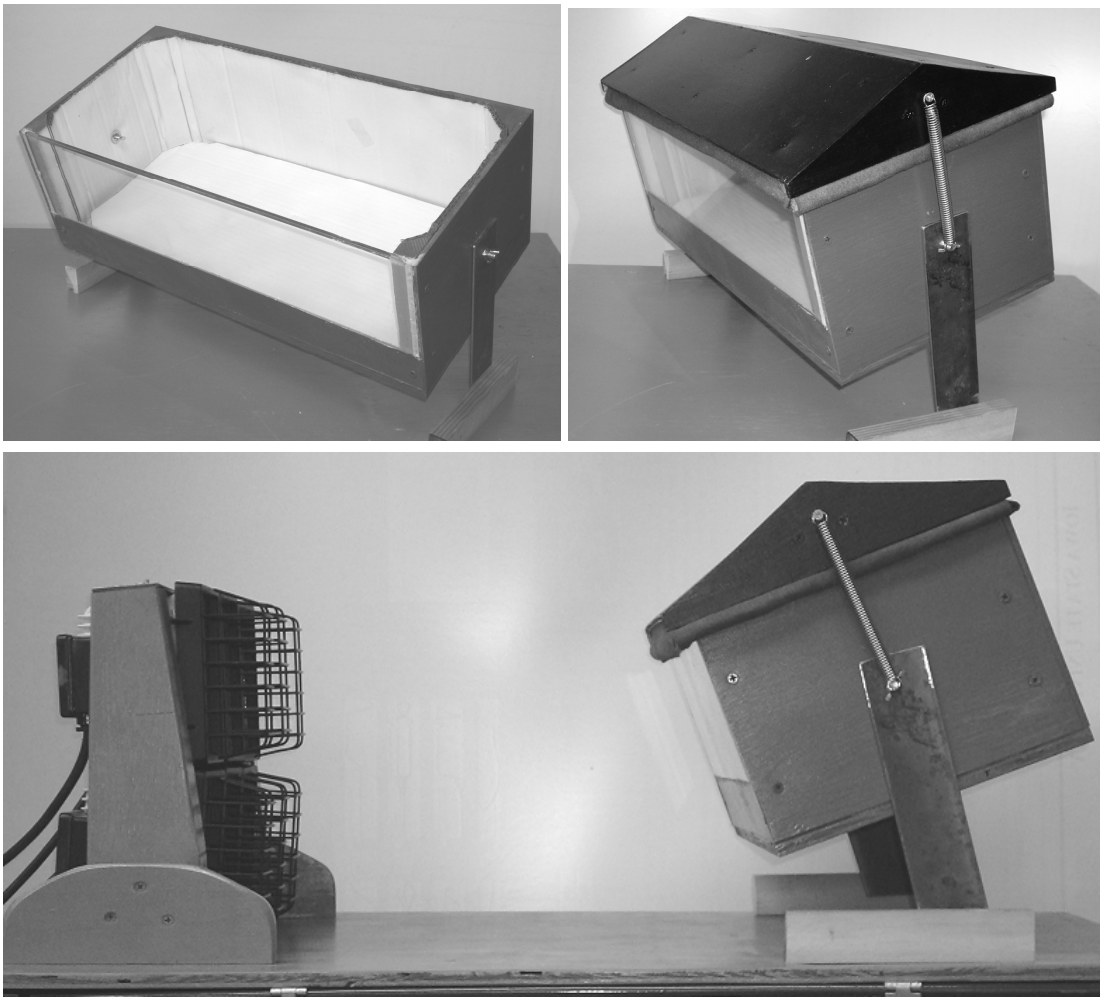

**Figure 8-5 Photographs of house model. Top left picture is without the roof, top right is with the roof attached, and bottom is in front of the light bank.**

The insides of the walls and floor are lined with thick cardboard for insulation. The roof is removable and has a cushioned bottom edge for an insulated, tight fit with the bottom half of the house model. Removal of the roof allows for the placement of several movable components into their positions for different experiments.

The whole house is mounted on the stands that are also used for the PV panels described in a previous section. This allows the orientation of the house relative to the lights to be adjusted. For convenience's sake and the constraints of mobility for the laboratory facility as a whole, the rotation of the house relative to the lights is a better choice than altering the position of the lights. The summer sun can be replicated with the cart rotated toward the

light source while the winter sun can be replicated with the house more horizontal, as shown in Figure 8-6 below.

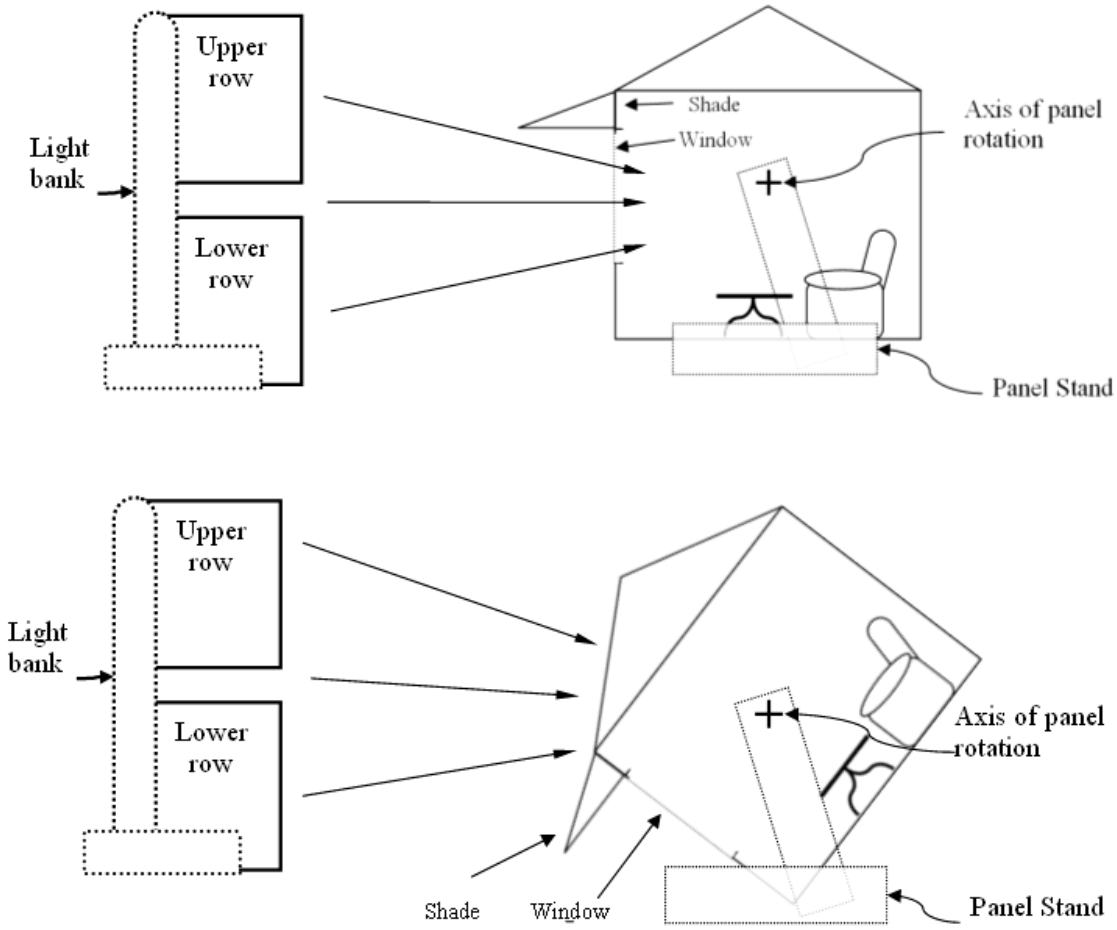


**Figure 8-6 Illustration of adjustable orientation of the house model relative to the light bank.**

A small electric fan is located within the enclosure and provides circulation for the Trombe wall as well as a means of keeping internal air temperature uniform for more accurate temperature measurements. The fan also provides the option for investigating internal air circulation as another variable contributing to building temperature.

A roughly 5/8'' thick Trombe wall was formed out of a mortar/plaster mix and painted with black paint on all sides and shown in Figure 8-7 and Figure 8-8. It was sized according to the window of the model house and is held in position within the model house by wooden stands that keep the wall roughly 3/8'' from the window as shown in Figure 8-7 below. It has clearance on both the bottom and the top to allow air circulation across the front side of the wall.

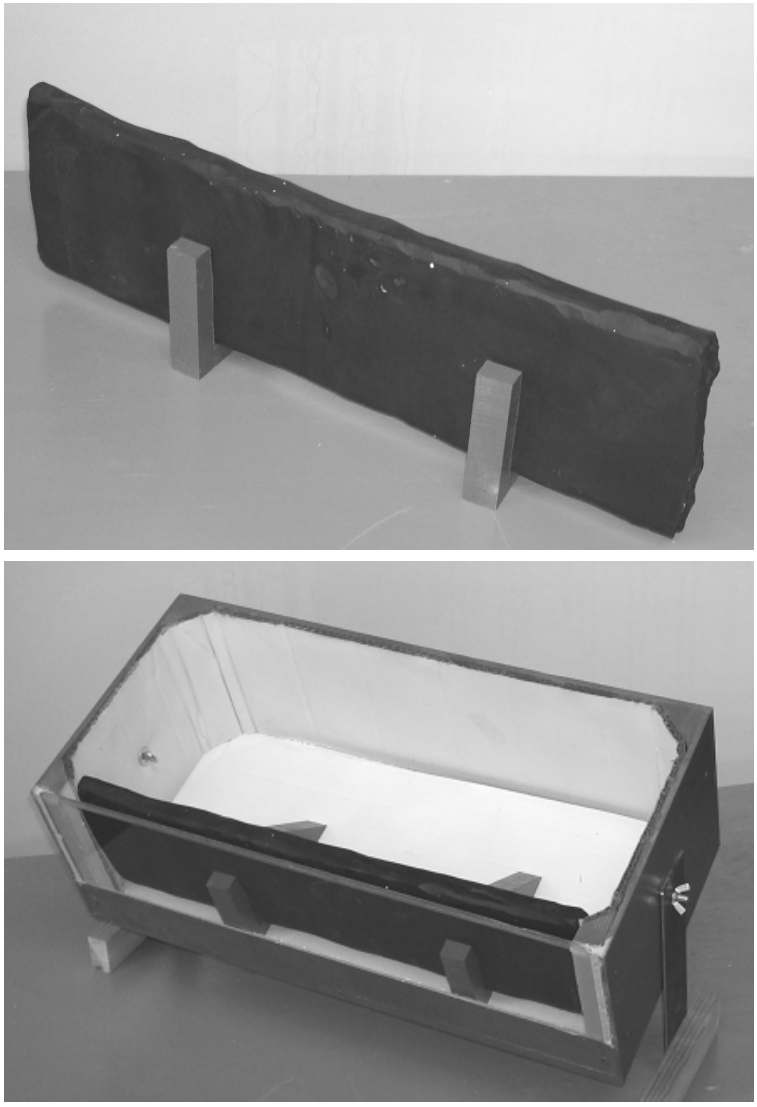

**Figure 8-7 Pictures of the Trombe Wall from various angles and in position in the model house.**

Another passive solar design feature included in the demonstration is a thermally massive floor. The floor was constructed with the same materials as the Trombe wall and painted black on the top side. It is about ¾'' thick and sized to cover the floor of the model house and is shown in Figure 8-8 below next to the Trombe wall.

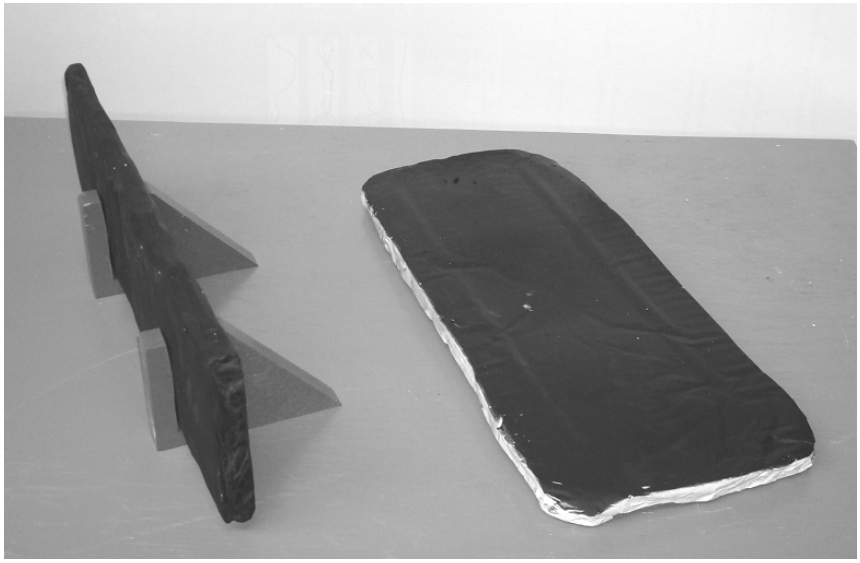

**Figure 8-8 Trombe wall and massive flooring.**

A final feature for experimental use is a thermally light floor sized the same as the thermally massive flooring but made of cardboard. One side is painted white and the other is painted black. This will allow for the analysis of the effect of both color and thermal mass.

Because no feature of the house is designed to scale, absolute value and quantitative results are not the goal. Rather, relative and qualitative results will be analyzed for trends and effects of each technology. Multiple temperature sensors placed in key locations will give additional insight onto the operation and performance of the components used.

## Reasonableness of Demonstration Developed

Major passive solar building technologies are represented in this demonstration and the cyclic lighting provides experience in their response and performance, and models real-world technologies at a reasonable classroom-scale. The possibility of various combinations of components and conditions to be experimented with using the demonstration lends itself to the variety of designs of passive technology available. This also allows for students to define their own experiments to test numerous issues not explicitly dealt with here. Temperature placement gives the ability to understand various characteristics not discernable with a single air temperature measurement. This allows for understanding of the motive for making variations on the passive solar building technologies included and gives more information suggesting avenues for new technical development. This demonstration gives a thorough exposure to the basic passive solar building technologies available and is a good platform for experimentation and investigation of these for deeper understanding.

## *Experiments*

Because the primary purpose of passive solar building technology is to regulate air temperature against daily fluctuating solar radiation, a small-scale replication of this is required for observing the performance of the various passive solar technologies available in the demonstration. After some initial experimentation, it was found that four minutes of the light bank being on followed by eight minutes of the light bank being off offered a significant temperature swing and mimicked typical winter time daytime-to-nighttime ratio. There are numerous combinations of the various interchangeable components and conditions—fan, Trombe wall, thermally massive wall, the thermally light wall with each color, orientation, and light bank strength (# of lights powered). Four experiments were chosen: Trombe wall, thermally massive floor, and the thermally light floor with both white and black sides exposed. The same orientation (window normal is 15º below horizontal as shown in Figure 8-5 and light power (all six light powered) was used for each run. The fan was used for each experiment as well. These choices highlight the effects of the components used within the model house by having the same conditions for run.

With these four experiments, many comparisons can be made to infer the effects of changes of particular variables. The experimental component for the particular experiment was placed within the model house and the light cycle was started. Steady state was reached after several hours and once reached, data was recorded every minute. The graphs below span two complete lighting cycles. On each graph, the time starts at zero with the beginning of an eight-minute cool-down period. At eight minutes, the light was turned on for four minutes followed by another eight-minute cool-down. The last four minutes shown on the graphs are the final four-minute irradiation period. The following acronyms were used to designate the results according to the components used:

| | |
|---|---|
| WC | Cardboard floor with the white side facing up |
| BC | Cardboard floor with the black side facing up |
| MF | Thermally massive floor |
| TW | Trombe wall |

The first graph (shown in Figure 8-9 below) displays the entire data set from all of the four runs plotted on the same graph. The experiments were run separately but all of the results are overlaid for general analysis and discussion.

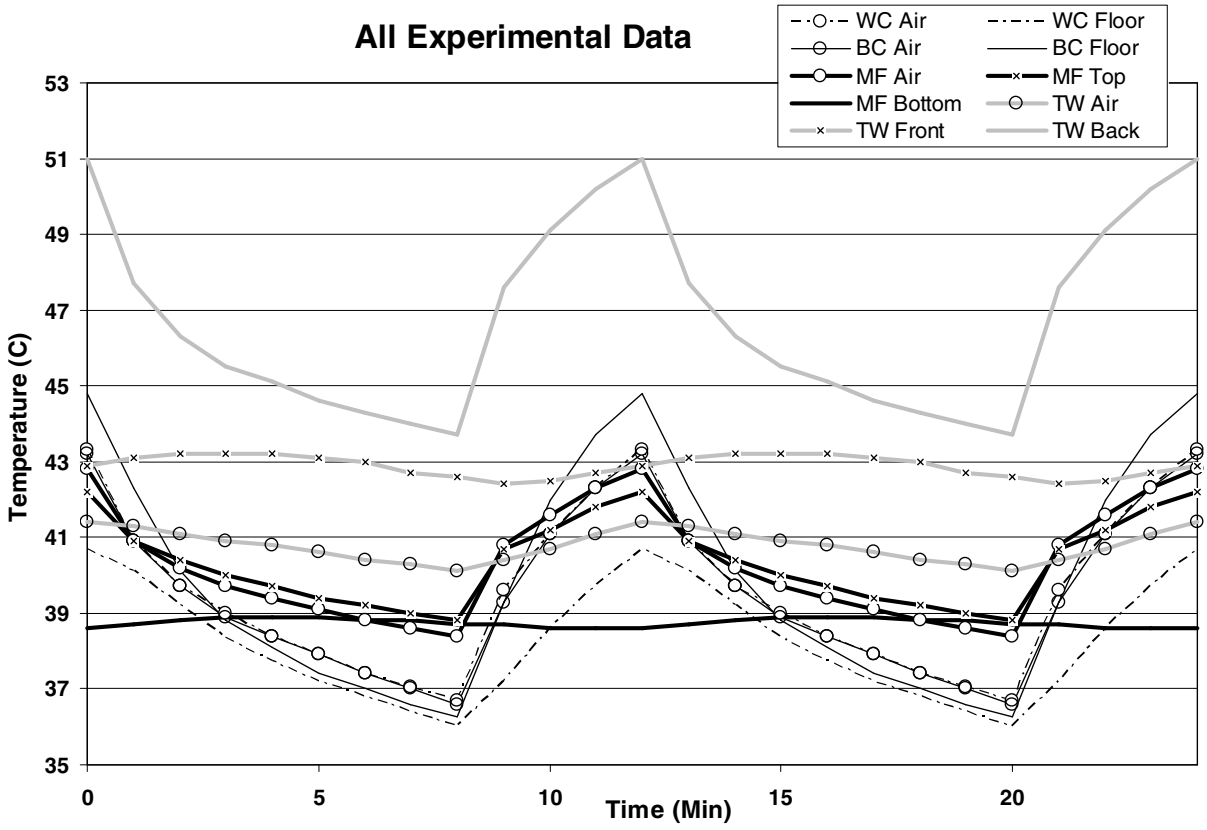


**Figure 8-9 Graph of all experimental data for general observation.**

Figure 8-9 shows the expected general trend of increasing temperature during the irradiation periods, except for two curves which look to be lagging about 90º. These are the temperatures of the sides of the wall and massive floor that are opposite the irradiation. The lag makes sense because of the time it takes for heat to travel from the irradiated side through the material and to the other side. Another general observation is that the front, exposed side of the Trombe wall is at a much higher temperature than anything else of any other run. This is expected given that the Trombe wall faces the irradiation directly, more directly than the floor. It is also painted black to absorb irradiation and though is it cooled by the circulating air, it also is insulated by the glass so the high temperature is not surprising. A final general observation is that there are curves which fluctuate drastically between the cool-down and irradiated periods, while others are more stable. More detailed analysis can be performed by isolating various curves for more specific comparison. Since the regulation and stabilization of air temperature is the primary purpose of passive solar building technologies, the four air temperature curves from Figure 8-9 are reproduced in Figure 8-10.

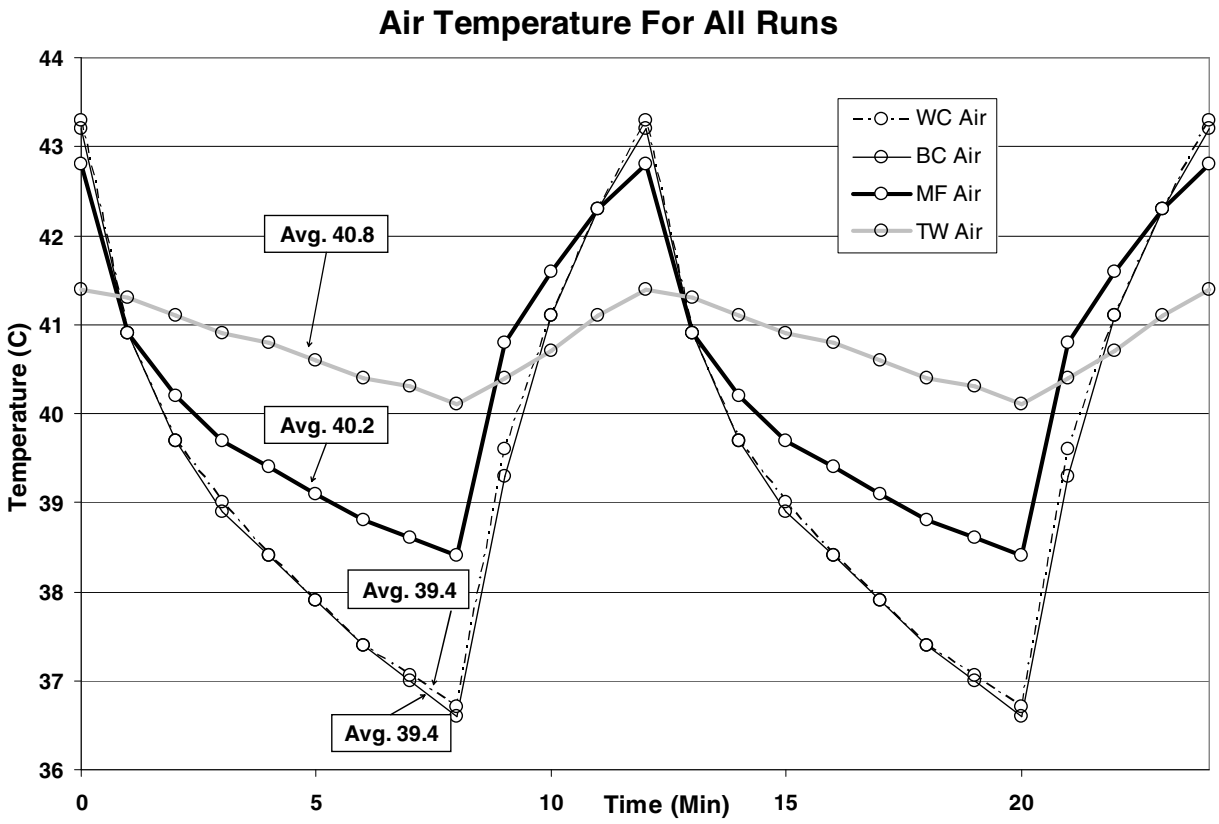


**Figure 8-10 Graph showing air temperature for each of the four experimental runs for comparison.**

The relative temperature stability can be seen clearly in Figure 8-10. The Trombe wall provides the most stable temperature across the cycle followed by the massive floor and, lastly, the cardboard floor resulted in wide air temperature swings. The color of the cardboard floor did not seem to effect temperature at all which is surprising. The average temperature over a cycle for each experimental run is displayed and as can be seen the average for the Trombe wall is the highest. This makes sense given that the black Trombe wall was completely covering the window of the model house. It thus would absorb more irradiation than either of the black floors since they make up only a fraction of the projected area of the window towards the light bank. The thermally massive floor had an average temperature less than that for the Trombe wall, followed by the cardboard floor with the lowest average temperature. More detailed analysis of the performance of the cardboard floors can be made based on all the cardboard run data shown in Figure 8-11 below.

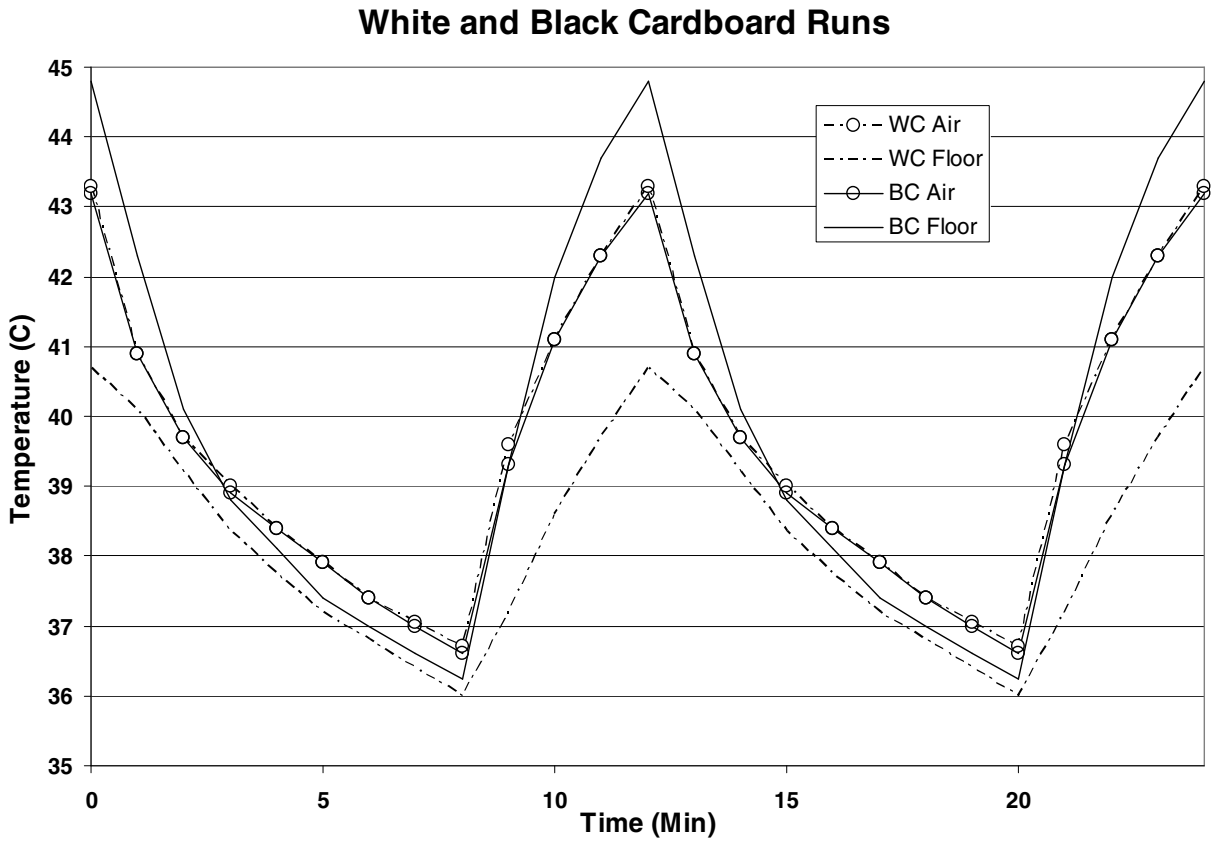


**Figure 8-11 Both black and white cardboard run data.**

Close inspection of Figure 8-11 reveals the surprising result that the air temperature was almost identical between the white cardboard floor and black cardboard floor. This is even more surprising given the fact that the black cardboard floor increased in temperature during the irradiation period significantly more than with the white floor. The explanation may be that even though the black cardboard conveyed more heat to the air, loss to the environment presented a limiting factor of air temperature so the air temperature ended up being very close between the two runs. Another possible explanation is that while the black cardboard did heat up more, the black cardboard was only a small fraction of the irradiated surfaces within the model house so the total result on air temperature was minimal. Even though floor color seems to be somewhat eliminated as a significant factor contributing to air temperature, further analysis based on Figure 8-12 uses both of the black colored floor combinations to isolate thermal mass as the only variable.

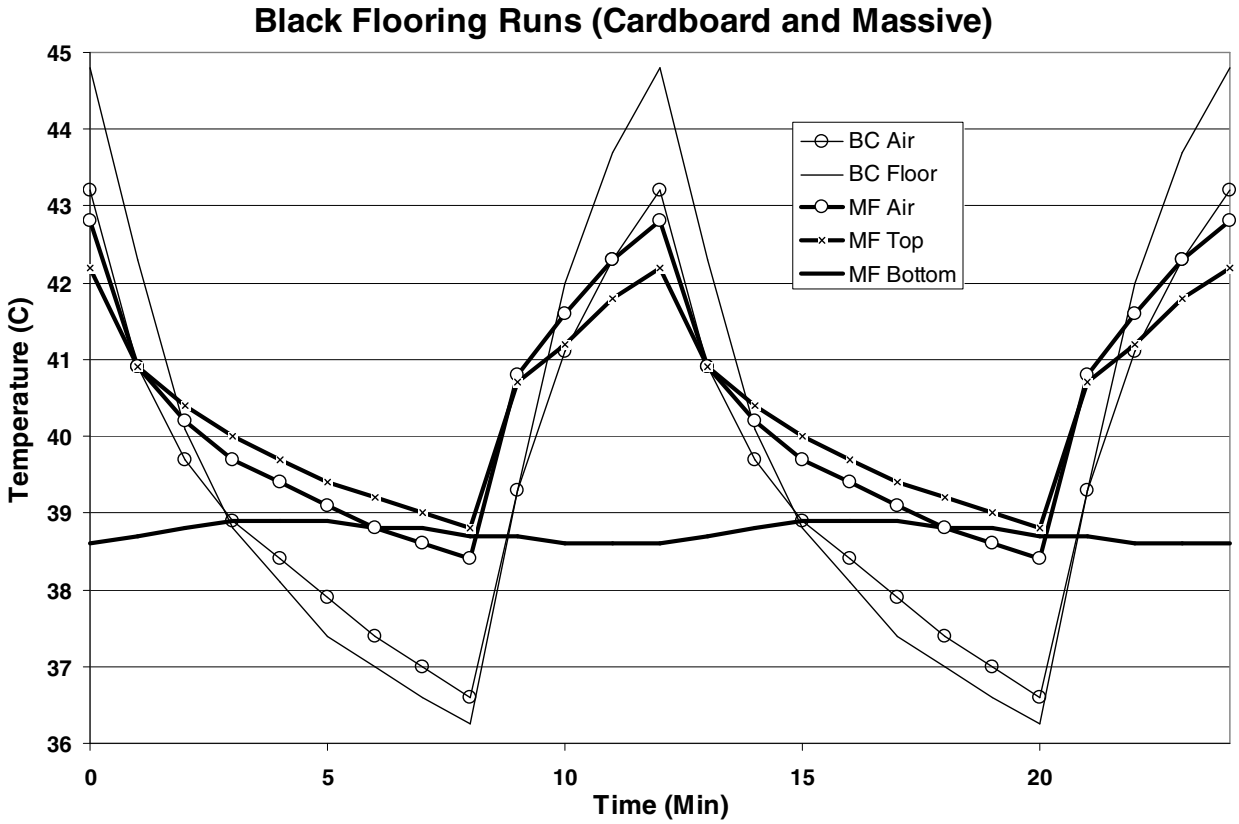


**Figure 8-12 Experimental results from black cardboard and thermally massive flooring.**

Since both of the runs included in Figure 8-12 used black colored floors, the main difference between them was in their thermal mass. The results show very clearly that thermal mass stabilizes temperature through cyclic irradiation. Even though both floors had the same surface coating, the thermally massive floor did not get as cold during the cool-down period or as hot during the irradiation period as did the cardboard floor. A final graph shown in Figure 8-13 shows the results of the Trombe wall experiment with the white colored cardboard run as a baseline for comparison.

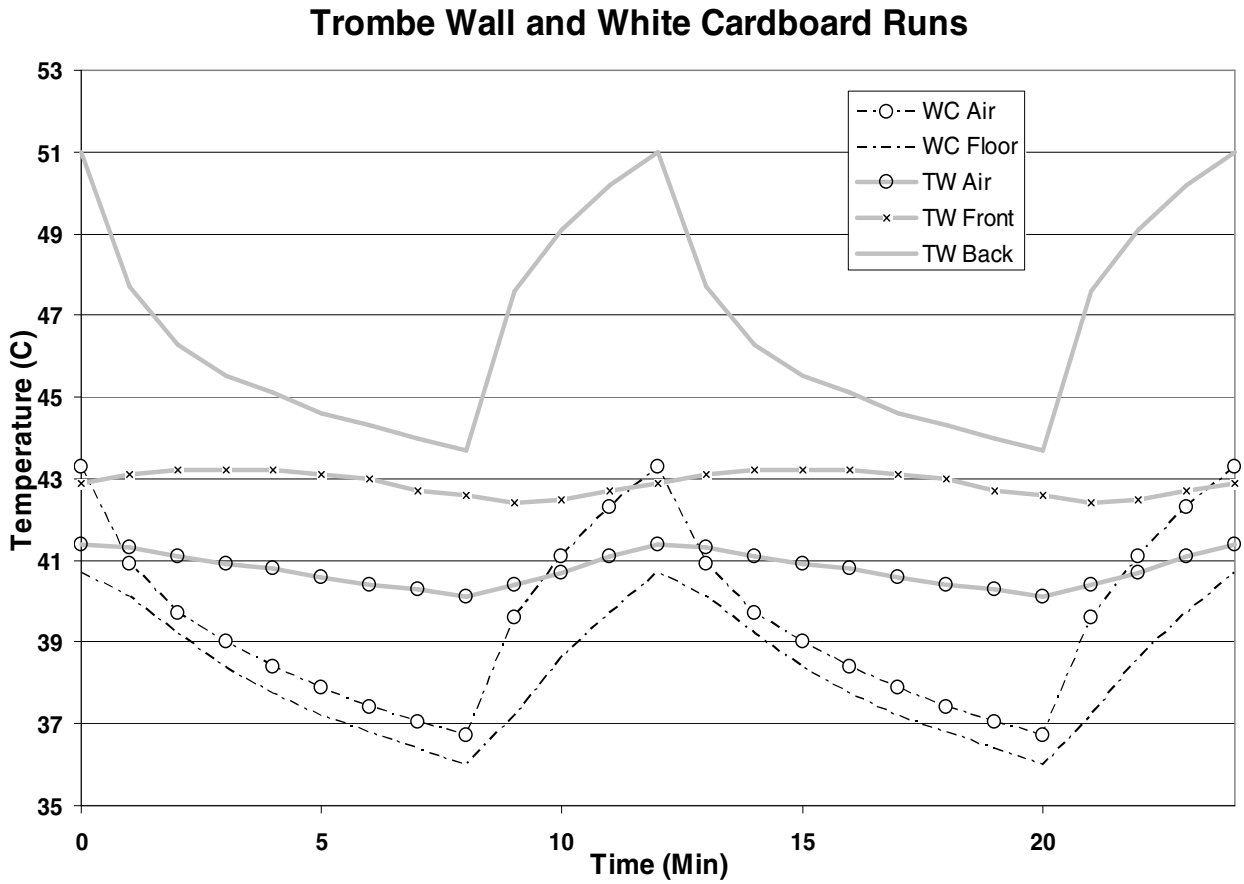


**Figure 8-13 Trombe wall and white colored cardboard experimental results.**

The Trombe wall shows the most stable air temperature and, as was seen before, has the highest average temperature. In real-world applications, further air temperature control can be accomplished through control of the circulation of air between the Trombe wall and the glass behind which it is situated. If this air is held still, heat must travel through the wall before entering the room, further delaying its release to heat up the air. This would practically result in a much higher rise in the rear wall temperature. Heating and cooling loads could be lessened by this passive technologies' regulation of building air temperature.

While the details of the optimal operation in real-world applications of the technologies just considered will inevitably require more complicated quantitative analysis and modeling, the basic concepts and potential usefulness of passive solar building technologies has been clearly seen. The effect of the color of flooring seems to be inconclusive from the experiments performed, but expanding the interchangeable colored surfaces to include all internal surfaces of the model house may offer more conclusive results. The Trombe wall

experiment showed promise for Trombe wall use as well as thermally massive flooring use for regulating and stabilizing the temperature building air temperature in spite of fluctuating irradiation levels. In this way more beneficial use can be made of the sun and unnecessary energy expenditures can be displaced.

## Accuracy of Demonstration

As there were no particular quantitative predictions for these experiments to live up to, the accuracy of this demonstration to real-world passive solar technologies much be qualitative. The general trends observed from experiments using the demonstration are those that are predicted by passive solar theory and desired to attain the goals of passive solar technology. The lack of difference the color of the floor seemed to make was unexpected but not completely unexplainable, though further investigation of this result would be appropriate for students. This demonstration, then, accurately presents some passive solar technologies and allows for accurate qualitative experimentation and analysis to aid and support the furthering of student understanding of this technology.